UNIVERSITÀ POLITECNICA DELLE MARCHE

FACOLTÀ DI INGEGNERIA

Corso di laurea in Biomedical Engineering
Curriculum eHealth and Clinical Engineering

Dipartimento di Ingegneria dell'Informazione

PHYSIOLOGICAL CIRCADIAN MODULATION OF ELECTROCARDIOGRAPHIC ALTERNANS IN HEALTHY SUBJECTS

Relatrice:

Prof.ssa **Laura Burattini**

Tesi di laurea di:

Raffaella Assogna

Correlatrice:

Dott.ssa **Ilaria Marcantoni**

A.A 2022/2023

ABSTRACT

The circadian rhythm is a cyclic process distinguished by a 24h periodicity. It is typical of the modulation of numerous physiological phenomena, including the ones of the cardiovascular system. The heart is a striated muscle organ and, as part of the cardiovascular system, its dynamics are modulated by a circadian pattern in many cases (e.g., heart rate). From the electrical viewpoint, the heart contraction and relaxation are possible due to a complex mechanism of depolarization and repolarization of the cardiac cells. In this context, the electrocardiography is a technique used to measure and record the electrical phenomena underlying the processes of cardiac depolarization and repolarization. The portable instrument that allows electrocardiography to be performed for extended durations, from hours to days, is called Holter. It usually made up of a precise set of electronic components. The result of the Holter exam is an electrocardiographic trace that is macroscopically composed of 3 fundamental sections: the P wave, the QRS complex, and the T wave. Through a detailed analysis of them valuable insights regarding the electrical vulnerability of the heart, the arrhythmias and the influence of the circadian rhythm on the cardiac activity can be deduced.

The electrocardiographic alternans (ECGA) is the alternation of the morphology, amplitude, or polarity of the P wave (PWA), QRS complex (QRSA) or T wave (TWA) from beat to beat, according to an ABAB pattern. Various methods can be used to automatically detect TWA but only the Enhanced adaptive match filter (EAMF) method can be utilized for all PWA, QRSA and TWA analysis. ECGA has been identified as index of cardiovascular risk, associated to the danger of developing arrhythmias. Since the cardiac activity is modulated by a circadian pattern in different aspects, it is expectable that ECGA follows a circadian rhythm too. The prior aim of this thesis was to assess the information regarding the circadian rhythm of ECGA present in literature. A systematic review was done in Scopus and Pubmed databases. After the screening following PRISMA guidelines 9 articles resulted (total population studied: 106 healthy subjects and 1380 diseased subjects). 8 papers concerned TWA (most used method of detection: modified-moving-average method (44% of papers)) and only 1 paper studied all 3 types of ECGA (used method: EAMF) highlighting the necessity to enlarge the knowledge in

this field. In all cases a circadian rhythm was identified with an increasing during day and a decreasing during night.

Moreover, this thesis aimed to verify whether PWA, QRSA and TWA are modulated by a circadian periodicity in real data. The Holter data (at least 24h; X, Y and Z leads) of 60 healthy subjects (mean age 39±16years) from "E-HOL-03-0202-003" database available on Telemetric and Holter ECG Warehouse were analysed. The signals were first subjected to a pre-processing phase and examined through the EAMF method. The EAMF was optimized for this application. Data were subjected to statistical analysis. Results were reported in terms of amplitude (ECGA-A) (μV), number of alternating heart beats (ECGA-D) and magnitude (ECGA-M) (μV*number of alternating beats (μV*n)) and fitted through a 2-sins-sum model. The trends of ECGA-A, ECGA-D and ECGA-M showed a circadian rhythm during the hours of the day with an absolute maximum in the afternoon (12:00-18:00) and a minimum during the night (19:00-7:00), proving the presence of physiological circadian modulation of ECGA in healthy subjects. The trend of ECGA was in line with the trend of arrhythmias reported in literature, confirming the ECGA as marker of cardiovascular risk. The circadian modulation was visible for PWA, QRSA and TWA, even if more evident for PWA. PWA oscillated between 11μV and 13μV in terms of amplitude, 67 and 96 in terms of number of alternating beats and 673μV*n and 1229μV*n in terms of magnitude; QRSA oscillated between 11μV and 12μV in terms of amplitude, 43 and 77 in terms of alternating beats and 428μV*n and 882μV*n in terms of magnitude; TWA oscillated between 12μV and 15μV in terms of amplitude, 100 and 107 in terms of alternating beats and 1314μV*n and 1684μV*n in terms of magnitude (median values over X, Y and Z leads). The values of ECGA-A, ECGA-D, ECGA-M were different among the 3 leads (X, Y and Z) validating the ECGA as a lead dependent event. Furthermore, the results in this thesis can be used as reference values of ECGA over the hours of the day in healthy population, giving a term of comparison for assessing the degree of cardiovascular risk according to the time of the day.

INDEX

1.
Introduction
and
Physiological contextualization

1.1. Electrical physiology of the heart

1.1.1 Fundamental aspects of cardiac anatomy

The heart is an organ located in the inferior mediastinum, in the center of the thoracic cavity and it is part of the cardiovascular system. From the shape viewpoint, it is a hollow organ that is generally described as a flattened cone. It is divided into 4 chambers: 2 upper ones, called the right atrium and left atrium, and 2 lower ones, called the right ventricle and left ventricle. This division is made by a structure called internal septa [1]. Arteries and veins originate and arrive at the heart: the pulmonary trunk and the aorta originate from the right and left ventricles, respectively; the vena cava opens into the right atrium, and the pulmonary vein into the left atrium. Externally, the heart has an anterior and posterior face separated by an acute edge and an obtuse edge. It has a coronary sulcus that separates the atria from the ventricles and contains the coronary vessels, used to supply the heart itself, and 2 interventricular sulci (anterior and posterior) [1].

The pericardium encases the heart. It is a sort of sac that is divided into the fibrous pericardium on the outside and the serous pericardium on the inside. The serous pericardium is composed of a double layer: the parietal layer that covers the inner surface of the fibrous pericardium and the visceral layer or epicardium. Below the epicardium, there is the myocardium which is made up of muscle tissue [1].

The heart's wall structure is reported in Figure 1.

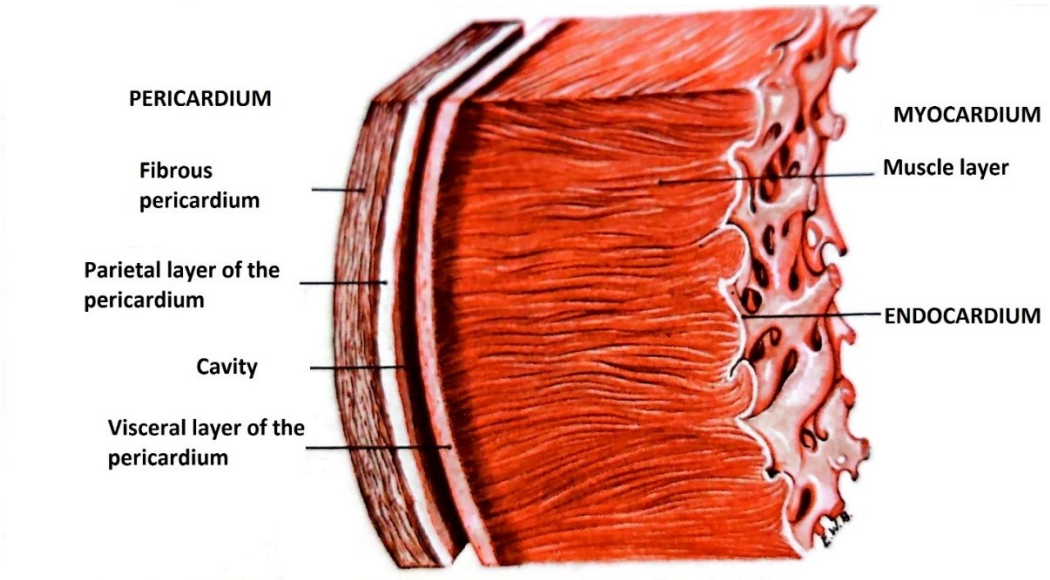

Figure 1 Heart's wall structure [2]

At cellular level, myocardial cells (myocytes) have a ramified and elongated morphology and are approximately 120µm long. They are delimited by a cell membrane which is formed by a double phospholipid sheet and is selectively permeable. Proteins are located in the membrane and extend from one or both sides of the sheet, thus acting as channels. The myocardium is characterized by elements of both smooth muscle tissue and striated muscle. Indeed, the myocardium can be considered as a functional syncytium, typical of involuntary muscles. In fact, the heart reacts to stimuli as a single fiber and contracts involuntarily. The cells form a 3-dimensional network and are self-contracting. However, it is not possible to identify the myocardium as an anatomical syncytium. Indeed, the cells appear to be distinct and striated. This hybridization allows the heart to resist high pressures and to carry out its function while maintaining an indispensable involuntary connotation. Between one cell and another, there is the intercalary disc which under the microscope appears as a clearly visible streak line. The nuclei, single or double, are located in the center of the cytoplasm called sarcoplasm. It is possible to distinguish the specific myocardium from the common one. The specific myocardium is less striated and the cells that compose it are characterized by a less effective but faster contraction. Therefore, these cells are essential in determining the right rate of self-contraction. Furthermore, particular myocytes are identified, i.e. nodal cells which will be indagated after [1].

The distinctive elements that make up the cardiac muscles are 2 proteins: actin organized into thin myofilaments and myosin organized into thicker filaments. Actin and myosin are grouped into units called sarcomeres (Figure 2) which are divided from each other by Z lines. These lines are disks made up of a lattice of actin from which thin filaments depart perpendicularly. This area is called the I-band and intersects with the myosin filaments organized in the A-band [1].

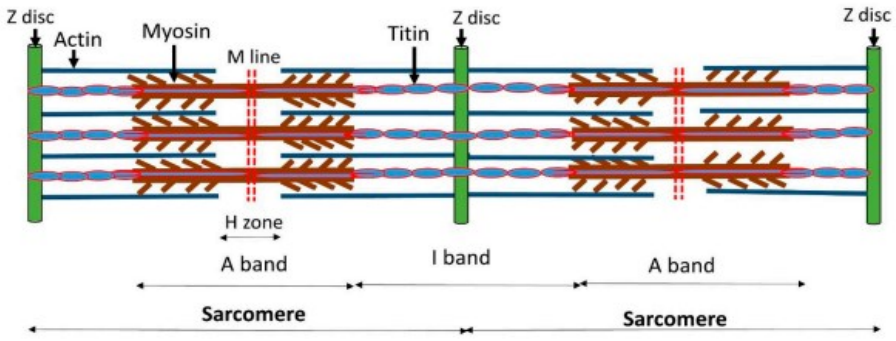

Figure 2 Sarcomere [3]

In the middle of the A-band, there is the M-line which is visually darker and holds the thick filaments in place. Sarcomeres are arranged in myofibrils surrounded by the sarcoplasmic reticulum. In the region adjacent to the Z line, the T-tubules are distributed perpendicular to the myofibrils. On either side of the tubule, the sarcoplasmic reticulum forms cisternae containing calcium ions. The tubule with the cistern represents a dyad. There are calcium ion channels on the sarcoplasmic reticulum membrane, and just behind these channels, there are protein filaments called calsequestrin. In the myocardium, the various sarcoplasm can communicate making it possible to define a functional syncytium. A myosin molecule consists of 2 polypeptide chains that form a structure with a tail and 2 round heads. The thick filament is created by the set of several myosin molecules that intertwine in a helix, placing the heads toward the outside. The thin filaments consist of 2 molecules of G actin linked to molecules of tropomyosin. Troponin proteins will be investigated later.

Internally the heart is characterized by a fibrous skeleton (Figure 3) which is organized into 4 fibrous rings. The rings surround 4 orifices in which the valves that connect the atria with their respective ventricles and the ventricles with the arteries are located. Between the right atrium and the right ventricle, there is the tricuspid valve which is made up of 3 leaflets: anterior, septal, and posterior. The base of each leaflet is anchored to the annulus fibrosus while the 3 edges are attached by chordae tendineae to the papillary muscles in the bottom of the ventricle. These muscles keep closed the valve when needed. The right ventricle communicates with the pulmonary artery through the

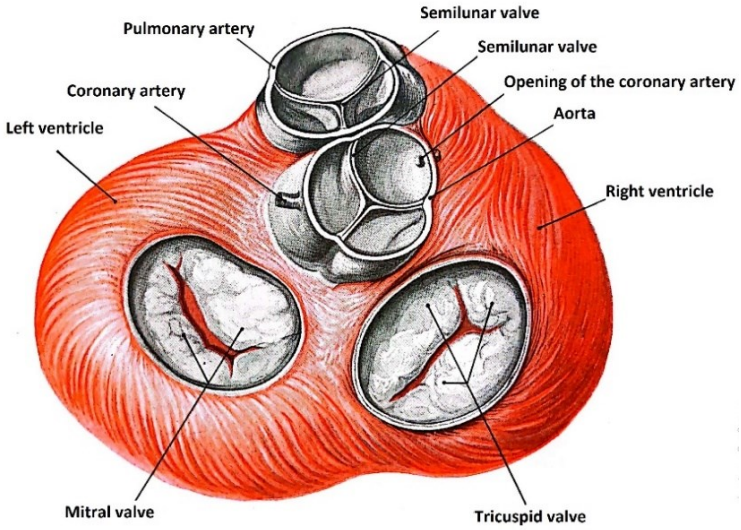

Figure 3 Heart's fibrous skeleton

pulmonary valve. The pulmonary valve is composed of 3 semilunar cusps which prevent the pumped blood from flowing back to the heart. The left atrium and ventricle are separated by the mitral or bicuspid valve (anterior and posterior), with a configuration similar to the tricuspid valve, except for the presence of 2 leaflets instead of 3. Finally, the aortic valve is morphologically similar to the pulmonary valve [1].

The fundamental role of the heart which acts as a sort of "pump" is pushing blood into the arteries and from the arteries to the entire body. The blood carries essential substances for body life such as oxygen, carbon dioxide, nutrients, immune defence agents, and hormones.

1.1.2 The heart electrical activity at the cellular level: the action potential

The extracellular and intracellular environment of cardiomyocytes are characterized by the presence of ions in different concentrations. This condition makes cellular electrical activity possible. More in details, these ions are sodium ions (Na+), potassium (K+), chlorine (Cl-) and calcium (Ca2+).

Overall, the electrical activity is the result of the combination of 2 transport mechanisms:

- diffusion or passive transport;
- active transport.

Moreover, diffusion is divided into free and ionic diffusion. Free diffusion is determined by the concentration gradient. In fact, the ions tend to move from an area with a lower concentration to a more concentrated one. The particle flux is proportional to the concentration gradient according to Fick's law:

$$J_d = -D\nabla C \quad (1)$$

J_d=flow of particles due to free diffusion

D=Fick coefficient

∇C=concentration gradient

Ionic diffusion is caused by the fact that an electric field is created in the presence of a potential difference. It results in a force is generation which tends to cause an electrical equilibrium. This process is described by Ohm's law:

$$J_I = -u\frac{Z}{|Z|}C\nabla\phi \quad (2)$$

J_I=flow of particles due to ionic diffusion

u=motility per unit electric field

Z=valence

C=concentration

$\nabla\phi$=potential gradient

The product $u\frac{Z}{|Z|}C$ can be written in terms of D using Einstein's law and thus J_I results:

$$J_I = -D\frac{ZCF}{RT}\nabla\phi \quad (3)$$

F=Faraday constant

T=temperature expressed in Kelvin

R=universal gas constant

The current generated by the passive transport mechanisms is therefore described by the following equation:

$$J_p = J_d + J_l = -D\left(\nabla C + \frac{ZCF}{RT}\nabla\phi\right) \quad (4)$$

The ions pass from one side of the membrane to the other trying to reach the equilibrium of concentration between the outside and inside of the cell. The phenomenon leads to a potential difference which, in turn, generates a passage of charges. This mechanism continues until a dynamic equilibrium is reached so until the Fick force equals that of Ohm and the current J_p reported in equation (4) is equal to 0.

Passive transport alone is not sufficient to correctly describe the events that occur at level of the cell membrane. In fact, the previously described process would lead to a variation of the concentrations of the ions which would move according to the law (4). Experimentally it has been noted that the concentrations remain instead constant. This is due to active transport. That type of transport is called "active" because it requires energy consumption to be completed. Indeed, differently from the passive transport that is done without energy usage, the active transport consumes ATP. In particular, sodium-potassium pumps are present in the cell membrane and use ATP to move sodium ions outside and potassium ions inside according to constant and well-defined ratios. For each molecule of ATP, 3 sodium ions are pushed into the extracellular environment and 2 potassium ions enter the cell. The cell membrane can be represented through a parallel conductance model (Figure 4). In the figure I(K), I(Na), I(Cl) indicate the currents referred to potassium, sodium and chlorine ions. For each ion a conductance and a generator are inserted which represent the potential that would be reached if only the ion itself would be present. The effect of the calcium ion is neglected since it has very low concentrations. The potential difference V_m between the outside and inside of the cell can be calculated using the laws of electrotechnics and it is:

$$V_m = \frac{g(K)V(K) + g(Na)V(Na) + g(Cl)V(Cl)}{g(K) + g(Na) + g(Cl)} \quad (5)$$

From this equation Goldman provides a pragmatic formula for calculating the membrane potential:

$$V_m = \frac{RT}{F}\ln\frac{[K,external] + \frac{P(Na)}{P(K)}[Na,external]}{[K,internal] + \frac{P(Na)}{P(K)}[Na,internal]} \quad (6)$$

[]=internal or external concentration of each ion

P()=permeability coefficient of each ion

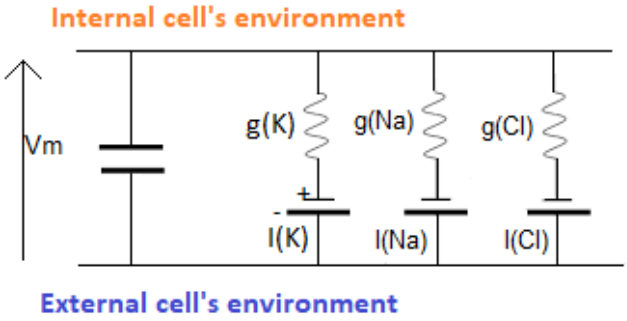

Figure 4 Parallel conductance model representing the cell membrane in relation to the electrical effects produced by the movement of potassium (K), sodium (Na) and chlorine (Cl) ions. I(K), I(Na), I(Cl) indicate the currents referred to potassium, sodium and chlorine ions. For each ion a conductance (g(K), g(Na), g(Cl)) and a generator are inserted which represent the potential that would be reached if only the ion itself were present. V_m indicates the potential difference between the outside and inside of the cell.

By applying equation (6) the potential difference characterizing the cell membrane, called resting potential, is calculated. The value of this potential difference, also in agreement with the empirical results, is approximately -90mV. Since the potential is negative, the cell is said to be polarized at resting condition.

Starting from this initial condition, the cell can vary its polarity. In fact, if stimulated by an electrical signal or if subjected to a chemical stimulus, the value of the potential difference can change from negative to positive. In this case, the cell is said to be depolarized. A positive electric potential difference can be measured across the membrane, between the extracellular space and the intracellular environment. The mechanisms underlying this phenomenon can be better explained by looking at Figure 5. The potential, initially, is equal to about -90mV, as previously reported, until, in the presence of the right stimulus, the opening of the sodium channels located in the membrane takes place. The positive sodium ions begin to enter the cell, producing an increase in the concentration of Na+ inside the cell itself, and a decrease outside it. Therefore, using the Goldman equation (6) it is easy to understand how the potential difference increases. The variation of the potential is represented in phase 0 and it has a very rapid increase. In phase 1 the peak of the potential is reached, of approximatively 20mV which subsequently begins to decrease due to the opening of the potassium channels. Indeed, the entry of Na+ ions give to the cell an increasingly positive nature from the point of view of the charges present. Then, the opening of potassium channels leads to the release of K+ ions. Since K+ ions are positive ions, when present inside the cell they give to the intracellular environment a positive nature. With the release of K+

ions, the positivity of the intracellular environment decreases, and a further depolarization is not possible. However, when the potassium channels open, the potential does not drop suddenly because the calcium channels open too. The Ca2+ ions cross the membrane and make the cell positive, counteracting the effect of the opening of the potassium channels. In phase 2, a condition of dynamic equilibrium is reached between the outgoing and incoming charges. The cell is still polarized but there are no significant changes in the action potential which morphologically describes a plateau. Therefore, in the graphical representation, the action potential is represented as an almost stationary path. At some point, the sodium channels close completely and the incoming Ca2+ ions are no longer able to counteract the effect of the outgoing K+ ions. The inside of the cell becomes increasingly negative and the potential difference decreases (phase 3). As can be seen in Figure 5, during phase 3, the potential follows a declining curve with a large negative slope. Subsequently, there is progressive repolarization of the cell until the return to the initial condition in which the potential re-establishes itself at about -90mV and describes a constant stretch (phase 4). To prevent the cell from being stimulated before it is completely depolarized, there is a refractory period between phase 3 and phase 4. In the refractory period, even if a stimulus reaches the cell, the action potential is not generated. Thus, during that period the cell can not be stimulated. The phenomenon that occurs between phase 0 and phase 4 is called action ion potential and has a duration in the order of milliseconds (ms).

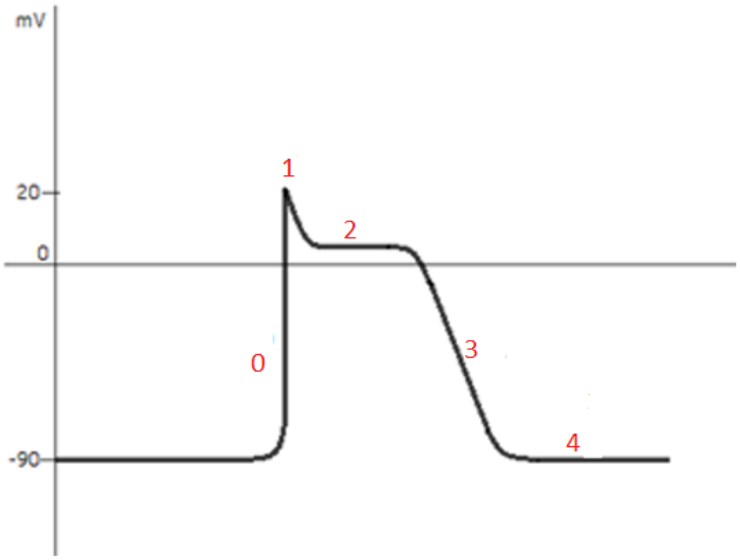

Figure 5 Ventricular cell's action potential (mV)

1.1.3 The conduction system and the heart circle

The action potential, at the cellular level, makes possible electrical activity. Indeed, the action potential travels from one cell to the other one which depolarizes and repolarizes, causing a current flow from one cardiomyocyte to the other. From the viewpoint of the entire heart, the current flow can be studied highlighting the points from which it is generated and how it propagates. The area of generation is called the sinus node and it is located in the left atrium, at the level of the opening of the superior vena cava in the right atrium. It is made up of a set of particular cells, known as nodal cells [1]. It is a sort of natural pacemaker from which pulses are born with a frequency, in resting conditions, of around 60-100bpm [4]. Subsequently, the stimuli spread to the atrial myocardium and the result is the depolarization of the atria. The impulse then reaches the atrioventricular node. The atrioventricular node is located in the atrioventricular septum and acts as a center for the reorganization and amplification of the impulse. In the meantime, the atria repolarize and the electrical signal continues along a fibrous structure that is able to conduct the electrical impulse and originates from the atrioventricular node. Moreover, that fibrous structure crosses the fibrous skeleton and it is called the bundle of His. To reach the ventricles, the bundle divides into 2 branches: right and left. The excitation is finally transmitted to all the muscles of the heart by means of the Purkinje cells. The ventricles also depolarize and then repolarize at the end of excitation [1]. The conduction system of the heart is schematized in Figure 6.

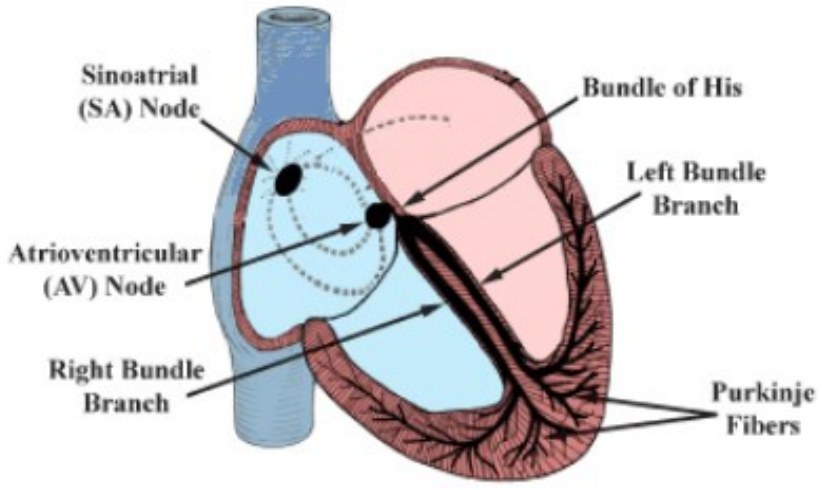

Figure 6 Conduction system of the heart [5]

Some parameters such as heart rate, contraction intensity or cardiac output are controlled by the peripheral nervous system. However, the heart has an autonomous ability to contract [1].

The previously described electrical conduction events are the basis of cardiac contraction which determine the functioning of the myocardium in the role of "pump". In this regard, the heart fills with blood and ejects it throughout the body in a cyclical process. In this context it is necessary to define the phenomena of systole and diastole. Systole refers to the contraction aimed to push blood out of the atrium or ventricle. Diastole is the filling phase in which the atrial or ventricular chambers dilate. As far as the cardiac cycle is concerned, initially the blood coming from the vena cava fills the right atrium. The blood coming from the pulmonary vein fills the left atrium. At this point the atria are in diastole. The tricuspid and bicuspid valves open and there is a passive filling of the ventricles. The aortic and pulmonary valves are closed. Subsequently, the electrical impulse generated by the sinus node and propagating to the atrial myocardium, causes the contraction of the atrial. The contraction of the atrial muscles leads the atria to be in systole that causes the pumping of blood into the ventricles. Once the filling is completed, the tendon cords keep the atrioventricular valves tightly closed, preventing the blood flow from going back. The lobbies relax. At this point the ventricles contract triggered by the electrical impulse that from the atrioventricular node reaches all the ventricular myocardium through the Purkinje fibres. So the ventriculi enter in systolic phase. The opening of the semilunar valves allow blood to be pushed into the pulmonary and aortic arteries. Subsequently, the aortic and pulmonary valves close. A small part of the blood flow tries to flow back into the ventricles but, as the valves are closed, the blood is diverted to the coronary arteries which supply the heart. The ventricles relax and the cycle can begin again [1].

As previously stated, actin and myosin are characteristic elements of the myocardium and are grouped into sarcomeres. Within these structures, the A band, the I band, the M line and the Z disks are distinguished. The contraction of the cardiac muscle is possible thanks to the sliding of the actin filaments of the I band on those of myosin of the A band, making the Z disks to near each together as shown in Figure 7. More specifically, the sliding of the thin filaments of actin on the thick ones of myosin is linked to the action of calcium present in the cisternae adjacent to the T tubules. In fact, following the

electrical stimulation of the myocardial cells, the action potentials travel in the tubules T and cisternae release Ca^{2+}. Tropomyosin molecules, associated with troponin, a protein that binds calcium, are present in the thin filaments. Therefore, Ca^{2+} ions bind to troponin which cause tropomyosin to move to show the active sites of actin. Myosin activates and elongates its head and places it in the active sites of actin creating a bridge. The so-called power stroke is carried out. Thus, myosin produces the movement of actin: the thin filaments are pulled by the thicker ones towards the M line. Myosin head activation and power stroke are processes that require energy expenditure. Subsequently, the myosin detaches from the actin, the calcium ions are reuptake inside the terminal cisternae through the calsequestrins and the muscle fibres return to the initial condition of relaxation [1].

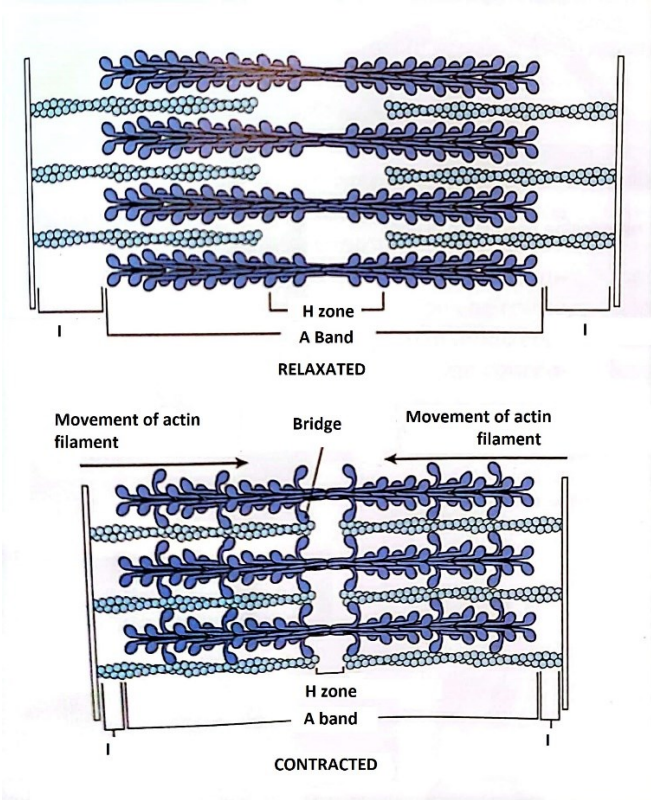

Figure 7 Contraction mechanism of the cardiac muscle fibre [6]

1.1.4 Arrhythmias and anomalies of the electrical activity

An alteration of the normal heart rhythm (between 60bpm and 100bpm in resting state) is called arrhythmia. The arrhythmias can be divided into 2 main categories:

- tachycardia, if the heart rate increases over 100bpm in resting conditions;
- bradycardia, if the heart rate decreases over 60bpm or, most definitely, under 40bpm in resting conditions.

The main causes of tachycardia are the stimulation of the cardiac muscle by the sympathetic system, as a consequence for example of a shock state, some particular conditions like fever [4], dehydration, heart failure, pulmonary embolism, hyperthyroidism and the presence of heart pathologies such as the postural orthostatic tachycardia syndrome and myocarditis. The tachycardia can be of different types, among which 2 main branches are distinguishable: the supraventricular tachycardia and the ventricular tachycardia. In the supraventricular tachycardia, the areas above the ventricles contract with an accelerated frequency, causing the increasing of the heart rate. It is generally less dangerous than the ventricular one and in most of the cases it is not subject to treatments. The ventricular tachycardia, instead, affects the ventricles. It is generally characterized by the presence of 3 or more ventricular beats that occur in succession, originating independently from the sinus node. It is considered as a serious form of arrhythmia as it can degenerate and lead to death. The tachycardias include atrial fibrillation, ventricular fibrillation and atrial flutter. During the fibrillations, the conduction of the cardiac electrical impulse is abnormal and leads a contraction, atrial or ventricular, completely disorganized and irregular. In this field, the ventricular fibrillation is one of the leading causes of sudden cardiac death [7]. During the atrial flutter, the abnormal contraction of the atria is regular but not perfectly followed by ventricular contraction. Indeed, the atrial contraction is too rapid, reaching between 200bmp and 350bpm, leading generally to 3 atrial contractions before 1 ventricular contraction [4].

The bradycardia can be a result of heart pathologies such as ischemic heart disease [7]. Other possible causes are the stimulation the vagus nerves or a non-pathological condition common in athletes [4]. The bradycardia can be classified according to its source in sinus bradycardia (if the decreasing heart rate is caused by a malfunction in the sinus node) and atrio-ventricular bradycardia (if the decreasing heart rate is caused

by a malfunction in the atrio-ventricular node). The phenomenon of atrio-ventricular node malfunction is referred to atrio-ventricular blocks condition. It is characterized by the partial or complete interruption of the transmission of the electrical impulse from the atria to the ventricles. The severity of the interruption can vary from the atrio-ventricular block of the first order (less sever one because the conduction is slowed but no missing beat is present) to the atrio-ventricular block of the third order (most sever one because the transmission of the electrical impulse is totally interrupted) [7].

Another phenomenon associated with anomalies of the heart electrical activity is the long QT syndrome. It is a disorder that occurs when the ventricular cells repolarize later than in a normal healthy state resulting in a protract depolarization of ventriculi. The QT interval is a parameter that reflects the period or depolarization and depolarization of the ventriculi [4] and it will be indagated later. The long QT syndrome is detected when the QT interval exceeds the normal values (normal values reported as less than 450ms in men and less than 470ms in women) [7]. The long QT syndrome has been reported as a sever heart pathology since it is related to the risk of developing arrhythmias, tachycardia and ventricular fibrillation. The long QT syndrome can be a inherited disorder or it can be acquired. For what concerns the hereditary form, it is a phenomenon that occurs in relation to mutations of sodium or potassium channel genes. The acquired form is more spread and can be triggered by a multitude of factors. Some examples of these factors are conditions like hypomagnesemia, hypokalemia and hypocalcemia and the intake of antiarrhythmic drugs or some antibiotics [4].

1.1.5 Circadian rhythm influencing the electrical activity of the heart

The expression biological rhythm indicates a cyclic change of the human body functions, processes or chemicals. According to the periodicity, 3 types of biological rhythms can be distinguished: circadian rhythms characterized by a period of 24h, ultradian rhythms with a period of some hours, minutes or seconds but anyway much shorter day 24h and infradian rhythms with a period larger than 24 hours, thus of some days, months or even more. The circadian ones are the most reported in literature since they are the most common in physiology. The reason why processes follow a circadian rhythm is found in the fact that they have to adapt to the different demands of human body during the different hours of night and day [8].

Circadian rhythms can be described through a mathematical technique based on a cosine fitting. According to that methodology, the data that are thought to follow a circadian rhythm are fitted through a cosine function using the least squares approach. Subsequently 3 parameters are extracted (Figure 8):

-the so-called midline estimating statistic of rhythm (MESOR) which is the half value between the maximum and the minimum of the cosine function;

-the amplitude that is the measure of one half of the magnitude of the cosine;

-the acrophase that is a measure of the time needed to reach the maximum of the cosine function.

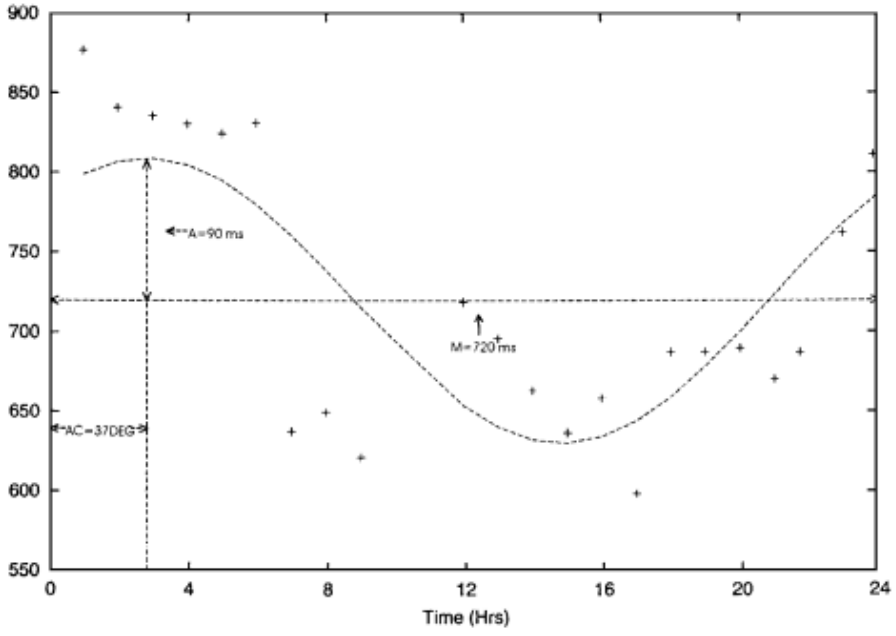

Figure 8 Example of cosine function fitting data following a circadian rhythm, where A=amplitude; AC=acrophase; M=MESOR [8]

Ones extracted, these parameters allow to characterize the circadian rhythm. Moreover they allow to compare different data that follow a circadian rhythm [8].

For what concerns the heart, it has been shown that many activities related to it are characterized by a circadian rhythm. One example is the heart rate. Indeed it has been demonstrated that the heart rate increases just after the awakening or around it and reaches the acrophase between the 10:00 and 12:00. Then the heart rate registers a decreasing. In some studies, a second peak is reported in the afternoon and in others a continuous general decrease is recorded. Anyway, it is generally recognized that the heart rate reaches its lowest values during night with a minimum between 3:00 and 5:00 or a couple of hours before awakening [8].

Even atrioventricular conduction and arrhythmias may have a circadian periodicity. Indeed, it has been reported that arrhythmias are characterized in general by a peak in terms of frequency in the morning and a depression during the sleeping hours. These results have been found both in terms of ventricular and atrial arrhythmias even if the atrial ones have been less studied in these terms [8], [9], [10], [11].

More in details, atrial flutter, atrial fibrillation and atrial premature beats exhibit a peak between 6:00 and 12:00. Atrial fibrillation is characterized by a major peak between 23:00 and 6:00 and a minor peak between 14:00 and 16:00. Ventricular premature beats show a maximum between 6:00 and 12:00, ventricular tachycardia between 10:00 and 18:00 and ventricular fibrillation has a major peak between 7:00 and 11:00 and a minor peak between 16:00 and 20:00 [11].

In this context it is clear how the electrical activity of the heart is influenced by circadian rhythm. Indeed an increasing heart rate needs to be supported by an increasing frequency in depolarization/repolarization events. The atrioventricular conduction is, by definition, an electrical event of the heart and, as reported before, the arrythmias are strongly associated with the heart's electrical behaviour.

To deeply understand the base of the circadian nature of the heart's electrical activity, some research concentrated on ion channels' gene expression. As explained before, the role of the ion channels is essential to keep a difference of potential between the external and internal environments of the heart's cells and even to allow the generation of action potential. In particular, it has been studied the transcription of ion channels (process in the field of gene expression, on the basis of the ion channels' synthesis) in

mice. It has been shown that the transcription process of ion channels follows a circadian rhythm [12]. Moreover, another study, conducted on mice too, underlined the circadian nature of potassium' channel gene expression [13]. That conclusions suggest that the circadian gene expression of ion channels may be related to circadian cardiac arrhythmogenesis even in humans.

Moreover, it has been reported that some characteristic elements of the cardiac electric behaviour exhibit a circadian rhythm such as the sinoatrial and atrioventricular nodes and the ventricular refractory period. Indeed, it has been reported that sinoatrial recovery time has a circadian behaviour with the shortest period at 7:00. The atrioventricular circadian rhythm has been reported to have the acrophase between 24:00 and 7:00 [14]. The refractory period of the ventriculi has been studied both with invasive and non-invasive techniques, thus using both intracardiac catheters and telemonitoring implanted pacemakers. In both cases, it has been found that the refractory period has a minimum in terms of duration during the day and a peak during night hours [11].

1.2 Electrocardiographic signal

1.2.1 Origin, definition, nomenclature and general properties

The electrocardiography is a non-invasive technique which origins date back to 1893. This technique is carried out in the field of the diagnostic analysis of the state of health of the human heart. It is done through a spatio-temporal recording of the pattern of action potentials of cardiac cells. As result from the electrocardiography, it is obtained a graph that represents the electrical activity of the myocardium associated with the processes of depolarization and repolarization of the cells. The resulting graph is known as electrocardiogram (ECG) [15].

The ECG measures the cell's electrical activity through conducting elements placed on the subject's skin called electrodes. They will be described more in details later.

The duration of the recording is not standard, but the ECG acquisition time can vary from a few minutes to days as in the case of the use of a particular instrument called Holter.

The brief ECG generally lasts for 10s. It is an ambulatory diagnostic examination that is done with no portable instrument and in controlled conditions that favour the recording. Thus, the subject is asked to not move and, in some cases, to keep the breath. However, since the recording covers only a small part of the day of the subject and it is done in particular conditions, represents a limited view on the subject' heart conditions.

The Holter takes is name from its inventor, N. J. Holter, who invented the Holter in 1962. It is a portable instrument, equipped with batteries, that allows the continuous acquisition and memorizing of ECG signal during 24 hours or even more, when the subjects performs daily activities of normal life. The analysis of the ECG is then performed offline. Since the acquisition covers at least 1 entire day, it is indicated for a more detailed examination of the heart' electrical behaviour. In particular it is used to detect some cardiac pathologies such as arrhythmias [16]. Indeed, as previously reported, the heart behaviour changes according to needs of the subject. Thus, it depends on the time of the day and on the activity the subject is performing. Anyway, one intrinsic limitation of that type of exam consists in the fact that since the recoding is acquired during the normal life of the subject, in non-controlled conditions, it is more prone to movement artifacts and more affected by noise. Therefore, the subsequent analysis of the ECG signal may be more difficult and may require a more careful processing of the data. Moreover, even if the technological progress tries to lead to

more and more comfortable Holter instruments, the presence of the instrumentation for the entire day may make the Holter exam more annoying than the ECG obtained in 10s.

1.2.2 Parameters deductible from electrocardiography

For each cardiac cycle, the ECG in the absence of pathologies, is characterized by a distinctive shape and amplitude. Concerning the shape, firstly it is necessary to consider that the ECG is a graph, as previously stated. It is possible to identify a line representing the zero that is defined as isoelectric. With respect to this line there are fluctuations in the electrocardiographic tracing. Thus, the amplitude of the ECG signal taken non-invasively, respect to the isoelectric, varies in the order of mV [17]. Moreover, from the point of view of the morphology of the ECG, 3 fundamental sections are macroscopically distinguishable as represented in Figure 9:

- P wave. Denotes atrial depolarization and in terms of amplitude, the P wave is the smallest of the 3;
- QRS complex. Represents repolarization of the atria and ventricular depolarization. It is composed of 2 negative waves, Q and S, and a positive R wave;
- T wave. It is characterized by a large and low amplitude "hump". It Indicates ventricular repolarization which is rapid and begins at the apex and then expands towards the base.

In the frequency range, P and T waves are low frequency, while the QRS complex is characterized by a rapid temporal variation. The periods of time that elapse between one wave and another also need to be carefully observed. In particular, the PR interval, the PR segment, the QT interval, and the ST segment must be considered. The PR interval goes from the beginning of the P wave to the beginning of the QRS complex and represents the time required for the atria to completely depolarize and the electrical impulse to reach the ventricles. The PR segment is contained within the PR interval, which is the distance between the end of the P wave and the beginning of the QRS complex. The QT interval starts at the beginning of the Q wave and ends at the end of the T wave. It is interpreted as the time required for the ventricles to fully depolarize and repolarize. Finally, the ST segment is the part of the electrocardiographic tracing contained in the QT interval, between the conclusion of the S wave and the beginning of the T wave. Morphologically, the PR and ST segments have a constant trend since they represent no variation of potential difference and are aligned with the isoelectric. Another interval that has been haighlited in literature is the TQ interval (TQI) which is identified as the time between the end of the T wave of one beat and the start of the QRS complex of the subsequent beat. It is also called diastolic interval [18].

When recording the ECG signal with at least 10 electrodes, it can be calculated the dispersion of the QT interval that is a parameter that reflects the heterogenicity of the vetricular repolarization process [11].

Another paramter related to repolarization istability that can be obtained through the ECG signal is the Short-term variability of the QT-interval (STV-QT). It represents the variability of 30 consecutive QT segments [19].

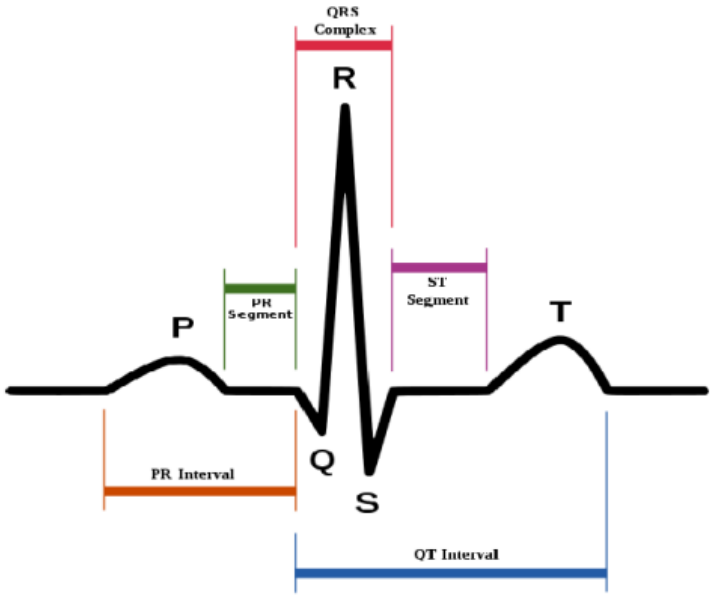

Figure 9 ECG morphology [5]

1.2.3 Electrocardiographic machine and electrocardiographic Holter

The instrument used to perform electrocardiography for 10s is the electrocardiograph. In contemporary times, due to the technological improvement, 2 types of electrocardiographs are distinguishable: digital electrocardiographs and analogical electrocardiographs that are becoming progressively obsolete. Because of that reason, this thesis will concentrate in describing the analogical electrocardiographs. At a macroscopic level, they consist of a set of electronic components that record the cardiac signal acquired by means of the electrodes. These components can be divided into functional blocks as shown in Figure 10. Each block has its own function and characteristics:

-Block 1: patient cable that makes the connection between the patient and the electrodes. It is a flexible, shielded and preferably not very long cable so that it is less sensitive to electromagnetic interference;

-Block 2: system that protects the electronics from overvoltage. There is one system of that type for each electrode. The basic elements that make it up are a gas discharge lamp, a low-pass filter and 2 polarized diodes. If the voltages are too high, the circuit becomes at minimum impedance and the current discharges through the lamp to earth. Otherwise, the lamp does not become conductive and the current continues. Moreover, the filter prevents high frequency signals from entering the circuit. If the current is not in the correct range, the 2 diodes start conducting, blocking its passage. Otherwise, the current continues and meets an amplifier downstream of the circuit;

-Block 3: selector and branch box. It is formed by a group of resistances with the task of making the selection of the various derivations possible. The input data are the signals coming from the electrodes, while the leads are present in the output. A lead can be defined as the difference of potential between an electrode and another one;

-Block 4: amplifiers and filters. Differential amplifiers boost the signal to be able to drive all the remaining electronics. They ensure high and stable gain and a high common-mode rejection ratio. The filters minimize the effects of noise such as those caused by muscle tremors;

-Block 5: analogical/digital and digital/ analogical converters;

-Block 6: optical and electromagnetic coupler. This element has a fundamental importance for patient safety. Indeed, it allows a non-direct connection between the

part of the electrocardiograph referred to the subject and the part referred to the ground. In the optical coupler, a LED diode emits a light proportional to the heart signal. The light is captured by another diode and is transformed into current. Any overvoltage from the side referred to earth cannot be transmitted to the part connected to the patient. The system is powered by batteries. The electromagnetic coupler transfers the power supply and setting information from the digital elements to the analogical part. It consists of an oscillator, a rectifier and a transformer;

-Block 7: graphical interface and related tools. There are items such as computers and monitors. Their function is to allow the operator to view and analyse the ECG trace. Moreover, they provide information to the electrocardiograph such as, for example, which derivation the operator wants to observe;

-Block 8: electrode sensor. It ensures that electrodes are well attached to the patient. A feedback amplifier generates a signal that oscillates with a frequency that depends on the input impedance. A comparator compares this frequency with a reference one and, if the values do not match, produces an alarm signal;

-Block 9: right leg driving circuit. In the presence of an electromagnetic field generated by alternating current, the subject behaves like a sort of antenna. The resulting effect is a common-mode disturbance to the electrodes. Therefore the circuit allows to eliminate this disturbance. The Holter instrumentation is very similar to the electrocardiograph because it is based on the same principle to record the ECG signal. Indeed it uses the electrodes to record the difference of potential associated to the heart electrical events.

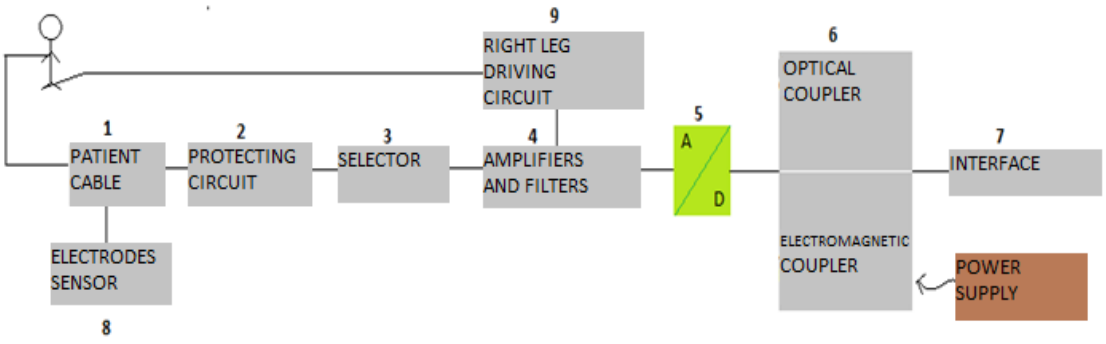

Figure 10 Electrocardiograph block diagram

However, the Holter instrumentation ensures the continuous recording for prolongated times and allows the subject to perform normal activities during the day when wearing the Holter. Indeed, a minor electrodes number is generally present (the electrocardiograph generally is used with 10 electrodes). Thus between 3 and 8 leads are usually used for the Holter recording (for the electrocardiograph the number of leads is up to 12). Anyway, even Holter instruments that are equipped for a 12 leads recording exists. The power supply is ensured by the presence of batteries, so differently from the electrocardiograph the external power supply is never present. Another essential difference between Holter instrumentation and electrocardiograph is the presence of a storage system with retrieval capability, thus memorizing the ECG signal until its remote analysis is made by an operator. From the global view point the Holter appears like a rigid small box at which cables connected to the electrodes are connected [20].

1.2.4 Electrodes and leads

In the measurement chain, the electrodes represent the interface elements that transduce the ionic currents generated by the cardiac cells. The input data to the electronic component of the electrocardiograph or to the Holter is always a potential difference (ddp) acquired through the electrodes. In this context, bipolar and unipolar electrodes can be distinguished. For bipolar electrodes, the potential difference is measured between 2 separate electrodes. In the case of unipolar electrodes, the potential of a single electrode is calculated with respect to a reference potential. In general, electrodes consist of a metal part that is kept in contact with the patient through various methodologies. Depending on the chosen method there are: button electrodes using an adhesive disk; suction electrodes in which a sucker is used; electrodes with a clamp system. Usually, the metal part is made up of silver plates. The silver is placed in contact with silver chloride and immersed in a gel rich in chlorine ions. An oxidation-reduction reaction takes place in the electrode with a consequent release of electrons which travel towards the electrocardiograph or the Holter.

As regards the efficiency of the measurement, it is necessary to evaluate the contact impedance between the electrodes and the skin. In fact, 3 layers made up the skin: epidermis, dermis and subcutaneous. Unlike the other 2, the epidermis is not vascularized and its most superficial portion, called stratum corneum, is made up of dead cells. Therefore, it acts as a good insulator whose effect must be minimized. Generally, acetone or sandpaper are used to thin the thickness of the stratum corneum. During the analysis, the electrodes must remain firmly on the skin and fixed in their position. Otherwise, the contact impedance varies and motion artifacts are generated. This represents an issue in particular with regard to the Holter type of exam, since the electrodes must be kept in place for long times and while the subject is moving.

In the field of the electrocardiography that lasts for 10s, the electrodes are placed in a standardized manner. For the common electrocardiography at 12 leads, a total of 10 electrodes are used. 4 of them are placed at the level of the limbs, 2 on the legs and 2 on the arms, identified as RA (right arm), LA (left arm), RL (right leg), LL (left leg). Through the use of these 4 electrodes, are computed the so called “Eindhoven leads” and “augmented leads”. In the Einthoven leads the following differences of potential are computed:

-D1, calculated between RA and LA;

-D2, calculated between RA and LL;

-D3, calculated between LA and LL.

D1, D2 and D3 make up the Einthoven triangle observable in Figure 11.

In the augmented leads the following potentials are computed:

-aVR, defined as the absolute potential of RA;

-aVL, defined as the absolute potential of LA;

-aVF, defined as the absolute potential of LL.

The other 6 electrodes represent the “precordial leads” that are named V1, V2, V3, V4, V5, V6 and are defined in the following manner:

-V1 in the right parasternal fourth intercostal space;

-V2 in the left parasternal fourth intercostal space;

-V4 in the fifth intercostal space on the left midclavicular;

-V3 in the space between V2 and V4;

-V5 in the fifth intercostal space on the left anterior axillary;

-V6 in the fifth intercostal space on the left mid-axillary.

For what concerns the Holter, instead, there is not a unique way to place the electrodes. So, their location is not identified following a standardized protocol. Anyway, the guidelines followed for the short-term electrocardiogram can be taken as reference even in case of Holter exam.

Since generally in the Holter exams 3 leads are used, the protocol for the positioning of the electrodes for the short ECG in case of 3 leads can be followed. The protocol is named “three pseudo-orthogonal lead configurations”. Historically it was invented by E. Frank in 1954 [21] and establishes a standard way through which the electrodes must

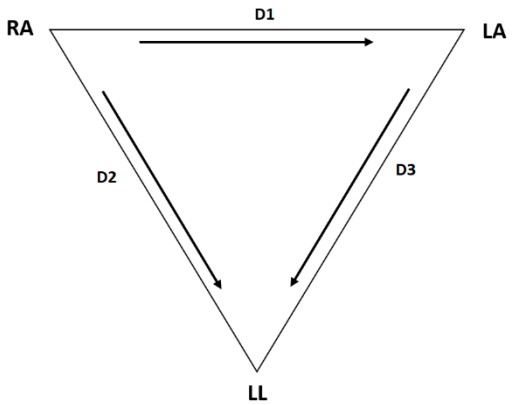

Figure 11 Eindhoven triangle

be placed in order to allow the extraction of ECG from 3 leads that are mutually orthogonal. Indeed these 3 leads can be visually represented through 3 mutually orthogonal axes that cross the body in vertical (Y), transversal (X), and sagittal directions (Z). A total of 7 electrodes are used named I, E, C, A, M, F, and H (Figure 12).

The position of the 7 electrodes is specified as follows:

-E electrode placed in the middle of the chest, in the frontal plane;

-M electrode placed in the opposite way respect to E electrode on the back;

-I electrode placed in the right central axillary line;

-A electrode placed in the left central axillary line;

-C electrode placed in the middle between A electrode and E electrode;

-F electrode placed on the left leg;

-H electrode on the neck [22].

Then, the potentials of X (P_x), Y (P_y) and Z (P_z) leads are extracted as follows [22]:

$$P_X = 0.610A + 0.171C - 0.781I \quad (7)$$

$$P_Y = 0.655F + 0.345M - 1.000H \quad (8)$$

$$P_Z = 0.133A + 0.736M - 0.264\,I - 0.374E - 0.231C \quad (9)$$

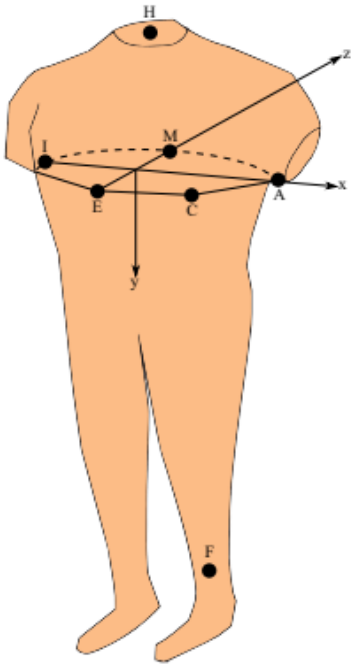

Figure 12 Electrodes' positioning according to pseudo-orthogonal lead configurations [22]

1.2.5 Evidence of circadian rhythm on electrocardiographic signal

As reported before, the heart electrical activity is characterized by a circadian rhythm from many points of view. The heart electric behaviour is measured and recorded by the EEG. Thus, it is expectable that circadian changes in electrical activity and in arrhythmias are reflected by circadian changes in the electrocardiographic parameters. Indeed, even for some electrocardiographic parameters it is possible to talk about circadian changes: P wave area and duration, PR interval, QRS complex duration. All these parameters have been studied in literature and show an increasing during the night, reaching a peak between 24:00 and 6:00. Then they start to decrease, with a minimum between 10.00 and 12.00. These results reflect the fact that probably depolarization and repolarization events follow a circadian rhythm to adapt to daily needs [8]. Moreover, an increasing in P wave duration, PR interval and QRS complex duration during night is understandable since, as reported before, the heart rate decreases during nocturnal hours. The decreasing of the electrocardiographic parameters, on the other hand, is related to the increasing of heart rate during daytime.

Moreover, a circadian path has been observed even in the context of the QT interval duration. It has been shown an increasing of the QT interval between 6:00 and 9:00 in healthy subjects. This peak is followed by a decreasing reaching lowest values during night [23].

Furthermore, even the dispersion of the QT intervals has circadian features in subjects with heart diseases. It has been shown to be shorter during night than during daytime in patients with coronary artery disease and suffering of heart failure [11]. Healthy subjects show a circadian rhythm characterizing the dispersion of the QT intervals too, with some differences according to the gender. Indeed, the dispersion of QT intervals has been reported to have a peak just after awakening. That result is understandable thinking about the fact that QT interval has been related to the risk of developing arrhythmias and many arrhythmias are more common just after waking up. Studies performed on males, generally, report an higher variations of the dispersion than those done on females [24]. In the same field, the STV-QT has been reported to follow a circadian rhythm both in subjects suffering from arrhythmias and in healthy ones with 2 peaks at 8:00 and 18:00 [19]. A more detailed report of the circadian rhythm in the field of P wave, T wave and QRS complex will be given later.

1.3 Electrocardiographic alternans

1.3.1 Origin, definition and modalities of manifestation

The electrocardiographic alternans is a beat-to-beat variation according to an ABAB scheme of the morphology, the polarity or the amplitude of the P wave (PWA), QRS complex (QRSA) or T wave (TWA) [25].

TWA was, historically, the first alternans to be studied. Thus, it is nowadays the most investigated in literature [25]. TWA has been seen to be present, particularly, with an increased heart rate. For that reason, it is usually studied by means of an exercise ECG, causing a controlled increase in heart rate. Usually, a heart rate between 95bpm and 110bpm is reached and kept from 1min up to 3min. Anyway, frequencies higher than 110bpm are undesirable. In this context it has been observed that the TWA increases after a certain frequency threshold according to a monotonic function. Moreover it has been seen that after TWA has been caused, it is a stable phenomenon [18].

Anyway, TWA has been identified even during exams using Holter instrumentation. Indeed Holter has been underlined as a proper technique to detect TWA over a larger period of time (generally minimum 24h) than exercise ECG (few minutes) [26].

At the physiological level, TWA is the consequence of a non-homogeneous repolarization from both the temporal and spatial point of view, due to the alternation from beat to beat of the duration of the action potential of the cardiac cells. The origins of this phenomenon are not uniquely identified and there is not a fully recognized theory. For example, TWA may be caused by the presence of groups of ventricle myocytes that have longer refractory periods, thus being depolarized each 2 beats (instead of at every beat). Anyway, this theory has been overcome because it seems to be not in line with evidence. Indeed, following this theory TWA would occur dependently on QRSA. So, TWA would be related to QRSA of the same order or even greater. That association has been disproved [18].

Among the most accredited hypotheses, an interpretation called calcium cycling hypothesis has been formulated. According to it, TWA would occur when the cell is no longer able to maintain the balance between calcium released and reuptake into the sarcoplasmic reticulum. Knowing the role that calcium has inside the cells and the basis of mechanisms underlying electrical conduction at the biological level, this theory could provide a valid explanation to the TWA [18].

Another accredited theory is called action potential duration (ADP) restitution hypothesis. According to it, there is a relationship between the TQI, and the action potential duration of ventricle's myocytes of the subsequent beat. Thus, a decreasing in one TQI would be followed by a decreasing even in the ADP. But a decreasing in ADP would be followed by an increasing in TQI. Then an increasing in TQI would be followed by an increasing in ADP. Subsequently there would be a decreasing in TQI and so on. The relationship between TQI and ADP can be represented through a graph. The slope of the curve describing that relationship may be used to identify the presence of TWA. Indeed, TWA would be present when the slope of the curve is higher than 1. Anyway, even that theory has been at the same time discredited and supported [18].

Moreover, it has been suggested that some parts of the ventricle are more prone to cause TWA than other. Indeed myocytes that are located in more external zones of the heart seem to be more incline to TWA than the ones in more internal areas [18]. However, more studies are needed and the causes of TWA still remain uncertain.

From the viewpoint of the singular myocyte, 2 types of TWA are reported in literature:

-concordant TWA. It is characterized by an in phase alternans of the myocytes (all myocytes altern in the same way for example according to a short-long-short path);

-discordant TWA. It is characterized by an out of phase alternans of the myocytes (for example a group of myocytes alternating according to a short-long-short path and another according to a long-short-long path) [18].

From the point of view of amplitude, the TWA can be divided into 2 categories:

-macroscopic and visible. It was reported in 1909 by Herring and Lewis [27] and is considered a rare condition [18];

-microscopic and not visible to the naked eye. Historically it was highlighted for the first time in 1980 [26]. Thus, to show microvolt changes of the ECG, the electrocardiographic signal needs to be processed in order to be able to detect a phenomenon that happens at microscopic level.

Among the 3 types of alternans (PWA, QRSA, TWA) the less studied is the PWA. Indeed, the origins and causes beyond that phenomena are not described in literature. This lack may suggest a new field of research, in particular in relation to the reported association between PWA and some heart issues that will be described in the following paragraph.

Even QRSA may be a heart-rate dependent phenomena and can be distinguished into microvolt and microvolt one. The visible QRSA may be caused by conduction problems concerning the His-Purkinje fibres. Some hypothesis relying on calcium cycling at cellular level have been proposed to explain QRSA too. Anyway these hypothesis seem to be less reliable than the ones regarding His-Purkinje fibres [28]. Another theory links the QRSA with the thickness of the left ventriculi. According to that theory, a high thickness of the ventriculi may lead to QRSA [29]. However, like in the case of TWA, the opinions regarding the origin of the alternations are in conflict and more studies are required [28].

Generally speaking, electrocardiographic alternans is considered as non-stationary phenomenon since it is characterized by variable duration and amplitude [30]. It is probability a channel dependent condition. Indeed, the electrocardiographic alternans may be detected in one lead but not in another. Thus, it is important to analyse it in all available channels [25].

1.3.2 Role

PWA has been showed to be probably associated to atrial fibrillation, being related to the electrical instability of the atria. P wave represents atria depolarization, thus it is understandable that PWA has been highlighted as a phenomenon that can indicate an increased propensity to develop atrial fibrillation [31]. Moreover PWA may be indicative of imminent atrial flutter [32]. This associations are limited since they are reported only as case reports. Anyway, they underline the necessity to increase knowledge regarding the PWA.

Even the QRSA has been associated with some pathologies like ventricular tachycardia and supraventricular tachycardia [29]. This associations seem to be plausible since the QRS complex represents the ventricular depolarization. QRSA has been seen in subjects with cardiomyopathies, both together with TWA and alone. When present with TWA, QRSA has been detected with a higher amplitude. Moreover QRSA, in cardiomyopathic subjects, indicates a higher risk of developing ventricular tachyarrhythmia when it is present without TWA [28].

For what concerns TWA, it has been shown that TWA can be related to electrical instability. Thus, it can induce heart to be more incline to develop ventricular arrhythmias being identified as a precursor of a wide range of arrhythmias. Some examples are polymorphic or monomorphic ventricular tachycardia and ventricular fibrillation [18]. The association between TWA and arrhythmias has been underlined both in subjects with heart with structural abnormalities and even in healthy hearts [27]. Moreover TWA has been associated with myocardial ischemia and long QT syndrome [18].

TWA has been highlighted as an important risk factor of sudden cardiac death. The sudden cardiac death is defined as the unexpected death of the subject due to cardiac causes. It develops in a complex and still unclear way, thus it is important to underline the possible associations with any phenomena such as TWA [18].

Thus, generally speaking, PWA, QRSA and TWA are indexes of several cardiac problems such as, in particular, arrhythmias and sudden cardiac death [25].

1.3.3 Algorithms and methods for automatic detection

The microvolt electrocardiographic alternans as said, is non-visible. Thus, it requires automatic techniques to be identified. Anyway only the Enhanced adaptive match filter (EAMF) method has been proposed in literature, to indagate all types of electrocardiographic alternans (PWA, QRSA and TWA) [25]. A modified version of that methodology was used in this thesis to analyse data and will be fully described in the following chapter. Apart from that method, no other technique is available for the detection of all 3 types of electrocardiographic alternans. TWA is instead, deeply studied and several methods have been proposed for its identification and quantification in an automatic way. Some of the most used methods are the following: adaptive-match-filter method (AMFM), modified-moving-average method (MMAM), fast-Fourier-transform spectral method (FFTSM), complex demodulation method (CDM) and Laplacian-likelihood-ratio method (LLRM) [33].

The adaptive-match-filter method (AMFM) is the precursor of EAMF, so it's very similar to it from the methodology viewpoint. Anyway, differently from EAMF, AMFM is used only for TWA. It is characterized by an excellent robustness to noise. Therefore, its use is appropriate even in presence of very noisy ECGs. First, in order to use the adaptive method, the ECG signal must be divided into windows of 128 beats. At this point, the method evaluates each window based on the stability of the heart rate and on good signal quality. To define the heart rate as stable, the standard deviation of the RR intervals must not exceed 10% of the average RR interval. For the quality of the signal, each beat is correlated with the median beat of the window under consideration. If the correlation coefficient is lower than a certain threshold (generally 0.85) then the beat is replaced. With too many beats replaced (typically 10%), the signal is not reputed to be of good quality. If the window is deemed suitable (i.e. both conditions of stable heart rhythm and sinus rhythm, not affected by ectopic beats or noisy), the TWA is analysed. The adaptive method filter is a Butterworth bidirectional filter of the 6^{th} order with a very narrow passband centred in the frequency of the TWA. The TWA frequency is half of the heart rate by definition. If there is TWA, as output there is a pseudo-sinusoidal signal whose amplitude is half the width of the TWA in μV and which has its maximums and minimums in correspondence with the ST segments or of the T wave. Otherwise, if there is no alternans phenomenon, the output signal is a constant, and the TWA is

considered equal to 0. If the signal quality and/or heart rate stability are not adequate, the window is rejected and the TWA cannot be studied [34].

MMAM, which works in time domain, is widely used since it is available on ECG machines that are present on the market such as Milwaukee, GE Medical and others [33]. For MMAM method application, it is necessary to pre-process the signal to obtain an ECG beat series without high frequency noise or arrythmias and to identify the end of QRS complex, T wave and ST segment for each beat. Then the ECG beat series is separated into 2 subseries: one constituted by even beats (A) and one constituted by odd beats (B). To do that, the signal can be divided in windows of desired duration. Anyway in [35] windows of 15s are considered. At this point, the modified moving average beats of each subseries is calculated. Thus, each modified moving average beats subseries starts with the first even or odd beat, respectively for A and B subseries. For example, considering A subseries, at the starting point, the current modified moving average beat is the first even beat. If second even beat of A is greater than the current modified moving average beat, the second modified moving average computed beat will be determined as higher than the current one of a certain quantity Δ_A. If instead it is lower, it will be determined as lower than the current one of a certain quantity Δ_A. The quantity Δ_A is a fraction of the difference between the current modified moving average beat and the second beat of the A subseries. The second modified moving average computed beat will then become the current modified moving average beat and the process can be iterated for all the following beats of A subseries. Thus, Δ_A will be fraction of the difference between the current modified moving average beat and the next beat of the A subseries. Moreover Δ_A, which represents the innovation, has boundaries, thus it cannot be too big. This limitation is used to avoid the presence of noise. The analogous process is applied for B subseries. That process is applied since the modified moving average is demonstrated to be able to produce a beat series with reduced noise. At the end, the maximum difference between the 2 subseries modified moving average beats is calculated, in absolute terms, within the area between the end of QRS complex to the end of the T wave and within ST segment to identify alternans [35].

FFTSM works in frequency domain and it is very used since it is available on commercial ECG machines such as CH2000 and Heartwave, Cambridge Heart Inc. and others [33]. A pre-processing step is required to identify ST segment, T wave and an estimation of

noise. After that, for each beat, are identified 2 non-overlapping and adjacent windows: a depolarization window centred at R peak with 150ms of duration and a repolarization window just after the depolarization window with 225ms of duration. A consequent check is made to be sure that the depolarization phase is fully contained within the depolarization window. For each study, 128 beats are considered. So, a *nxm* matrix is determined containing data of the repolarization window. Each row corresponds to a beat, so *n* is equal to 128. Each column contains 1 data sample of the repolarization window. So *m* is equal to the number of samples contained in the 200ms repolarization window. For each column of the matrix the power spectral density is estimated using Fast Fourier Transform. Then these power spectral densities are summed up algebraically. Thus, the power spectral density is obtained for the matrix. If the power for the TWA frequency, calculated as half of the heart rate, is higher than the mean noise power at that frequency, the alternans is considered significant. The difference between the power of TWA and the power of mean noise is calculated and normalized for the average energy of the beats and represents the TWA amplitude. The FFTSM can be applied even for evaluating the QRSA [36].

For CDM application, in the ECG series, the R peaks are identified, and premature beats are removed. Then, for each R peak, the section between 60ms and 290ms after the R peak is identified (for a total of 230ms). The section is divided into windows of 10ms (in total there are 23 windows for one section). For each window, the area between the ECG signal and the baseline is computed. Thus, a total of 23 areas are extracted for each window. These 23 areas compose a series that is then filtered through a 16th-order Butterworth filter. The TWA in each time series is estimated using the so-called complex demodulation method [37].

LLRM considers successive windows composed by 32 beats and with their centres aligned to the analysed heartbeat. In each window, to identify the presence of TWA, it calculates the difference between each T wave and previous one. Then, the computed difference between the T waves is represented through a signal which is a combination of alternans waveform and noise, following a Laplacian distribution with zero mean. With the aim of validating the accuracy of the estimated alternans, a generalized likelihood ratio test is applied at the end [38].

It is possible to make a comparison among the cited methods (AMFM, MMAM, FFTSM, CDM, LLRM), highlighting the advantages and disadvantages of each of them. Indeed, these methods have been applied to simulated data with both stationery and time-varying TWA. It has been shown that MMAM is susceptible to provide false-positive TWA if applied to ECG signals that have T wave variability in amplitude but not really alternans. Anyway, TWA, when truly present, it is well identified by MMAM even if this method introduces a time delay in the TWA signal. On the contrary, all other methods, provide underestimated TWA results with respect to MMAM. Moreover, AMFM has been shown to be able to detect time-varying TWA. Instead, the FFTSM has not this ability because it identifies time varying TWA as stationary. CDM and LLRM can properly identify time-varying TWA only if the variation is low. The AMFM has been demonstrated to best one in reaching the trade-off between the necessity to detect only true positive TWA and to be capable to distinguish between stationary and time varying TWA [33].

2. Rationale of this thesis

As previously stated, the circadian rhythm is a cyclic process characterized by a periodicity of 24h and it is typical of many physiological processes. Even the dynamics of the cardiovascular system are characterized by a 24h periodicity. Indeed it can be affirmed that the heart rate, the atrioventricular conduction and the arrhythmias follow a circadian pattern [8], [9], [10], [11]. Heart rate, atrioventricular conduction, arrhythmias and ECGA are all linked to the heart's electrical activity. Moreover, ECGA is a marker of cardiovascular risk, related to the development of arrhythmias [18], [25], [28], [29], [31], [32]. Thus, expecting that ECGA is modulated by a circadian rhythm is reasonable.

The first aim of this thesis is to assess what is already known about the circadian periodicity of the ECGA investigating and reviewing in a systematic manner the information present in literature.

Furthermore, this thesis aims to verify if in real data the 3 ECGA types (PWA, QRSA, TWA) are characterized by a periodicity of 24h in healthy subjects. So, if the trend of its features is describable by a circadian rhythm. Thus, the first issue is to detect and measure PWA, QRSA and TWA in Holter tracers of healthy subjects lasting at least 24h. A possible solution is the EAMF, a noise-robust method already used for ECGA identification [25]. The EAMF method was optimized and used in this thesis.

ECGA circadian rhythm can be evaluated in terms of the trend of the amplitude (ECGA-A), in terms of the trend of the number of alternating heart beats (ECGA-D) and in terms of the trend of the magnitude (ECGA-M) [39].

Evaluating the circadian behaviour of PWA, QRSA and TWA may add an important element to the study of ECGA. In fact, increasing the information relative to the ECGA in healthy subjects would offer a more solid basis for evaluating diseased subjects. Since ECGA is a cardiovascular risk index, enlarging the knowledge in that field is crucial.

3. Materials and Methods

3.1 Systematic literature research

To have a comprehensive view of the state of art of the circadian rhythm of ECGA, a systematic research was done in Scopus and Pubmed databases, with no time or language limitation. The inclusion search keywords were:

-ECG or ECGK or electrocardiogr*. Those terms were included in order to select articles in which the ECG was investigated;

-alternans. That term was included in order to select articles in which the alternans was treated;

-circadian. That term was included in order to select articles in which the circadian rhythm was treated.

From the combination of the keywords previously reported, the following queries resulted:

-in Scopus: "TITLE-ABS-KEY (ecg OR ekg OR electrocardiogr*) AND TITLE-ABS-KEY (alternans) AND TITLE-ABS-KEY (circadian)";

-in Pubmed: "((ECG[Title/Abstract]) OR (EKG[Title/Abstract]) OR (electrocardiogr*[Title/Abstract])) AND (alternans[Title/Abstract]) AND (circadian[Title/Abstract])".

The inclusion criteria were the following:

-concerning human beings;

-being related to the theme of this thesis (treating the circadian rhythm of PWA, QRSA or/and TWA).

The literature scanning was done by reading the full text. Thus, the exclusion of papers was performed through the full text exclusion.

3.2 Analysis of real data

3.2.1 Database description

The data analysed in this thesis come from the "E-HOL-03-0202-003" database available on Telemetric and Holter ECG Warehouse (THEW) [40]. The database contains 24h Holter traces of 202 healthy subjects. The eligibility criteria were the following:

-not being affected by cardiovascular disease or having cardiovascular disorders history;

-not having high blood pressure (>150/90mmHg) history;

-not taking medication;

-not having other chronic illness such as diabetes, asthma, chronic obstructive pulmonary disease;

-not being previously evaluated by a physician for cardiovascular-related syndrome such as chest pain, palpitation, syncope;

-having a normal physical examination;

-having a normal sinus rhythm in 12-lead ECG, thus without signs of ventricular hypertrophy, inverted T wave , intraventricular conduction disturbances;

-having a normal echo and a normal ECG exercise testing;

-not being pregnant [40].

All subjects were asked to rest in supine position for 20minutes prior to the start of the recording.

The Holter recordings were acquired using the SpaceLab-Burdick digital Holter recorder (SpaceLab-Burdick, Inc., Deerfield, WI) with 10000nV of resolution and through pseudo-orthogonal lead configuration (X, Y, Z). The sampling frequency was of 200Hz.

Among the 202 subjects present in the database, 60 were selected in a random manner and analysed in this thesis, therefore constituting the population of this thesis. The population was characterized by 39±16years of mean age (range 13years-76years). The 25% of subjects (15 subjects) had an age between 13years and 25years; the 52% of subjects (31 subjects) had an age between 26years and 50years and the 40% of subjects (12 subjects) had an age between 51years and 76years. The 48% of subjects were males (31 subjects). The 30% of subjects (18 subjects) were smokers. 2 subjects took beta-blockers. The 55% of subjects (33 subjects) had a BMI (Body Mass Index) between 18.5 and 24.9 (normal weight); the 40% of subjects (24 subjects) had a BMI greater than 25 (overweight) and the 3% of subjects (2 subjects) had a BMI lower than 18.4

(underweight). The population main features are reported in details in Table 1A in Appendix A.

3.2.2 Data pre-processing

All data were analysed using MATLAB software (version R2022b, through ASUSTeck Computer Inc. Model F555L).

For each subject consecutive windows of ECG signal 120s long were load each second in an iteratively manner. Thus, each second a window of 120s containing ECG data of all 3 leads have been load until the end of the subject's signal. The average value was subtracted to each lead signal. Moreover, it was multiplied for 10000nV to obtain the data in nV. Then it was divided for 1000000 to convert the data from nV into mV. At this point it was evaluated the standard deviation of each lead signal: if it was equal to zero the window was rejected and the analysis proceeded considering the following window. Otherwise, each lead signal was filtered through a bidirectional 6th-order Butterworth low pass filter with cut-off frequency of 45Hz and a bidirectional 6th-order Butterworth high pass filter with cut-off frequency of 0.2Hz. At this point the Pan-Tomkins algorithm was used to individuate the R peaks on the ECG signal coming from lead Y. Then the R peaks position was corrected. So, each R peak computed through Pan-Tompkins algorithm was selected. It was considered a region of ECG between 8 samples (0.04s) before the R peak and 8 samples (0.04s) after R peak. Then the local maximum of that region was identified as the true R peak. At this point, the number of detected R peaks was counted. If that number was major than 60 and minor than 230 the analysis continued. Otherwise, the window was rejected and the analysis proceeded with the following window. After that primary check (number of R peaks major than 60 and minor than 230) another control of R peaks' number was made: if it was minor than 140 the window was enlarged in an iterative manner (10s at a time up to a maximum of 60s). If the number of beats was not at least 140 despite the window enlargement, the window was rejected and the analysis proceeded with the following window. Otherwise, in the lead Y the fiducial points of each electrocardiographic beat (Figure 13) were found:

-the beginning of P wave (Pon), the peak of P wave (Pmax), the end of P wave (Poff);

-the beginning of QRS complex (Qon), the peak of QRS complex (R), the end of the QRS complex (J);

-the beginning of the T wave (Ton), the peak of T wave (Tmax) and the end of the T wave (Toff).

The fiducial points were estimated using experimental formulas. Thus, for each beat, J was identified 50ms after the R peak, Qon was identified 50ms before R peak. Ton, Toff and Pon were estimated on the basis of the mean distance between 2 consecutive R peaks (mean RR). So, if the mean RR was minor than 600ms (average heart rate major than 100bpm), Ton was identified 60ms after R peak, Toff 330ms after R peak and Pon 180ms before Qon. Otherwise, if the mean RR was major than 600ms but minor than 1100ms (average heart rate minor than 100bpm and major than 55bpm), Ton was identified 100ms after R peak, Toff 380ms after R peak and Pon 200ms before Qon. In all other possible cases (average heart rate major than 100bpm) Ton was evaluated 150ms after R peaks, Toff 430ms after R peak and Pon 250ms before Qon. Poff was identified 20ms before Qon, independently from the heart rate. Pmax, R and Tmax were identified as the maxima or minima (depending on the polarity of the waves) of the segment between Pon and Poff, the segment between Qon and J and the segment between Ton and Toff respectively.

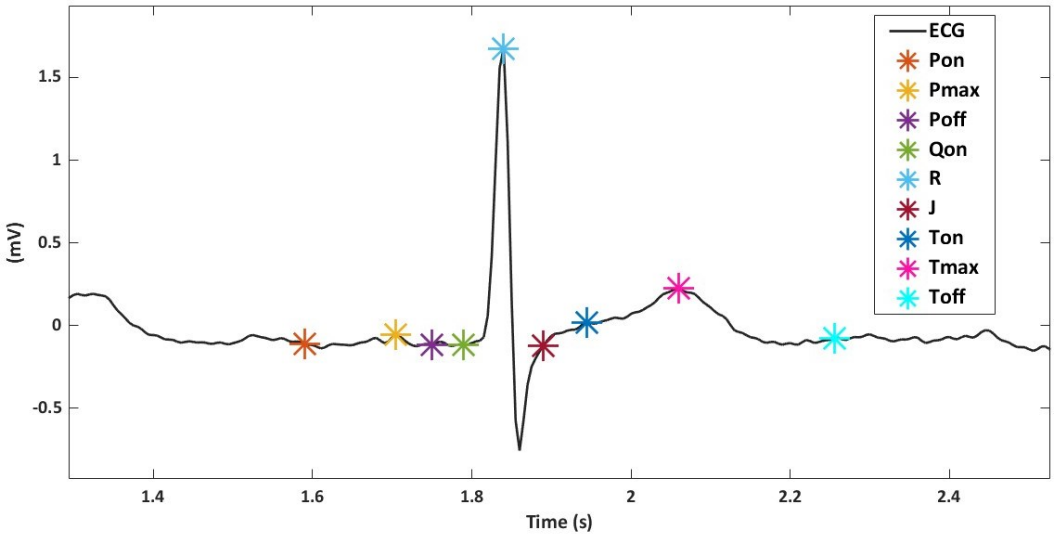

Figure 13 Example of detected fiducial points of one heartbeat. Pon=beginning of P wave, Pmax=maximum of P wave, Poff=end of P wave, Qon=beginning of QRS complex, R= R peak, J= end of QRS complex, Ton=beginning of T wave, Tmax= maximum of T wave, Toff=end of T wave

3.2.3 Data processing

At this point the pre-processed data were processed through the EAMF method [25], modified for the application in this thesis.

First of all, the EAMF method requires windows of ECG signal containing at least 140 heart beats. That condition was ensured in the pre-processing phase. At this point, the signal was filtered with a 6th-order bidirectional Butterworth low pass filter with cut off frequency equal to 35Hz and its baseline was removed. The method evaluated each window based on heart rate stability and good signal quality. To define the heart rate as stable, the standard deviation of the RR intervals should not exceed 10% of the mean RR interval. For the quality of the signal, each beat was divided into 3 consecutive sections:

-P section, defined between Pon and Qon;

-QRS complex section, defined between Qon and J;

-T wave section, defined between J and Tend.

At this point, a modification with respect to the original EAMF method was added. Indeed, the corrected median sections' waveform was computed. To calculate it, for the P waves, first of all were considered all the P sections and a median of them was calculated. Thus, all P sections of the considered windows were selected to compute the median P wave section waveform. After that, all P sections were aligned to their median section waveform. In order to align the P sections, for each P wave section a series was computed. A series was composed by a total of 11 P wave sections (P_n): the original P wave section and other 10 new ones. The first new one (P_1) was computed translating extremes of the original P wave section of 25ms backwards. Thus, the Pon and Poff of P_1 were identified on the ECG signal, 25ms before the Pon and the Poff of the original section respectively. Then the other new sections were identified in the same manner but translating the extremes of the original P wave section of N*5ms, where N is an integer and -5<N<5 (200/(5+N)ms). So for the new extremes:

-Pon_n=Pon+N*5ms;

-$Poff_n$=Poff+N*5ms.

Then, it was calculated the correlation between each section of the series P_n and the median P wave section waveform. After it, the P section with the highest correlation

value was selected for the following steps. At this point, the median waveform of the aligned P wave sections was computed.

Then, the corrected median P wave section was computed considering only aligned P wave sections with higher correlation coefficient than 0.3. The same process was applied to compute the corrected median QRS complex sections waveform and the corrected median T wave sections waveform. An example of aligned T wave sections and their corrected median T wave sections waveforms is reported in Figure 14. An example of the difference between the median T wave sections waveforms, the median aligned T wave sections waveforms and the corrected median T wave sections waveform is appreciable in Figure 15. Therefore another alignment was performed to align the P waves sections with respect to the corrected median P wave sections waveform. The correlation value between the corrected median P wave sections waveform and the new delayed P waves was calculated. At this point, the analysis continued following the original EAMF method. If the correlation coefficient was lower than a certain threshold (0.85) then the original P wave section was replaced with the corrected median one. All the previous steps were performed even for the T waves and QRS complexes. An example of ECG signal before the replacement of ectopic T waves was and ECG signal after the replacement of ectopic T waves is reported in Figure 16.

With too many sections replaced (more than 10% QRS complex sections or more than 10% T wave sections), the signal was considered not to be of good quality.

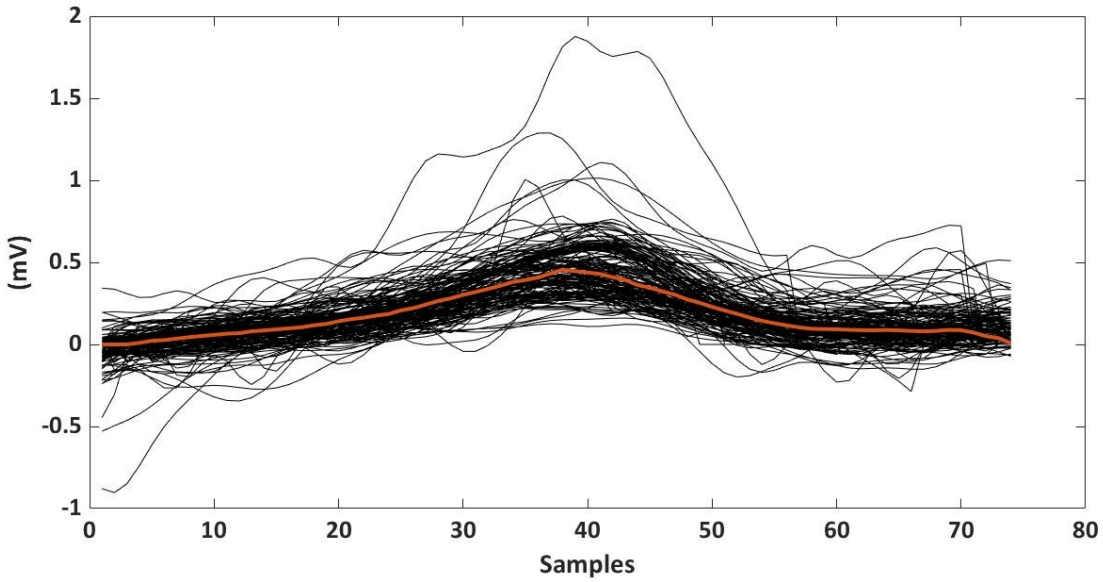

Figure 14 Example of aligned T waves (black lines) and their corrected median (red line)

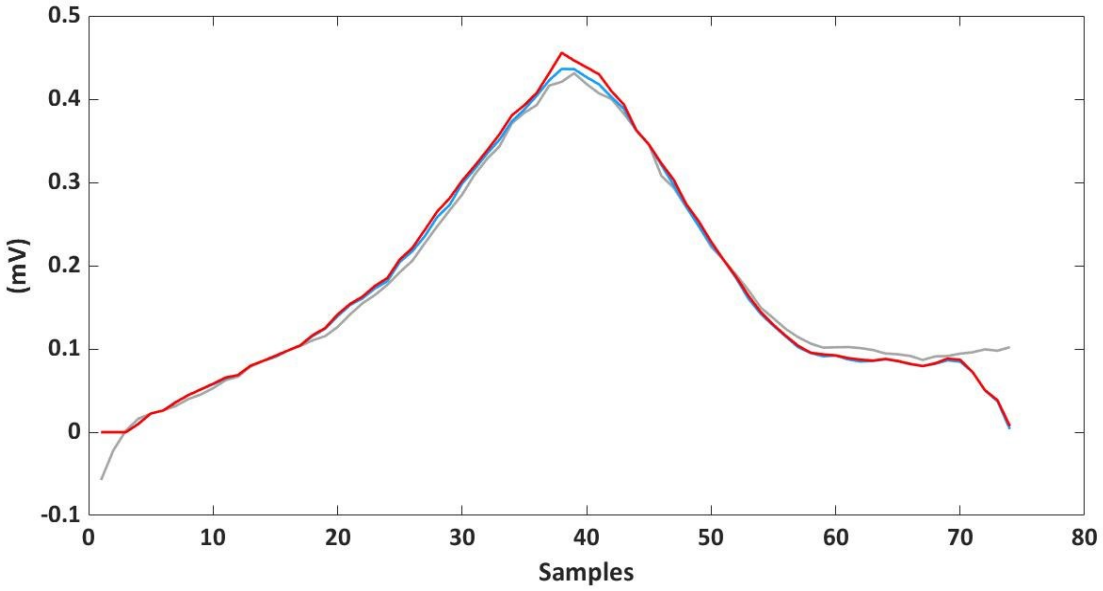

Figure 15 Example of the appreciable difference between the median T wave sections waveform before the alignment of the T waves sections (grey line), after the alignment (blue line) and after the correction (red line)

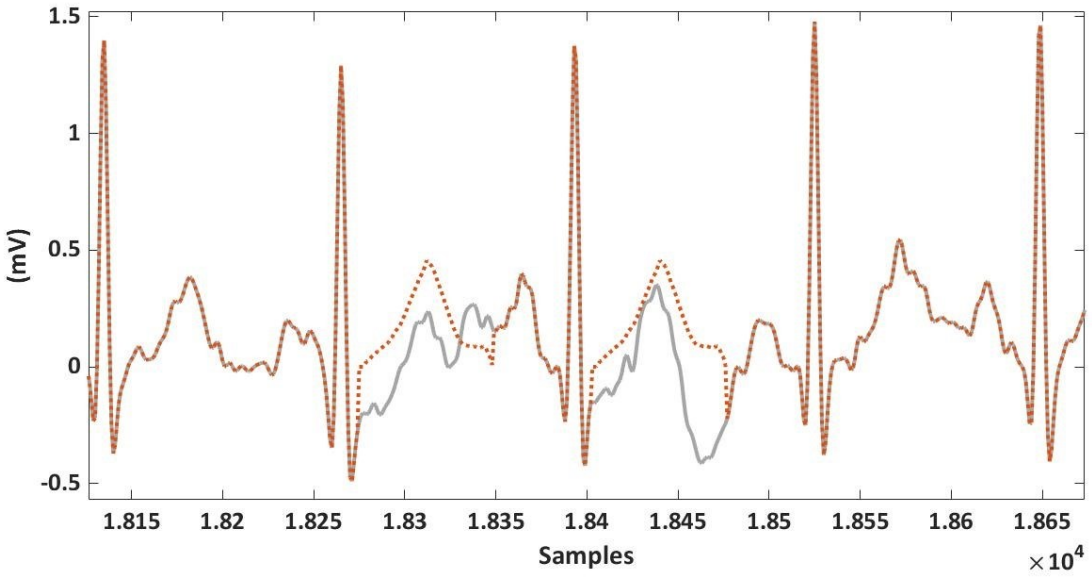

Figure 16 Example of ECG signal before the replacement of ectopic T waves was (grey line) and ECG signal after the replacement of ectopic T waves (dashed red line)

If the window was deemed suitable (i.e., both conditions of cardiac rhythm stability and sinus rhythm, unaffected by ectopic or noisy beats were met), the PWA, QRSA and TWA were analysed.

Thus, for each lead, the methods proceeded producing 3 signals:

-P wave signal. It was identified for the detection of PWA. The ECG tracing was all set to baseline with the exception of the P wave sections (Figure 17);

-QRS complex signal. It was identified for the detection of QRSA. The ECG tracing was all set to baseline with the exception of the QRS complex sections (Figure 18);

-T wave signal. It was identified for the detection of TWA. The ECG tracing was all set to baseline with the exception of the T wave sections (Figure 19).

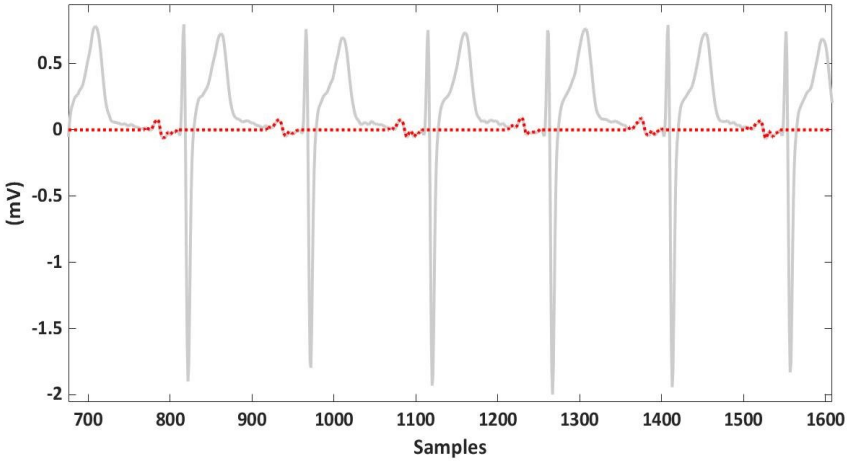

Figure 17 Example of P wave signal (red dashed line) computed through EAMF method over the ECG signal (grey line)

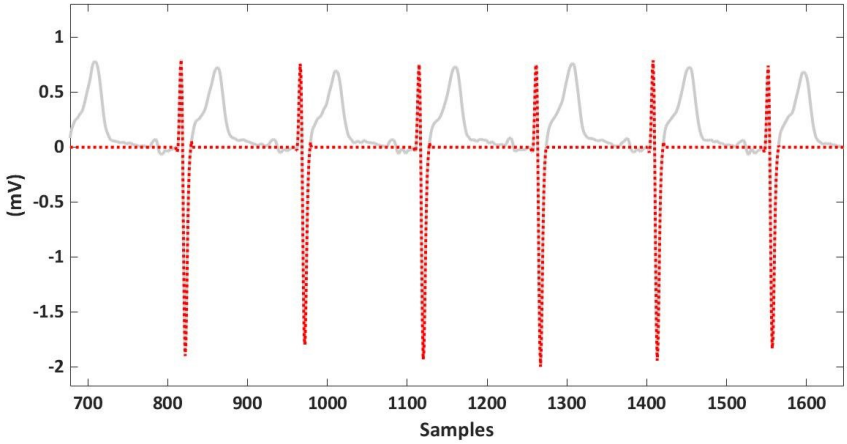

Figure 18 Example of QRS complex signal (red dashed line) computed through EAMF method over the ECG signal (grey line)

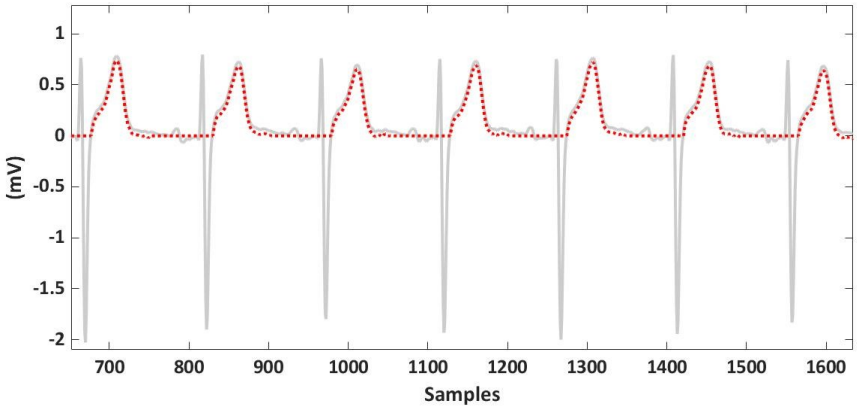

Figure 19 Example of T wave signal (red dashed line) computed through EAMF method over the ECG signal (grey line)

The electrocardiographic alternans is characterized by a narrow frequency band centred at the half mean heart rate (f_A) by definition. The EAMF method filter is a bidirectional 6th-order Butterworth filter with a very narrow passband and centred in the electrocardiographic alternans' frequency. The band is defined as b=($f_A \pm 0.06$)Hz. If there was alternans the output of the filter was a pseudo-sinusoidal signal whose amplitude was half the amplitude of the alternans in μV. Thus, if the input was the P wave signal, the output was a pseudo-sinusoidal signal with an amplitude of the half of P wave alternans and which had its maxima and minima in correspondence of the P wave. If the input was the QRS complex signal, the output was a pseudo-sinusoidal signal with an amplitude of the half of QRS complex alternans which had its maxima and minima in correspondence of the QRS complex. If the input was the T wave signal, the output was a pseudo-sinusoidal signal with an amplitude of the half of T wave alternans which had its maxima and minima in correspondence of the T wave. Otherwise, if there was no alternans phenomenon, the output was a signal constant in time and the electrocardiographic alternans was assumed to be 0 [25].

If the signal quality and/or heart rate stability were inadequate, the window was rejected and the alternans was not studied [25].

After the application of EAMF method, the following features for each lead of each window were extracted:

-median amplitude of PWA considering all beats;

-median amplitude of QRSA considering all beats;

-median amplitude of TWA considering all beats;

-median amplitude of PWA considering only the beats in which there was PWA (PWA-A);

-median amplitude of QRSA considering only the beats in which there was QRSA (QRSA-A);

-median amplitude of TWA considering only the beats in which there was TWA (TWA-A);

-median position of the PWA;

-median position of the QRSA;

-median position of the TWA;

-number of replaced P wave sections;

-number of replaced QRS complex sections

-number of replaced T wave sections;

-median amplitude of P wave;

-median amplitude of QRS complex;

-median amplitude of T wave;

-number of beats that manifested PWA (PWA-D);

-number of beats that manifested QRSA (QRSA-D);

-number of beats that manifested TWA (TWA-D).

Moreover, for each window even other 2 parameters were extracted which were common to all the leads, so they were extracted only for the lead 2:

-median distance between 2 consecutive R peaks (RR);

-standard deviation of RR.

After the extraction of all the features and parameters listed above, it was calculated a value of ECGA-M for each lead of each window, defined as the product between ECGA-A and ECGA-D in the considered window. Thus, PWA-M, QRSA-M and TWA-M were calculated.

3.2.4 Statistical analysis

The data extracted from the previous steps for each subject were mediated each 10minutes. For example, the PWA trend resulted from the previous steps consisted of a value for each second. Then it consisted of a median value each 10minutes. The same was done for all the extracted features.

The median of each extracted features with respect to all the subjects was computing, providing a cumulative trend. To do that, at each time instant (every 10minutes) the median cumulative value was calculated only if at least the 30% of the subjects (at least 21 subjects) reported a value at the considered time instant. Otherwise, the median cumulative value was defined as not admittable.

PWA, QRSA and TWA cumulative values were fitted (by the means of nonlinear least squares approach) through the sum of 2 sin functions as reported by the formula below:

$$Y=a1*\sin(b1*x+c1)+a2*\sin(b2*x+c2) \quad (7)$$

Y=function fitting of PWA, QRSA or TWA cumulative values

a1,b1,c1,a2,b2,c2=constants depending on the fitting

x=PWA, QRSA or TWA cumulative values

In addition the median of the cumulative values of PWA, QRSA and TWA among the 3 leads (X, Y and Z) was calculated and fitted through the formula (7).

Daily hours were defined between 7:00 and 19:00 [41].

4. Results

4.1 Systematic review

In Figure 20 are observable the literature search and the screening phases that were used to perform the selection of the articles included in this thesis.

25 papers resulted from Scopus and 7 from Pubmed, for a total of 32 papers. 8 articles were duplicated, so 24 papers were further analysed. Among them 1 paper concerned studies on animals, therefore it was rejected. 6 were not available, 8 were not pertinent with the topic of this thesis not reporting studies on ECGA possible circadian pattern. The remaining 9 papers were relevant for this thesis.

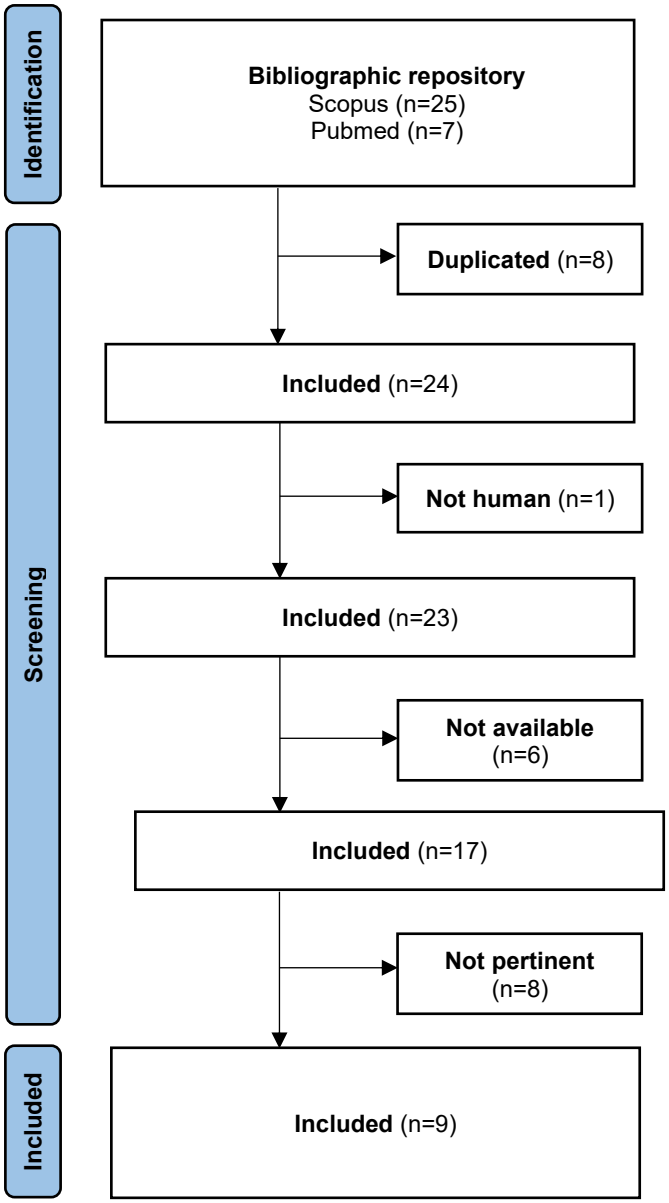

Figure 20 Literature search and the screening phases according to PRISMA guidelines [42]

Among the included articles, 8 concerned the circadian rhythm of TWA and 1 studied all 3 types of ECGA (TWA, PWA and QRSA). In 9 papers (100%) TWA was reported to have an increasing during day and a decreasing during night. 1 paper (11%) studied healthy subjects, 6 papers (67%) diseased patients and 2 papers (22%) examined both healthy and diseased subjects. Overall, 106 healthy subjects and 1380 diseased subjects were studied by the included articles. In 4 papers (44%) the method used to identify the TWA was the MMAM; in 2 papers (22%) the method was the FFTSM; in 1 paper the method was the LLRM. The article that evaluated all 3 types of ECGA used the EAMF method.
Below are reported more in details the important information in the field of circadian rhythm of ECGA of the 9 literature papers, ordered in a chronological manner.
Moreover, that information is summarized in Table 1.

F. Cruz Filho, et al., 2000

The 24-h Holter data of 11 patients (7 males, 4 females) with congenital long QT syndrome (QT interval range between 480ms and 580ms) were analysed in order to assess the characteristics of T wave polarity alternans (TWAP) in patients suffering of long QT syndrome. The Holter exams were performed using 2 or 3 leads (V2 and V5 or V2, V3 and aVF). 5 subjects (3 males, 2 females, QT interval range between 520ms and 580ms) presented more than 4 consecutive episodes of TWAP in 24h. The distribution of the TWAP was reported to be not uniform among the different hours of the day. Indeed, the 44% of episodes was registered between 8:00 and 12:00. The 19% occurred from 12:00 to 16:00, the 9% from 16:00 to 20:00, the 3% from 20:00 to 24:00 and another 9% from 24:00 to 4:00. Overall, the TWAP showed a major distribution during daytime hours with a peak between 8:00 and 12:00 and a large decrease during night hours [43].

Takasugi N., et al., 2009

The 24h Holter data of 40 subjects (27 males, 13 females; mean age 63.0+12.1years) suffering of congestive heart failure were studied to determine the implication of sleep apnoea in nocturnal sudden cardiac death. The Holter exams were performed with 2 leads (V1 and V5). TWA was used as index of vulnerability to arrhythmias. Subjects were divided according to the fact that TWA had a peak during daytime or night hours. Results

showed that 30 subjects (22 males, 8 females; mean age 61.5+11.8years) had a main TWA peak during daytime hours. The remaining 10 subjects (5 males, 5 females; mean age 67.5+12.6years) registered a TWA predominant peak during night. The method used to detect TWA was the MMAM [44].

Makarov L., et al., 2010

The 24h Holter data of 48 healthy subjects (age range 7-17years) and 85 paediatric patients (age range 7-17years) with heart diseases were analysed. Heart diseases included ventricular premature beats, dilated cardiomyopathy, inherited long QT syndrome, Brugada syndrome and catecholaminergic polymorphic ventricular tachycardia. The Holter exams were performed using 3 leads (V5, V1, and aVF). In both groups (healthy and diseased) it was found a circadian pattern of TWA with higher values during daytime hours. Healthy subjects showed a peak of TWA at 18:00. TWA peak was reported between 14:00 and 16:00 in diseased subjects. The method used to detect TWA was the MMAM [45].

S. Yamada, et al., 2013

The 24h Holter data of 50 subjects (33 males, 17 females; mean age 61.2±12.8years) with chronic heart failure were studied to determine the relationship between sleep-disordered breathing and risk for fatal ventricular tachyarrhythmias in patients with chronic heart failure. The Holter exams were performed with 2 leads (V1 and V5). The patients were divided into 2 groups according to the fact that they had more than 20 episodes for hour of sleep breathing disorders (24 subjects) or less (26 subjects). In that context, TWA detection was used as risk marker for arrythmias. TWA showed an increasing during daytime hours respect to night ones, with a peak between 12:00 and 18:00 in both groups. The method used to detect TWA was the MMAM [46].

A. Martin-Yebra, et al., 2015

The 24-hour Holter data of 626 subjects (mean age 62.7±11.9years) were studied to evaluate the circadian behaviour of TWA in patients suffering of chronic heart failure. Among all the subjects, 52 were victims of sudden cardiac death, 63 died because of other cardiac causes and 25 died due to non-cardiac reasons. The survivors were 486.

The Holter exams were performed using 3 leads (X, Y, Z). It was detected a correlation between the presence of TWA and the sudden cardiac death. TWA distribution was significant higher in daytime hours respect to and night ones. The peak was reached between 12:00 and 18:00. The method used to detect TWA was the LLRM [47].

Sakamoto S., et al., 2016

The 24h Holter data of 140 subjects were analysed. 129 patients had Brugada syndrome (122 males, 7 females; mean age 52±12years) and 11 were control subjects (11 males; mean age 50±9years). The Holter exams were performed using 12 leads (V1, V2, V3, V4, V5, V6, aVF, aVR, aVL, D1, D2, D3). TWA was used as predictor of ventricular fibrillation. Patients with Brugada syndrome showed an absolute peak of TWA during daytime hours between 12:00 and 18:00 and another peak during night hours, between 24:00 and 6:00. The method used to detect TWA was the MMAM [48].

K. Hashimoto, et al., 2019

The 24h Holter data of 47 subjects (20 males, 27 females; mean age 44.3±18.1years) without significant structural heart disease were analysed to assess the diurnal variation of the TWA. The Holter exams were performed using 3 leads (X, Y, Z). TWA reached a maximum between 12:00 and 18:00 and a minimum between 00:00 and 06:00. The method used to detect TWA was the FFTSM [49].

M. Uson, et al., 2022

The 24h Holter data of 388 patients (318 males, 70 females; mean age 65±10years) with heart failure were studied to verify the circadian rhythm of TWA. Each patient underwent 3 Holter exams (average time between first and second Holter exam was 3.6months; average time between first and third Holter exam was 12.7months). After 3.9years from the first Holter exam, there were reported 47 sudden cardiac deaths, 22 deaths due to cardiac causes and 16 deaths because of other causes. The Holter exams were performed using 12 leads (V1, V2, V3, V4, V5, V6, aVF, aVR, aVL, D1, D2, D3). In 76.8% of the data, it was possible to identify a pattern of TWA describable through a sinusoidal shape function. That function showed a minimum during the night hours and

reached a maximum during the daytime hours, between 11:00 and 15:00. The method used to detect TWA was the LLRM [50].

I. Marcantoni, et al., 2022

The Holter data (average 48h) of 51 patients (30 males, 21 females; age range 40-95years) with end stage renal disease were analysed to assess the circadian rhythm of TWA, PWA and QRSA in dialyzed subjects with kidney failure. The dialysis mean duration was 4h and started between 6:00 and 8:00 (20 patients), or between 10:00 and 12:00 (20 patients) or between 14:00 and 16:00 (11 patients). The Holter exams were performed using 12 leads (V1, V2, V3, V4, V5, V6, aVF, aVR, aVL, D1, D2, D3). Results showed that ECGA followed a circadian rhythm during days without dialysis, with maximum between 12:00 and 18:00 and minimum during night hours. The effect of dialysis treatment was the interruption of ECGA periodicity and a decrement of all types of ECGA. The method used to detect ECGA was the EAMF [41].

*Table 1 Information of the 9 articles reported in this thesis to assess the state of art of electrocardiographic alternans circadian rhythm. *Pop. Size= population size; **H.C.= Health condition. D=diseased, H=Healthy; ***Patol.=patology. LQTS=congenital long QT syndrome, CHF=congestive heart failure, BrS=Brugada syndrome, PVCs=premature ventricular beats, DCM=dilated cardiomyopathy, CPVT=catecholaminergic ventricular tachycardia, CrHF=chronic heart failure, HF=heart failure, KF=kidney failure; ****ECGA= electrocardiographic alternans. TWA=T wave alternans, PWA= P wave alternans, QRSA= complex QRS alternans. *****Method=method of detection ECGA. MMAM=modified moving average method, LLRM=Laplacian-likelihood-ratio method, FFTSM=fast-Fourier-transform spectral method, EAMF=Enhanced adaptive matched filter. N.A.=not available*

Ref.; Year	**Pop. Size*; males (%)**	**Age (mean±sd) years or (range)years**	**H.C. ******	**Patol. *****	**Leads**	**ECGA type ********	**Method *********	**Peak time**
[43]; 2000	11; 64%	N.A.	D	LQTS	2-3 (V2;V5 or V2;V5;aVF)	TWA	N.A.	Day 8:00-12:00
[44]; 2009	30; 73%	61.5±11.8	D	CHF	3 (V1;V5)	TWA	MMAM	Day
	10; 50%	67.5±12.6	D	CHF				Day
[45]; 2010	48; N.A.	7-17	H		3 (V1;V5;aVF)	TWA	MMAM	Day 18:00
	85; N.A.	7-17	D	LQTS/ BrS/ PVCs/ DCM/ CPVT				Day 14:00-16:00
[46]; 2013	50; 66%	61.2±12.8	D	CrHF	2 (V1;V5)	TWA	MMAM	Day 12:00-18:00
[47]; 2015	626; N.A.	62.7±11.9	D	CrHF	3 (X; Y; Z)	TWA	LLRM	Day 12:00-18:00
[48]; 2016	129; 95%	52±12	D	BrS	12	TWA	MMAM	Day 12:00-18:00
	11; 100%	50±9	H					N.A.
[49]; 2019	47; 43%	44.3±18.1	H		3 (X; Y; Z)	TWA	FFTSM	Day 12:00-18:00
[50]; 2022	388; 82%	65±10	D	HF	12	TWA	LLRM	Day 11:00-15:00
[41]; 2022	51; 59%	40-95	D	KF	12	TWA, PWA, QRSA	EAMF	Day 12:00-18:00
				KF				
				KF				

4.2 Real data

4.2.1 Amplitude

All results reported below are reported in terms of ECGA-A (μV).

Results show that 67% of subjects (40 subjects) registered at level of lead X a maximum value of PWA-A during daily hours, reaching between 12μV and 100μV. At level of lead Y, the maximum value of PWA-A was registered during daily hours by 67% of subjects (40 subjects), in a range between 12μV and 99μV. At level of lead Z, the maximum value of PWA-A was registered during daily hours by 67% of subjects (40 subjects), in a range between 10μV and 60μV. 53% of subjects (32 subjects) registered at level of lead X a minimum value of PWA-A during nocturnal hours, reaching between 6μV and 24μV. At level of lead Y, the minimum value of PWA-A was registered during nocturnal hours by 67% of subjects (40 subjects), in a range between 5μV and 14μV. At level of lead Z, the minimum value of PWA-A was registered during nocturnal hours by 62% of subjects (37 subjects), in a range between 6μV and 18μV. PWA-A maximum and minimum values for each subject are reported in Table 1B in Appendix B.

Results show that 57% of subjects (34 subjects) registered at level of lead X a maximum value of QRSA-A during daily hours, reaching between 11μV and 106μV. At level of lead Y, the maximum value of QRSA-A was registered during daily hours by 67% of subjects (40 subjects), in a range between 10μV and 33μV. At level of lead Z, the maximum value of QRSA-A was registered during daily hours by 72% of subjects (43 subjects), in a range between 11μV and 44μV. 58% of subjects (35 subjects) registered at level of lead X a minimum value of QRSA-A during nocturnal hours, reaching between 6μV and 21μV. At level of lead Y, the minimum value of QRSA-A was registered during nocturnal hours by 58% of subjects (35 subjects), in a range between 6μV and 17μV. At level of lead Z, the minimum value of QRSA-A was registered during nocturnal hours by 70% of subjects (42 subjects), in a range between 6μV and 17μV. QRSA-A maximum and minimum values for each subject are reported in Table 2B in Appendix B.

Results show that 48% of subjects (29 subjects) registered at level of lead X a maximum value of TWA-A during daily hours, reaching between 11μV and 102μV. At level of lead Y, the maximum value of TWA-A was registered during daily hours by 62% of subjects (37 subjects), in a range between 11μV and 132μV. At level of lead Z, the maximum value of TWA-A was registered during daily hours by 58% of subjects (35 subjects), in a range

between 8μV and 126μV. 60% of subjects (36 subjects) registered at level of lead X a minimum value of TWA-A during nocturnal hours, reaching between 4μV and 21μV. At level of lead Y, the minimum value of TWA-A was registered during nocturnal hours by 60% of subjects (36 subjects), in a range between 4μV and 17μV. At level of lead Z, the minimum value of TWA-A was registered during nocturnal hours by 39% of subjects (23 subjects), in a range between 3μV and 22μV. TWA-A maximum and minimum values for each subject are reported in Table 3B in Appendix B.

PWA-A cumulative values on lead X range between 10μV and 16μV (mean value 12μV, standard deviation(sd) of 1.2). The trend of the fitting of the PWA-A registered on lead X cumulative values is reported in Figure 20. The maximum of 14μV is reached between 16:00 and 18:00 and the minimum of 11μV is reached between 3:00 and 5:00.

PWA-A cumulative values on lead Y range between 10μV and 15μV (mean value 12μV, sd of 1.2). The trend of the fitting of the PWA-A registered on lead Y cumulative values is reported in Figure 21. The maximum of 13μV is reached between 15:00 and 17:00 and the minimum of 11μV is reached between 2:00 and 4:00.

PWA-A cumulative values on lead Z range between 10μV and 15μV (mean value 12μV, sd of 1.3). The trend of the fitting of the PWA-A registered on lead Z cumulative values is reported in Figure 22. The maximum of 13μV is reached between 16:00 and 18:00 and the minimum of 10μV is reached between 2:00 and 4:00.

QRSA-A cumulative values on lead X range between 10μV and 13μV (mean value 11μV, sd of 0.6). The trend of the fitting of the QRSA-A registered on lead X cumulative values is reported in Figure 23. The absolute maximum of 12μV is reached between 18:00 and 20:00, another maximum of 11μV is reached between 6:00 and 8:00 and the minimum of 11μV is reached between 1:00 and 3:00.

QRSA-A cumulative values on lead Y range between 10μV and 13μV (mean value 12μV, sd of 0.6). The trend of the fitting of the QRSA-A registered on lead Y cumulative values is reported in Figure 24. The absolute maximum of 13μV is reached between 16:00 and 18:00, another maximum of 12μV is reached between 6:00 and 9:00 and the minimum of 11μV is reached between 1:00 and 2:00.

QRSA-A cumulative values on lead Z range between 10μV and 15μV (mean value 12μV, sd of 1.2). The trend of the fitting of the QRSA-A registered on lead Z cumulative values

is reported in Figure 25. The maximum of 14µV is reached between 16:00 and 18:00 and the minimum of 11µV is reached between 1:00 and 4:00.

TWA-A cumulative values on lead X range between 11µV and 18µV (mean value 15µV, sd of 1.4). The trend of the fitting of the TWA-A registered on lead X cumulative values is reported in Figure 26. The maximum of 16µV is reached between 18:00 and 20:00 and the minimum of 13µV is reached between 5:00 and 8:00.

TWA-A cumulative values on lead Y range between 10µV and 15µV (mean value 12µV, sd of 1.2). The trend of the fitting of the TWA-A registered on lead Y cumulative values is reported in Figure 27. The maximum of 14µV is reached between 15:00 and 17:00 and the minimum of 11µV is reached between 3:00 and 5:00.

TWA-A cumulative values on lead Z range between 10µV and 18µV (mean value 13µV, sd of 1.6). The trend of the fitting of the TWA-A registered on lead Z cumulative values is reported in Figure 28. The absolute maximum of 15µV is reached between 17:00 and 19:00, another maximum of 13µV is reached between 6:00 and 9:00 and the minimum of 12µV is reached between 00:00 and 3:00.

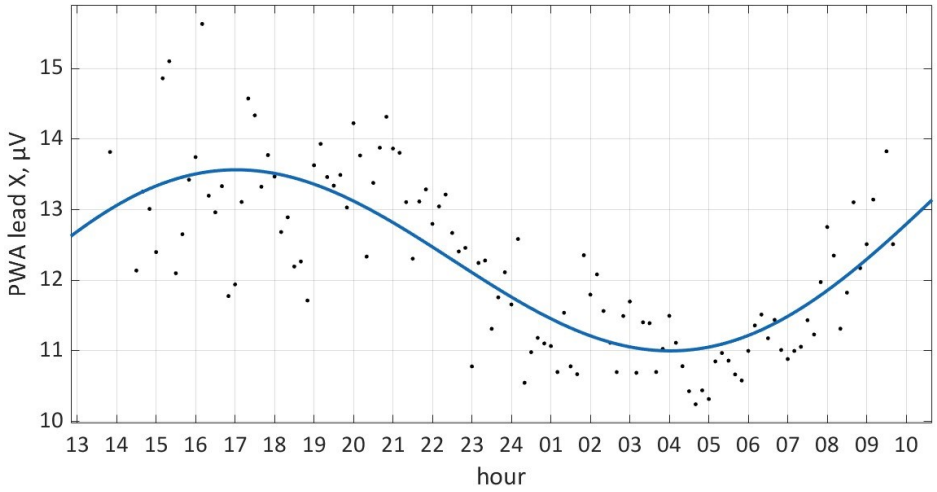

Figure 21 PWA (P wave alternans) in terms of amplitude (PWA-A) registered al level of lead X

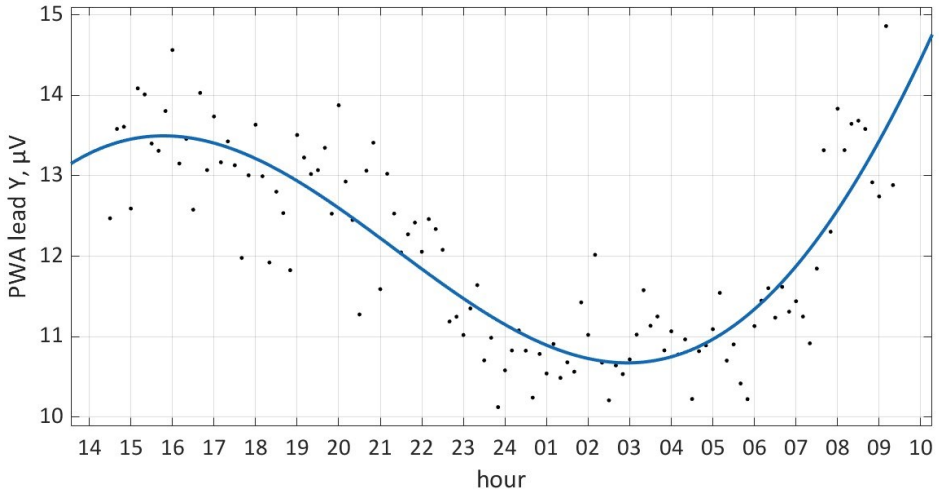

Figure 22 PWA (P wave alternans) in terms of amplitude (PWA-A) registered al level of lead Y

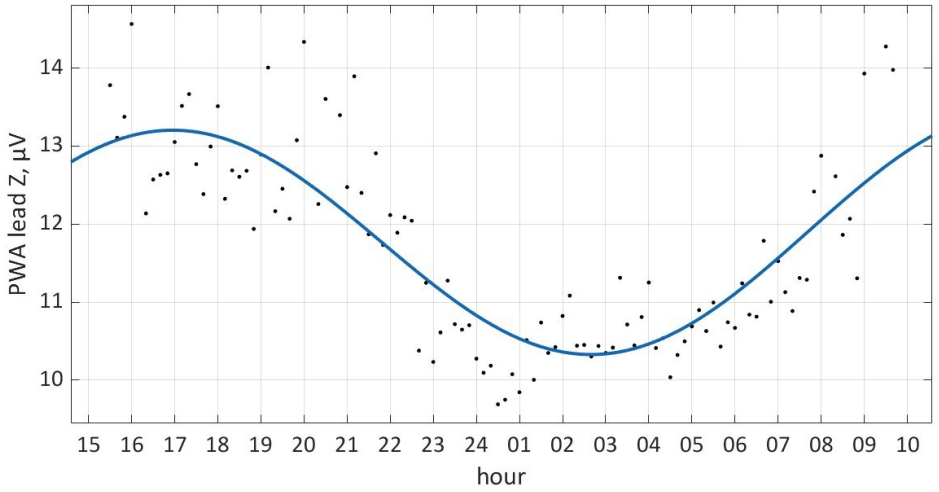

Figure 23 PWA (P wave alternans) in terms of amplitude (PWA-A) registered al level of lead Z

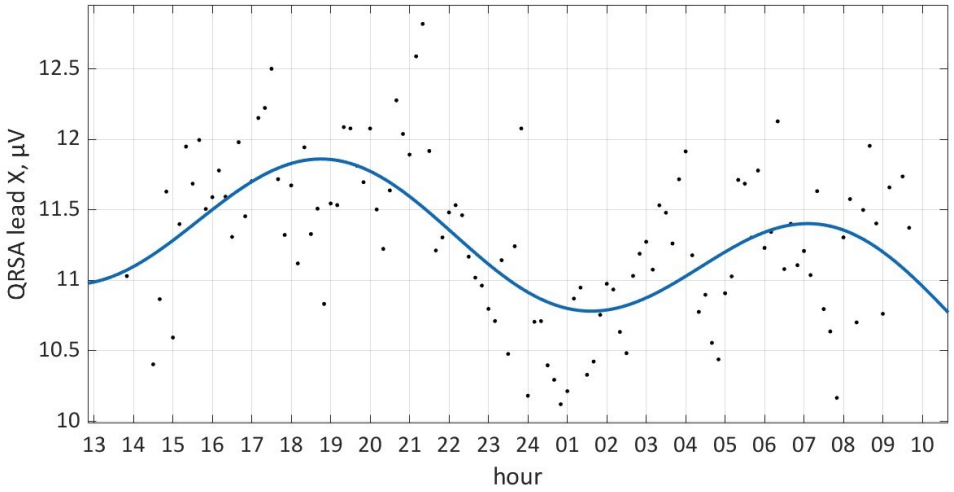

Figure 24 QRSA (QRS complex alternans) in terms of amplitude (QRSA-A) registered al level of lead X

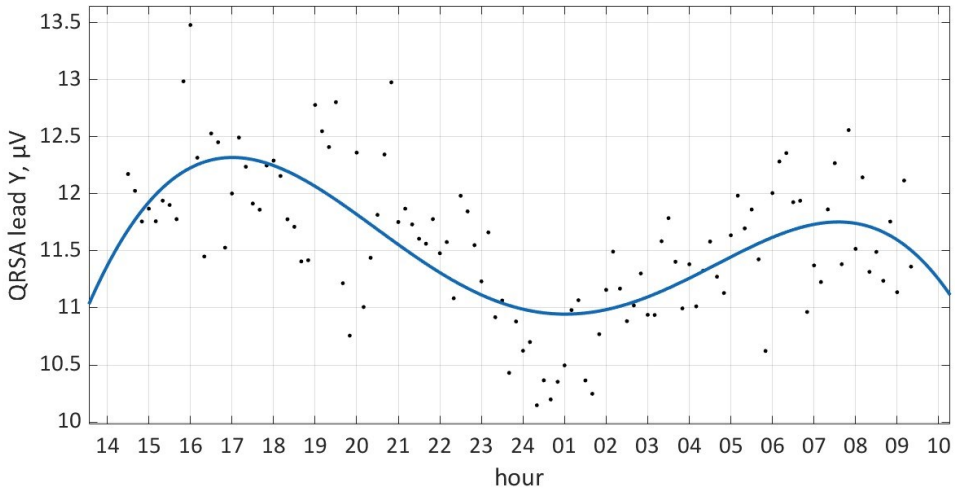

Figure 25 QRSA (QRS complex alternans) in terms of amplitude (QRSA-A) registered al level of lead Y

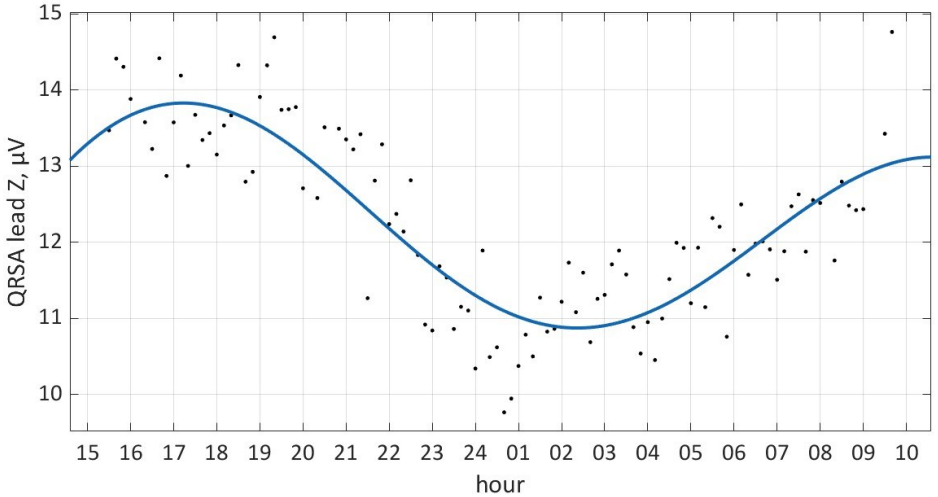

Figure 26 QRSA (QRS complex alternans) in terms of amplitude (QRSA-A) registered al level of lead Z

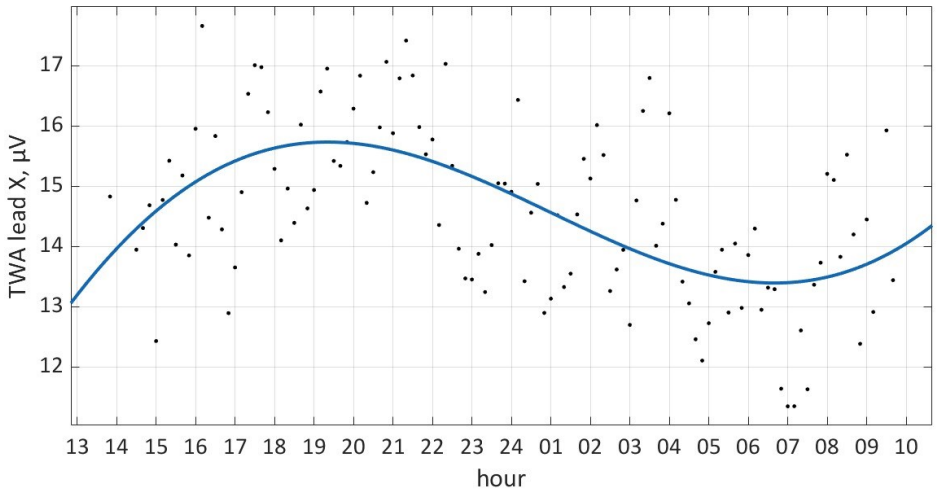

Figure 27 TWA (T wave alternans) in terms of amplitude (TWA-A) registered al level of lead X

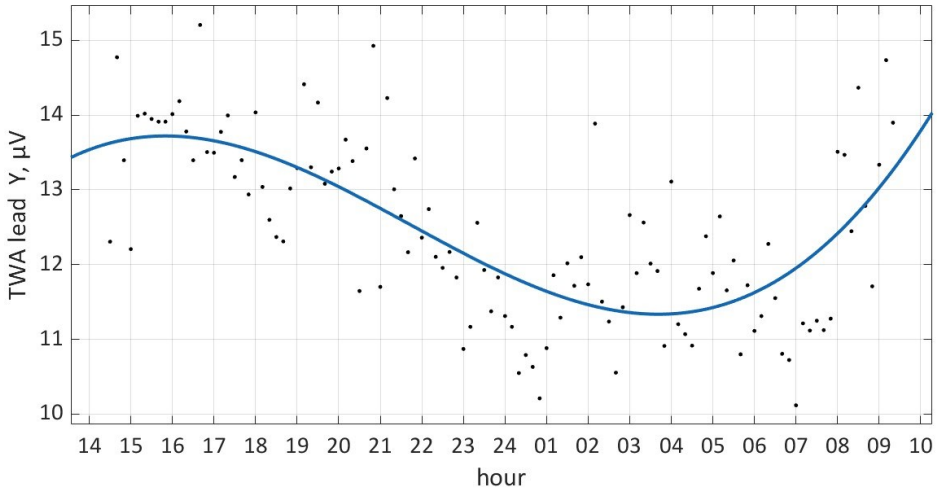

Figure 28 TWA (T wave alternans) in terms of amplitude (TWA-A) registered al level of lead Y

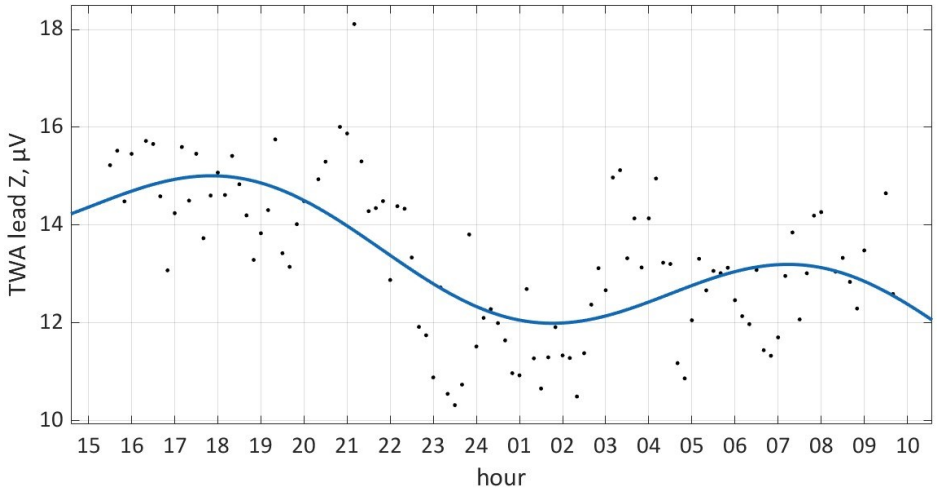

Figure 29 TWA (T wave alternans) in terms of amplitude (TWA-A) registered al level of lead Z

4.2.2 Number of alternating beats

All results reported below are reported in terms of ECGA-D.

Results show that 55% of subjects (33 subjects) registered at level of lead X a maximum value of PWA-D during daily hours, reaching between 105 and 136 heart beats per window. At level of lead Y, the maximum value of PWA-D was registered during daily hours by 63% of subjects (38 subjects), in a range between 107 and 129 heart beats per window. At level of lead Z, the maximum value of PWA-D was registered during daily hours by 51% of subjects (31 subjects), in a range between 99 and 130 heart beats per window. 53% of subjects (27 subjects) registered at level of lead X a minimum value of PWA-D during nocturnal hours, reaching between 13 and 97 heart beats per window. At level of lead Y, the minimum value of PWA-D was registered during nocturnal hours by 28% of subjects (17 subjects), in a range between 19 and 68 heart beats per window. At level of lead Z, the minimum value of PWA-D was registered during nocturnal hours by 38% of subjects (23 subjects), in a range between 17 and 76 heart beats per window. PWA-D maximum and minimum values for each subject are reported in Table 4B in Appendix B.

Results show that 53% of subjects (32 subjects) registered at level of lead X a maximum value of QRSA-D during daily hours, reaching between 83 and 136 heart beats per window. At level of lead Y, the maximum value of QRSA-D was registered during daily hours by 48% of subjects (29 subjects), in a range between 63 and 125 heart beats per window. At level of lead Z, the maximum value of QRSA-D was registered during daily hours by 53% of subjects (32 subjects), in a range between 79 and 128 heart beats per window. 60% of subjects (36 subjects) registered at level of lead X a minimum value of QRSA-D during nocturnal hours, reaching between 0 and 88 heart beats per window. At level of lead Y, the minimum value of QRSA-D was registered during nocturnal hours by 55% of subjects (33 subjects), in a range between 0 and 71 heart beats per window. At level of lead Z, the minimum value of QRSA-D was registered during nocturnal hours by 62% of subjects (37 subjects), in a range between 0 and 70 heart beats per window. QRSA-D maximum and minimum values for each subject are reported in Table 5B in Appendix B.

Results show that 52% of subjects (31 subjects) registered at level of lead X a maximum value of TWA-D during daily hours, reaching between 114 and 132 heart beats per

window. At level of lead Y, the maximum value of TWA-D was registered during daily hours by 50% of subjects (30 subjects), in a range between 117 and 130 heart beats per window. At level of lead Z, the maximum value of TWA-D was registered during daily hours by 57% of subjects (34 subjects), in a range between 113 and 132 heart beats. 42% of subjects (25 subjects) registered at level of lead X a minimum value of TWA-D during nocturnal hours, reaching between 60 and 103 heart beats. At level of lead Y, the minimum value of TWA-D was registered during nocturnal hours by 30% of subjects (18 subjects), in a range between 57 and 90 heart beats per window. At level of lead Z, the minimum value of TWA-D was registered during nocturnal hours by 33% of subjects (20 subjects), in a range between 50 and 100 heart beats per window. TWA-D maximum and minimum values for each subject are reported in Table 6B in Appendix B.

PWA-D cumulative values on lead X range between 58 and 101 (mean value 84, sd of 12). The trend of the fitting of PWA-D registered on lead X cumulative is reported in Figure 29. The maximum of 98 is reached between 16:00 and 19:00 and the minimum of 70 is reached between 2:00 and 5:00.

PWA-D cumulative values on lead Y range between 62 and 100 (mean value 83, sd of 12). The trend of the fitting of PWA-D registered on lead Y cumulative values is reported in Figure 30. The maximum of 97 is reached between 16:00 and 18:00 and the minimum of 69 is reached between 2:00 and 4:00.

PWA-D cumulative values on lead Z range between 61 and 99 (mean value 79, sd of 13). The trend of the fitting of PWA-D registered on lead Z cumulative values is reported in Figure 31. The maximum of 95 is reached between 16:00 and 19:00 and the minimum of 64 is reached between 2:00 and 5:00.

QRSA-D cumulative values on lead X range between 34 and 80 (mean value 60, sd of 14). The trend of the fitting of QRSA-D registered on lead X cumulative values is reported in Figure 32. The maximum of 76 is reached between 16:00 and 18:00 and the minimum of 44 is reached between 2:00 and 5:00.

QRSA-D cumulative values on lead Y range between 37 and 80 (mean value 61, sd of 13). The trend of the fitting of QRSA-D registered on lead Y cumulative values is reported in Figure 33. The maximum of 77 is reached between 16:00 and 18:00 and the minimum of 46 is reached between 2:00 and 4:00.

QRSA-D cumulative values on lead Z range between 39 and 88 (mean value 63, sd of 16). The trend of the fitting of QRSA-D registered on lead Z cumulative values is reported in Figure 34. The maximum of 83 is reached between 17:00 and 19:00 and the minimum of 43 is reached between 2:00 and 4:00.

TWA-D cumulative values on lead X range between 99 and 112 (mean value 107, sd of 3). The trend of the fitting of TWA-D registered on lead X cumulative values is reported in Figure 35. The maximum of 105 is reached between 16:00 and 19:00 and the minimum of 104 is reached between 2:00 and 5:00.

TWA-D cumulative values on lead Y range between 96 and 112 (mean value 105, sd of 4). The trend of the fitting of TWA-D registered on lead Y cumulative values is reported in Figure 36. The maximum of 110 is reached between 15:00 and 18:00 and the minimum of 101 is reached between 2:00 and 5:00.

TWA-D cumulative values on lead Z range between 96 and 112 (mean value 105, sd of 4). The trend of the fitting of TWA-D registered on lead Z cumulative values is reported in Figure 37. The maximum of 107 is reached between 17:00 and 19:00 the minimum of 100 is reached between 2:00 and 4:00.

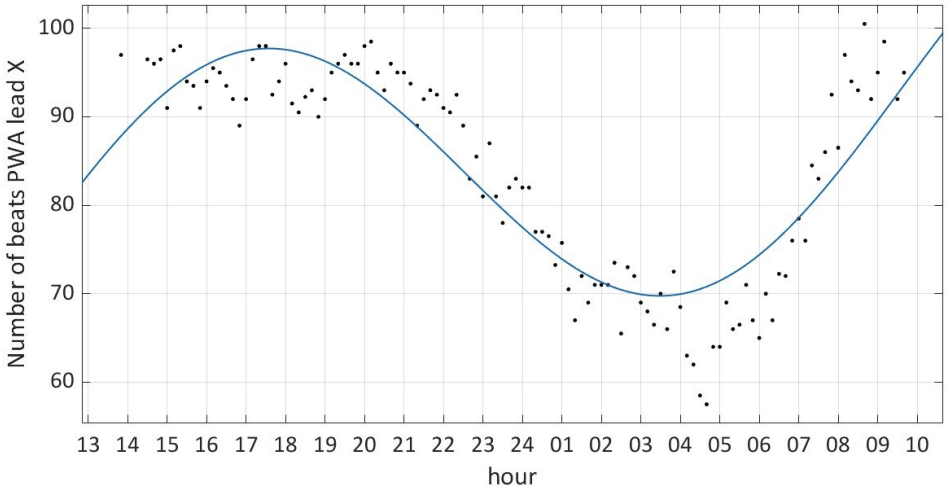

Figure 3 Figure 30 PWA (P wave alternans) in terms of number of heart beats per window (PWA-D) registered al level of lead X

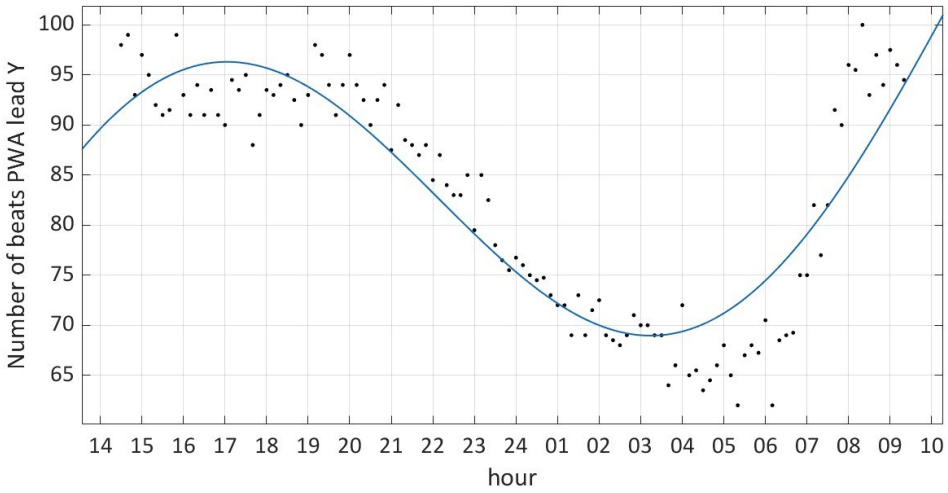

Figure 31 PWA (P wave alternans) in terms of number of heart beats per window (PWA-D) registered al level of lead Y

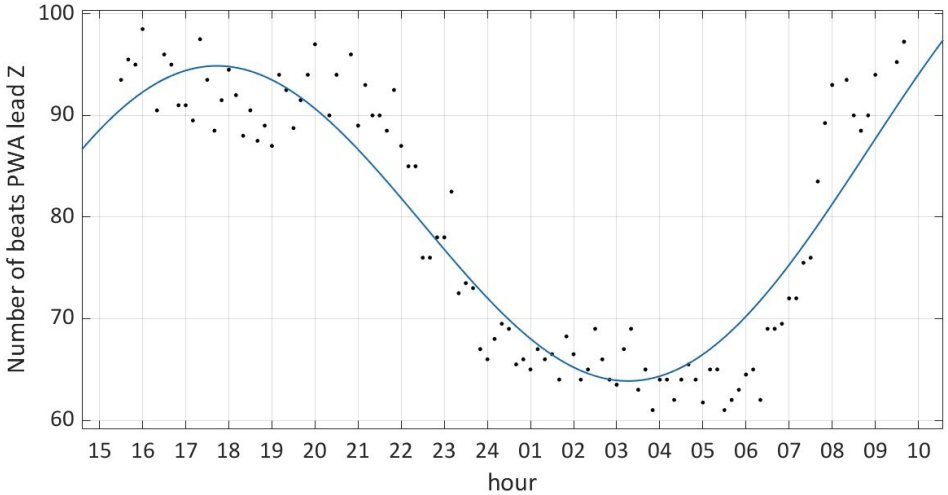

Figure 32 PWA (P wave alternans) in terms of number of heart beats per window (PWA-D) registered al level of lead Z

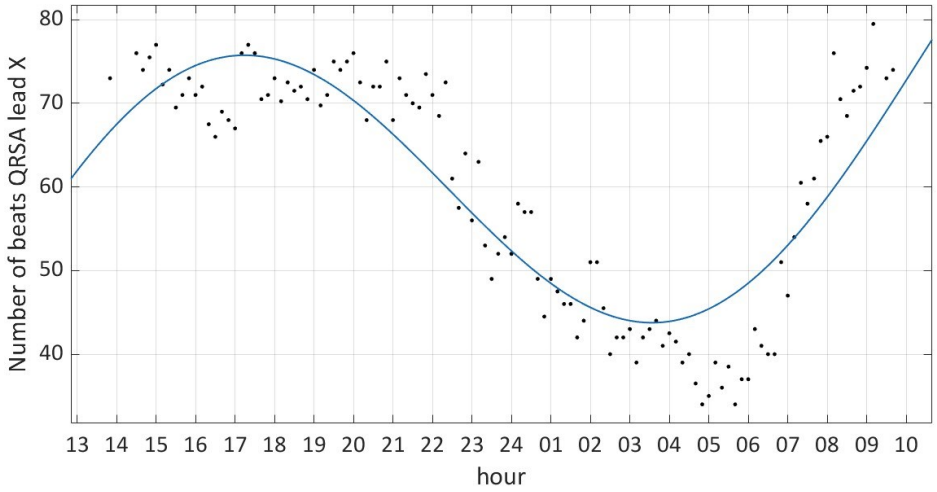

Figure 33 QRSA (QRS complex alternans) in terms of number of heart beats per window (QRSA-D) registered al level of lead X

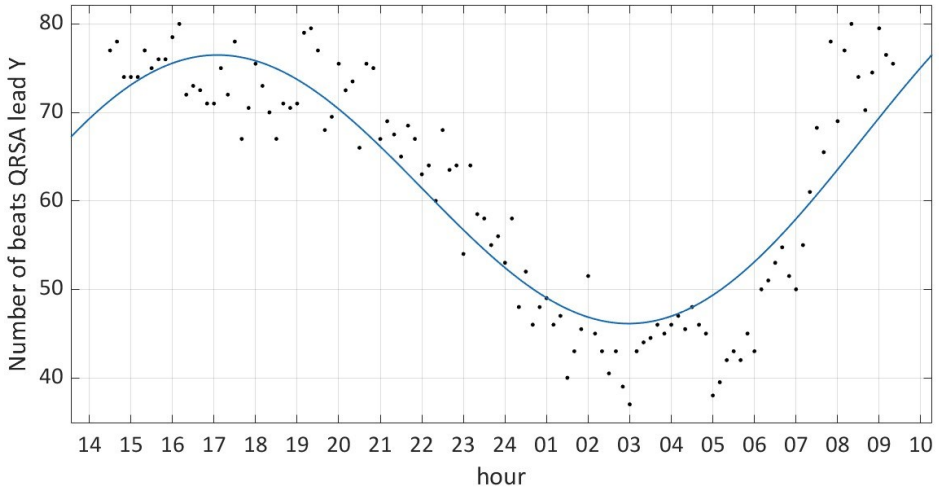

Figure 34 QRSA (QRS complex alternans) in terms of number of heart beats per window (QRSA-D) registered al level of lead Y

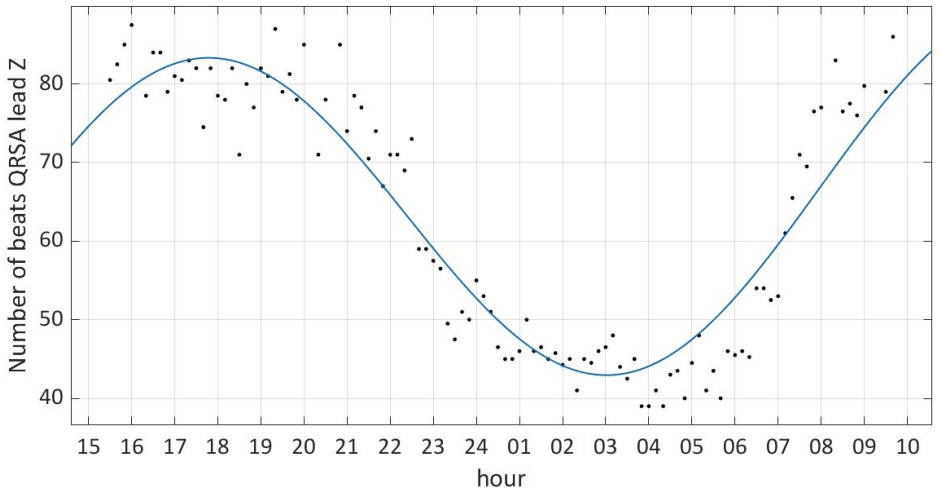

Figure 35 QRSA (QRS complex alternans) in terms of number of heart beats per window (QRSA-D) registered al level of lead Z

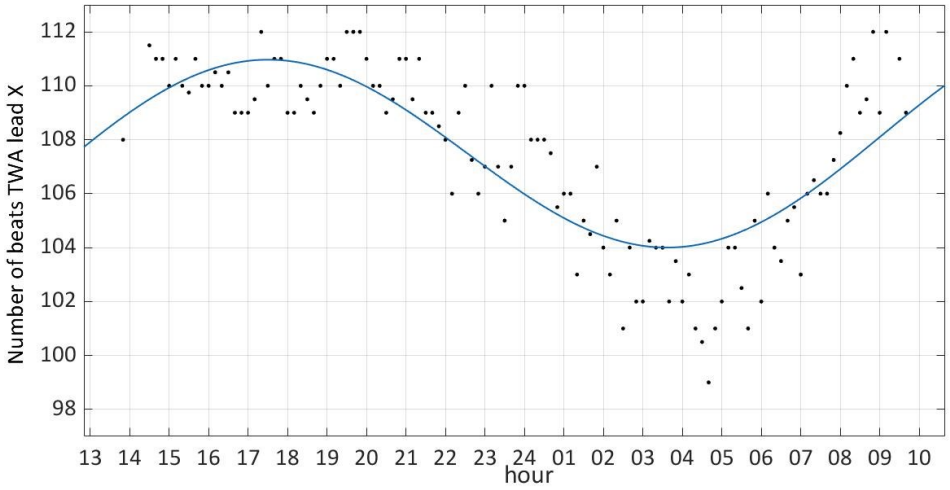

Figure 36 TWA (T wave alternans) in terms of number of heart beats per window (TWA-D) registered al level of lead X

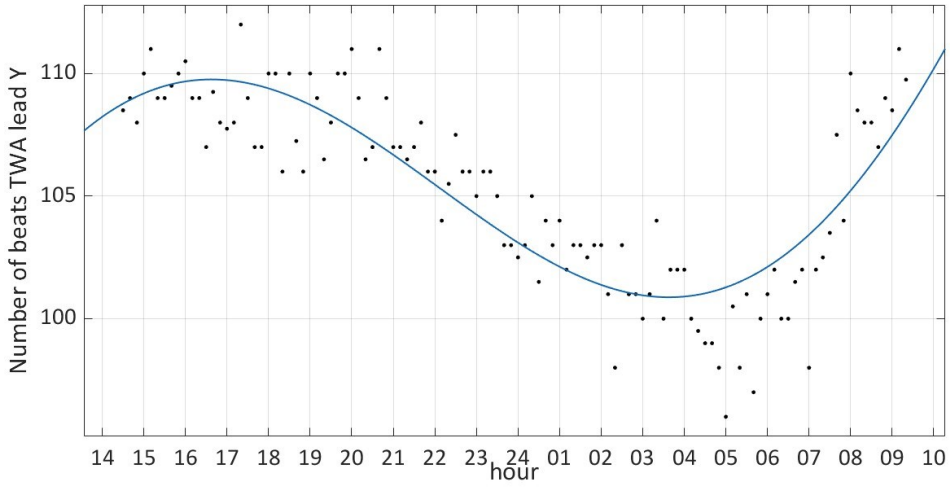

Figure 37 TWA (T wave alternans) in terms of number of heart beats per window (TWA-D) registered al level of lead Y

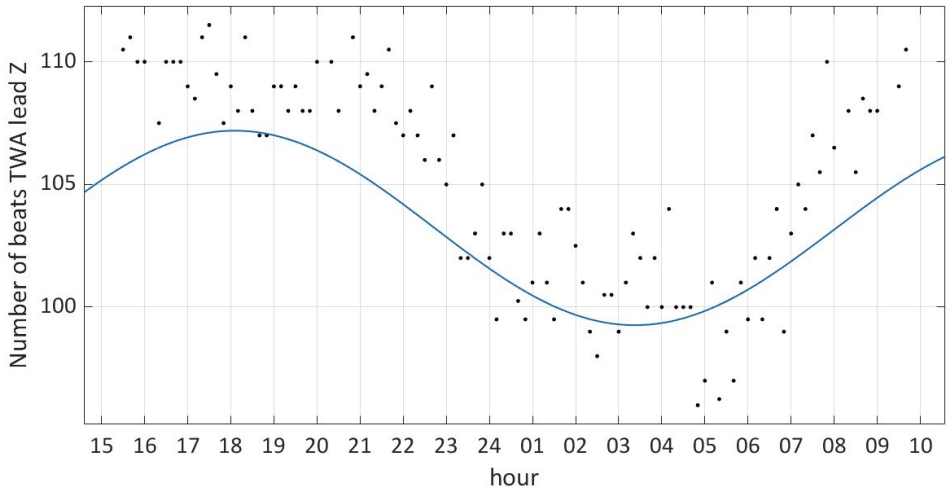

Figure 38 TWA (T wave alternans) in terms of number of heart beats per window (TWA-D) registered al level of lead Z

4.2.3 Magnitude

All results reported below are reported in terms of magnitude (ECGA-M) (μV*number of alternating heart beast (μV*n)).

Results show that 52% of subjects (31 subjects) registered at level of lead X a maximum value of PWA-M during daily hours, reaching between 1525μV*n and 21061μV*n. At level of lead Y, the maximum value of PWA-M was registered during daily hours by 52% of subjects (31 subjects), in a range between 1518μV*n and 20943μV*n. At level of lead Z, the maximum value of PWA-M was registered during daily hours by 42% of subjects (25 subjects), in a range between 1318μV*n and 16978μV*n. 42% of subjects (25 subjects) registered at level of lead X a minimum value of PWA-M during nocturnal hours, reaching between 108μV*n and 2055μV*n. At level of lead Y, the minimum value of PWA-M was registered during nocturnal hours by 40% of subjects (24 subjects), in a range between 175μV*n and 2041μV*n. At level of lead Z, the minimum value of PWA-M was registered during nocturnal hours by 43% of subjects (26 subjects), in a range between 135μV*n and 1247μV*n. PWA-M maximum and minimum values for each subject are reported in Table 7B in Appendix B.

Results show that 52% of subjects (31 subjects) registered at level of lead X a maximum value of QRSA-M during daily hours, reaching between 942μV*n and 7368μV*n. At level of lead Y, the maximum value of QRSA-M was registered during daily hours by 42% of subjects (25 subjects), in a range between 819μV*n and 5691μV*n. At level of lead Z, the maximum value of QRSA-M was registered during daily hours by 52% of subjects (31 subjects), in a range between 812μV*n and 6944μV*n. 33% of subjects (20 subjects) registered at level of lead X a minimum value of QRSA-M during nocturnal hours, reaching between 25μV*n and 1319μV*n. At level of lead Y, the minimum value of QRSA-M was registered during nocturnal hours by 40% of subjects (24 subjects), in a range between 0μV*n and 938μV*n. At level of lead Z, the minimum value of QRSA-M was registered during nocturnal hours by 35% of subjects (21 subjects), in a range between 30μV*n and 1388μV*n. QRSA-M maximum and minimum values for each subject are reported in Table 8B in Appendix B.

Results show that 52% of subjects (31 subjects) registered at level of lead X a maximum value of TWA-M during daily hours, reaching between 1645μV*n and 39076μV*n. At level of lead Y, the maximum value of TWA-M was registered during daily hours by 57%

of subjects (34 subjects), in a range between 1696μV*n and 40699μV*n heart beats per window. At level of lead Z, the maximum value of TWA-M was registered during daily hours by 53% of subjects (32 subjects), in a range between 1550μV*n and 13804μV*n. 40% of subjects (24 subjects) registered at level of lead X a minimum value of TWA-M during nocturnal hours, reaching between 292μV*n and 2056μV*n. At level of lead Y, the minimum value of TWA-M was registered during nocturnal hours by 45% of subjects (27 subjects), in a range between 324μV*n and 2044μV*n. At level of lead Z, the minimum value of TWA-M was registered during nocturnal hours by 37% of subjects (22 subjects), in a range between 171μV*n and 1578μV*n. TWA-M maximum and minimum values for each subject are reported in Table 9B in Appendix B.

The PWA-M cumulative values on lead X range between 560μV*n and 1450μV*n (mean value 1015μV*n, sd of 244). The trend of the fitting of the PWA-M registered on lead X cumulative values is reported in Figure 39. The maximum of 1307μV*n is reached between 16:00 and 19:00 and the minimum of 683μV*n is reached between 2:00 and 5:00.

The PWA-M cumulative values on lead Y range between 615μV*n and 1390μV*n (mean value 951μV*n, sd of 217). The trend of the fitting of the PWA-M registered on lead Y cumulative values is reported in Figure 40. The maximum of 1227μV*n is reached between 16:00 and 18:00 and the minimum of 696μV*n is reached between 2:00 and 5:00.

The PWA-M cumulative values on lead Z range between 594μV*n and 1478μV*n (mean value 907μV*n, sd of 247). The trend of the fitting of the PWA-M registered on lead Z cumulative values is reported in Figure 41. The maximum of 1235μV*n is reached between 15:00 and 18:00 and the minimum of 640μV*n is reached between 2:00 and 4:00.

The QRSA-M cumulative values on lead X range between 340μV*n and 1001μV*n (mean value 669μV*n, sd of 177). The trend of the fitting of the QRSA registered on lead X cumulative values is reported in Figure 42. The maximum of 863μV*n is reached between 17:00 and 19:00 and the minimum of 414μV*n is reached between 2:00 and 5:00.

The QRSA cumulative values on lead Y range between 398μV*n and 949μV*n (mean value 663μV*n, sd of 155). The trend of the fitting of the QRSA registered on lead Y

cumulative values is reported in Figure 43. The maximum of 857μV*n is reached between 16:00 and 19:00 and the minimum of 470μV*n is reached between 2:00 and 4:00.

The QRSA cumulative values on lead Z range between 398μV*n and 1344μV*n (mean value 767μV*n, sd of 277). The trend of the fitting of the QRSA registered on lead Z cumulative values is reported in Figure 44. The maximum of 1137μV*n is reached between 16:00 and 19:00 and the minimum of 434μV*n is reached between 2:00 and 4:00.

The TWA-M cumulative values on lead X range between 1103μV*n and 1923μV*n (mean value 1554μV*n, sd of 187). The trend of the fitting of the TWA-M registered on lead X cumulative values is reported in Figure 45. The maximum of 1740μV*n is reached between 17:00 and 20:00 and the minimum of 1370μV*n is reached between 4:00 and 7:00.

The TWA-M cumulative values on lead Y range between 1058μV*n and 1908μV*n (mean value 1491μV*n, sd of 191). The trend of the fitting of the TWA-M registered on lead Y cumulative values is reported in Figure 46. The maximum of 1670μV*n is reached between 17:00 and 19:00 and the minimum of 1313μV*n is reached between 5:00 and 7:00.

The TWA-M cumulative values on lead Z range between 995μV*n and 2072μV*n (mean value 1398μV*n, sd of 212). The trend of the fitting of the TWA-M registered on lead Z cumulative values is reported in Figure 47. The maximum of 1640μV*n is reached between 17:00 and 19:00 and the minimum of 1195μV*n is reached between 1:00 and 4:00.

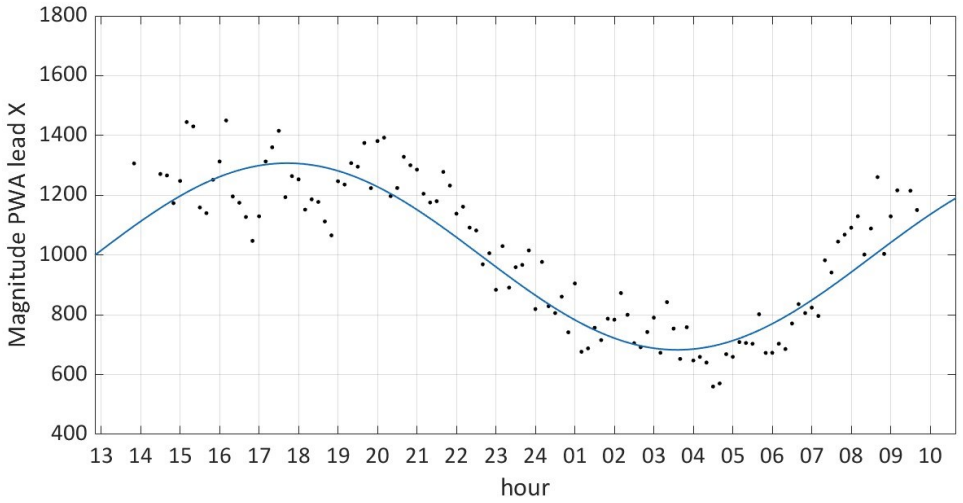

*Figure 39 PWA (P wave alternans) in terms of magnitude (PWA-M) registered al level of lead X (µV*n)*

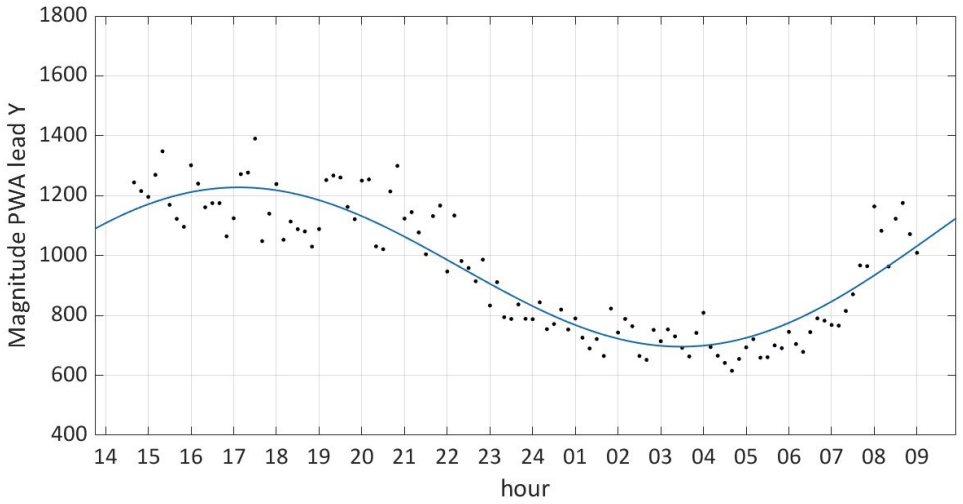

*Figure 40 PWA (P wave alternans) in terms of magnitude (PWA-M) registered al level of lead Y (µV*n)*

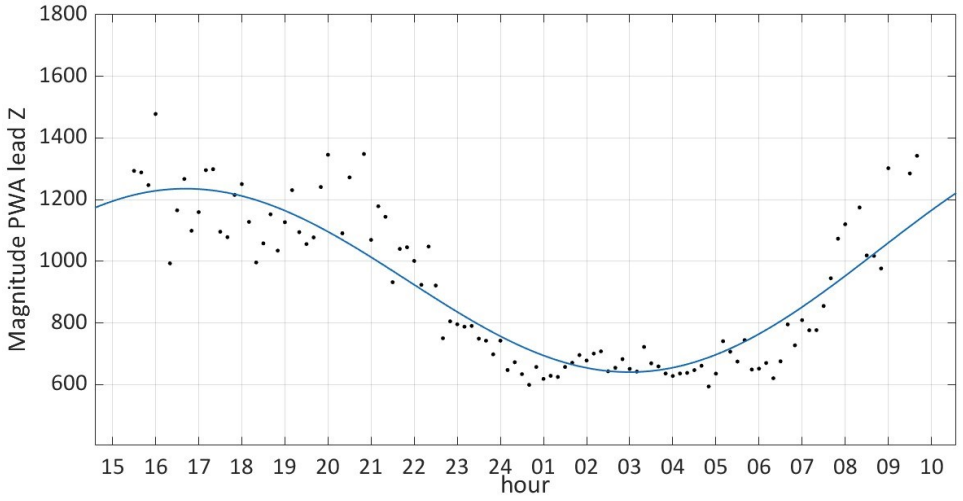

*Figure 41 PWA (P wave alternans) in terms of magnitude (PWA-M) registered al level of lead Z (µV*n)*

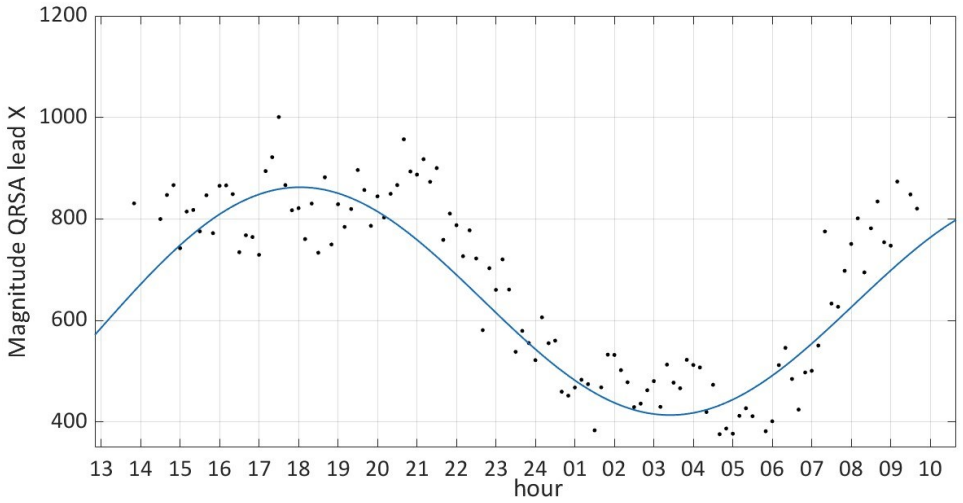

*Figure 42 QRSA (QRS complex alternans) in terms of magnitude (QRSA-A) registered al level of lead X (µV*n)*

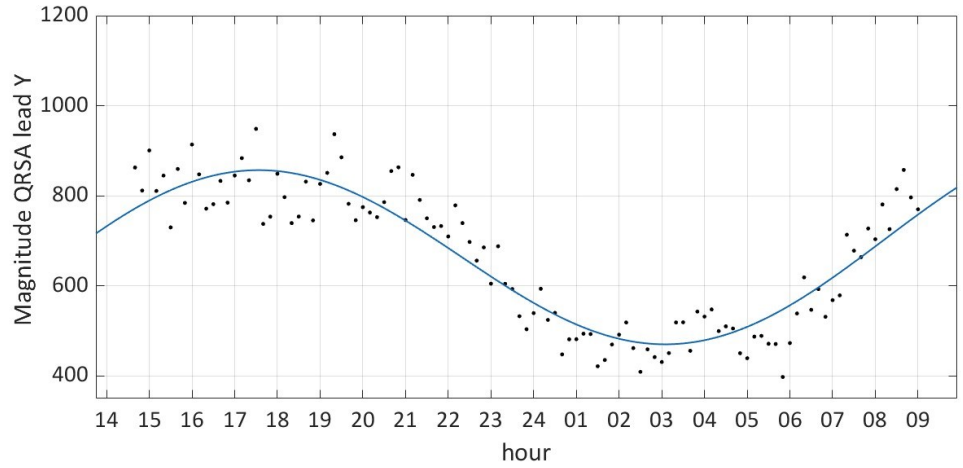

*Figure 43 QRSA (QRS complex alternans) in terms of magnitude (QRSA-M) registered al level of lead Y (µV*n)*

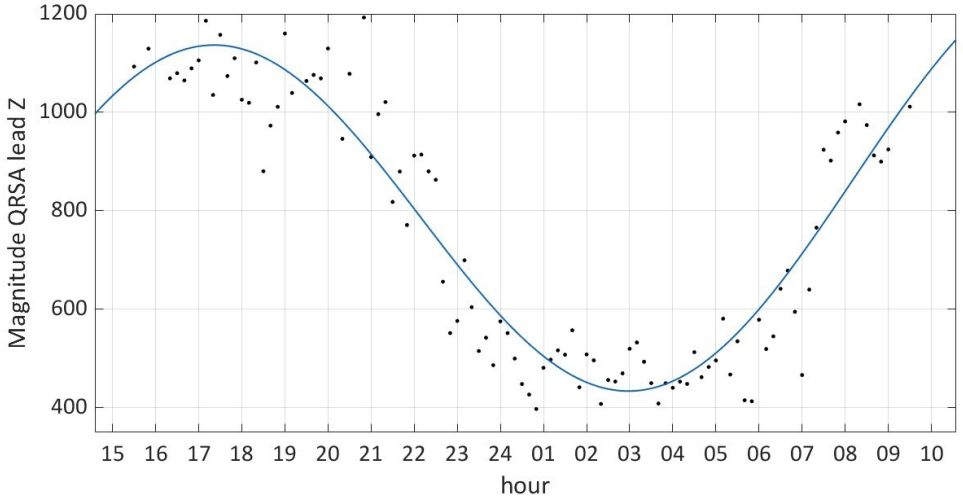

*Figure 44 QRSA (QRS complex alternans) in terms of magnitude (QRSA-M) registered al level of lead Z (µV*n)*

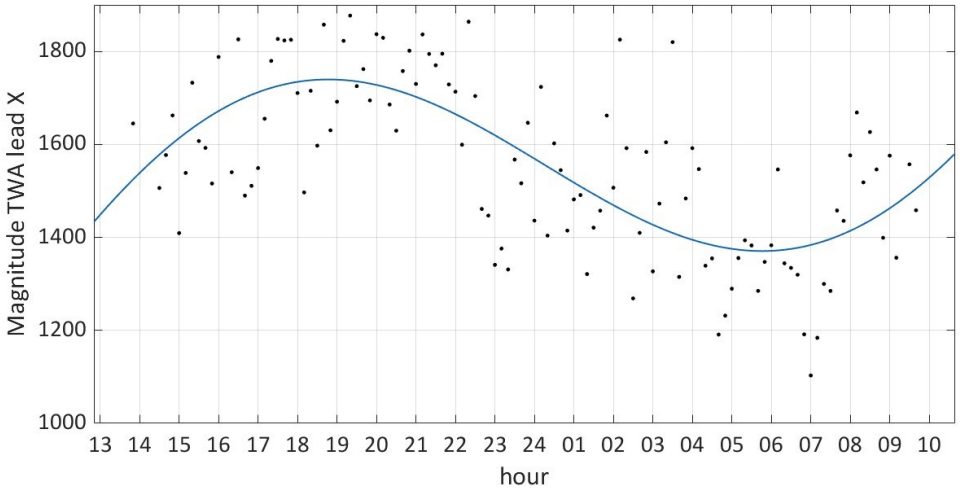

*Figure 45 TWA (T wave alternans) in terms of magnitude (TWA-M) registered al level of lead X (µV*n)*

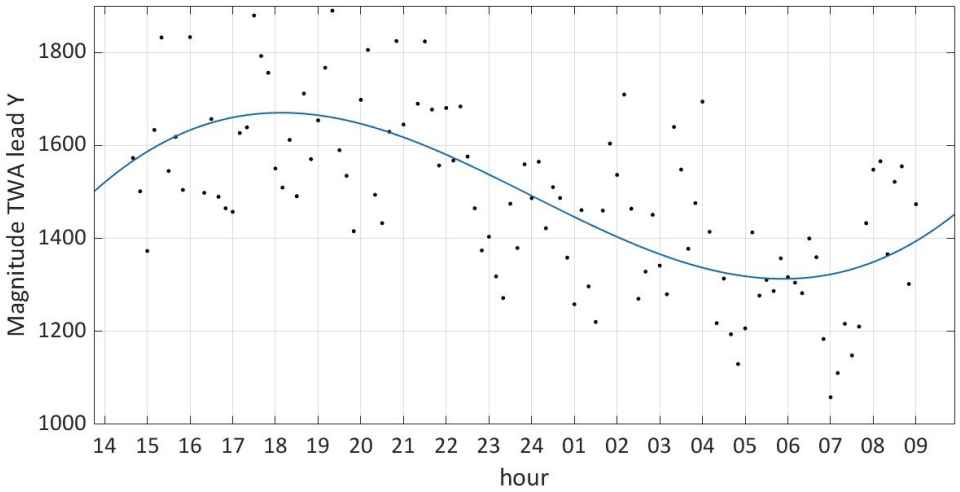

*Figure 46 TWA (T wave alternans) in terms of magnitude (TWA-M) registered al level of lead Y (µV*n)*

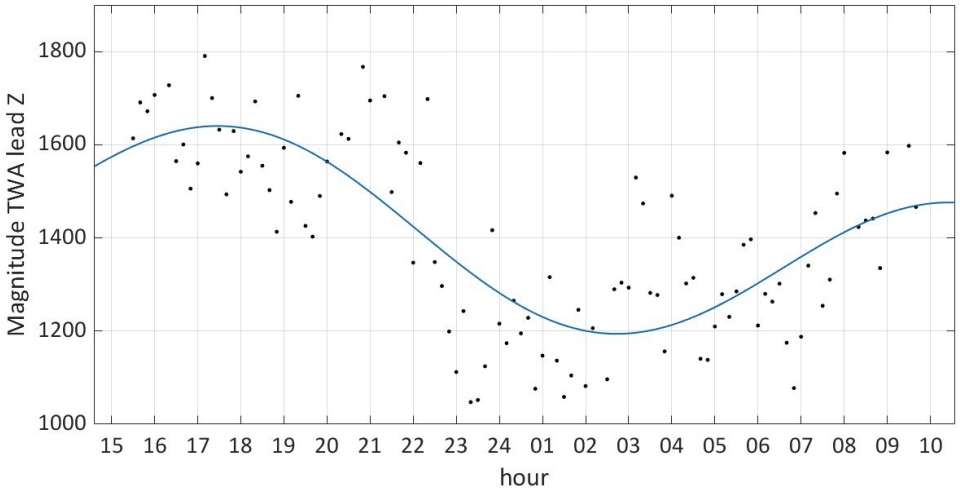

*Figure 47 TWA (T wave alternans) in terms of magnitude (TWA-M) registered al level of lead Z (µV*n)*

4.2.4 Overview

The total analysis (pre-processing and processing steps) required between 24h and 48h for each subject to be completed. The R-squared values associated to each fit of the cumulative values observable in Figure 21-47 ranged between 0.51 and 0.88.

The median PWA-A, QRSA-A and TWA-A over the 3 leads (X, Y and Z) and over all the subjects are reported in Figure 48. The absolute maximum and minimum values of PWA-A, QRSA-A and TWA-A mediated over the 3 leads and over all the subjects are reported in Table 2.

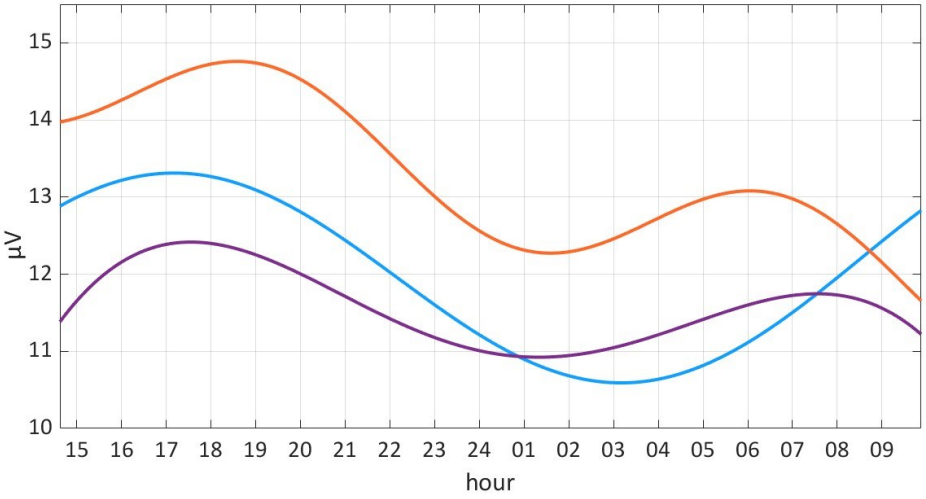

Figure 48 Median P wave alternans in terms of amplitude (PWA-A) (sky-blue line), QRS complex alternans in terms of amplitude (QRSA-A) (purple line) and T wave alternans in terms of amplitude (TWA-A) (orange line) over the 3 leads (X, Y and Z) and over all the subjects

Table 2 Maximum and minimum value of P wave alternans in terms of amplitude (PWA-A), QRS complex alternans in terms of amplitude (QRSA-A) and T wave alternans in terms of amplitude (TWA-A) mediated over the 3 leads (X, Y and Z) and over all the subjects

	PWA-A		QRSA-A		TWA-A	
	Value (μV)	Hour	Value (μV)	Hour	Value (μV)	Hour
Max	13	between 16:00 and 18:00	12	between 16:00 and 19:00	15	between 17:00 and 20:00
Min	11	between 02:00 and 04:00	11	between 24:00 and 02:00	12	between 24:00 and 03:00

The median PWA-D, QRSA-D and TWA-D over the 3 leads (X, Y and Z) and over all the subjects are reported in Figure 49. The absolute maximum and minimum values of PWA-D, QRSA-D and TWA-D mediated over the 3 leads and over all the subjects are reported in Table 3.

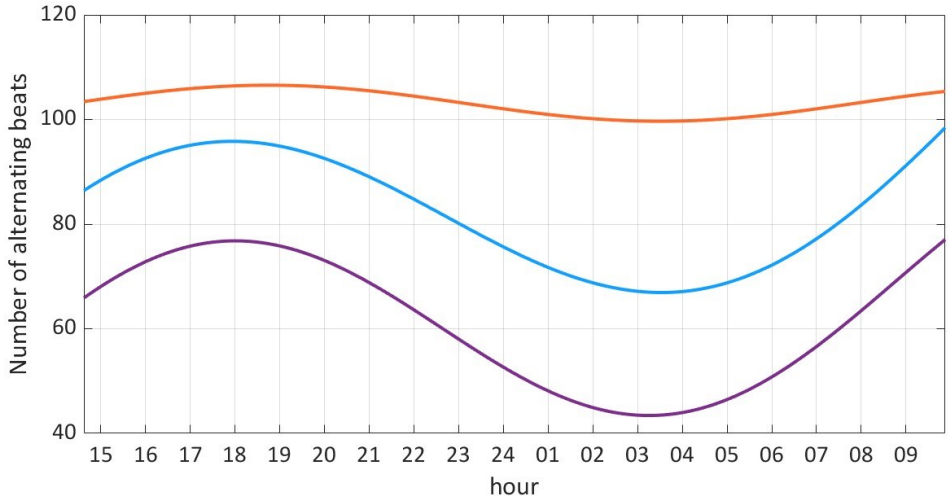

Figure 49 Median P wave alternans in terms of number on alternating beats (PWA-D) (sky-blue line), QRS complex alternans in terms of number on alternating beats (QRSA-D) (purple line) and T wave alternans in terms of number on alternating beats (TWA-D) (orange line) over the 3 leads (X, Y and Z) and over all the subjects

Table 3 Absolute maximum and minimum value of P wave alternans in terms of number on alternating beats (PWA-D), QRS complex alternans in terms of number on alternating beats (QRSA-D) and T wave alternans in terms of number on alternating beats (TWA-D) mediated over the 3 leads (X, Y and Z) and over all the subjects

	PWA-D		QRSA-D		TWA-D	
	Value	Hour	Value	Hour	Value	Hour
Max	96	between 17:00 and 19:00	77	between 17:00 and 19:00	107	between 17:00 and 20:00
Min	67	between 02:00 and 05:00	43	between 02:00 and 05:00	100	between 02:00 and 05:00

The median PWA-M, QRSA-M and TWA-M over the 3 leads (X, Y and Z) and over all the subjects are reported in Figure 50. The absolute maximum and minimum values of PWA-M, QRSA-M and TWA-M mediated over the 3 leads and over all the subjects are reported in Table 4.

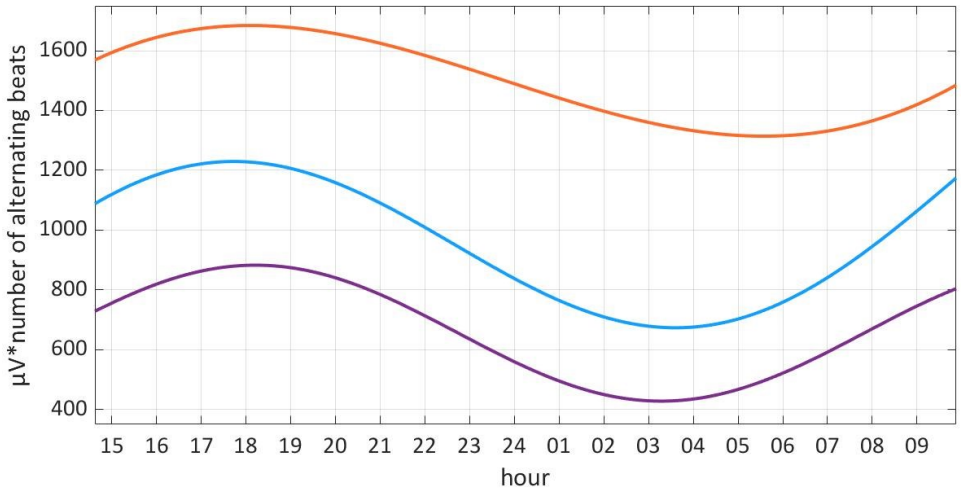

Figure 50 Median P wave alternans in terms of magnitude (PWA-M) (sky-blue line), QRS complex alternans in terms of magnitude (QRSA-M) (purple line) and T wave alternans in terms of magnitude (TWA-M) (orange line) over the 3 leads (X, Y and Z) and over all the subjects

Table 4 Absolute maximum and minimum value of P wave alternans in terms of magnitude (PWA-M), QRS complex alternans in terms of magnitude (QRSA-M) and T wave alternans in terms of magnitude (TWA-M) mediated over the 3 leads (X, Y and Z) and over all the subjects

	PWA-M		QRSA-M		TWA-M	
	Value (µV*n)	Hour	Value (µV*n)	Hour	Value (µV*n)	Hour
Max	1229	between 16:00 and 19:00	882	between 17:00 and 19:00	1684	between 17:00 and 19:00
Min	673	between 01:00 and 04:00	428	between 02:00 and 04:00	1314	between 04:00 and 07:00

5.
Discussion
and
Conclusion

The prior aim of this thesis was to review the information present in literature regarding the circadian rhythm of ECGA. The results show that only 1 paper concerns all types of ECGA (TWA, PWA and QRSA). That distribution of the articles is understandable since, as declared before, TWA is the most studied and reported in literature among all the electrocardiographic alternans typologies. Since the MMAM method provides good results when TWA is truly present and since it is integrated in many commercial ECG machines, it was expected that it was the most used method to identify TWA. Indeed, it was used in 44% of articles despite the fact that it is susceptible to provide false positive and introduces a time delay. Moreover, the results indicate that the only method that was applied to identify and measure all 3 types of ECGA is the EAMF, the same method optimized and used to analyse the data in this thesis. In 78% of papers (7 papers) the data derived from Holter exams were acquired through 3 leads. In particular, in 2 articles the Holter exams were recorded through the pseudo-orthogonal leads (X, Y and Z), pointing out the possibility of properly detecting the ECGA by the mean of that kind of leads as done in this thesis. In all papers the results show that the 3 ECGA types are modulated by a circadian pattern. Even if the papers concerning the circadian TWA rhythm are limited to a small number (8 papers), their results seem to be in accordance with what it is expectable. Indeed, as previously stated, TWA is an index of cardiovascular risk, in particular related to the risk of developing arrhythmias. In all papers TWA is reported to have an increasing during day and a decreasing during night, as observable in Table 1. Thus, it may seem to follow the same general pathway associated to the arrhythmias (major frequency during day and minimum during night). Even for all ECGA types, it is reported that is generally proper to talk about circadian rhythm with an increasing in daily hours, particularly in the afternoon, and a decreasing during night. These results are reported both for diseased and healthy subjects. Anyway, most of the studied population is composed by diseased subjects (1380 diseased; 106 healthy). The limited number of studies concerning the circadian modulation of ECGA present in literature, in particular analysing a healthy population, highlights the necessity of enhance the research in that field.

The other aim of this thesis was to assess the circadian rhythm of the ECGA analysing real data of healthy subjects. To do that, prior to the application of the optimized EAMF method, the ECG signals were pre-processed. The pre-processing involved the

conversion of the data into mV and the subtraction from each signal of its average to bring the isoelectric to the equivalent of 0mV, in order to facilitate further analysis and calculations. Then, it was necessary to evaluate the standard deviation of each lead signal and to reject the windows with a standard deviation equal to zero. That step was implemented to detect the windows in which the signal was constant and was equal to the isoelectric (0mV). That condition reflects that the acquisition of the signal had some problems, probably due to the detachment of the electrodes. Thus, it was necessary to remove that part of the data and to not analyse it. Indeed, when the electrodes are not attached and no physiological signal is detected, the recorded ECG is a constant. The standard deviation of a constant is equal to zero. Therefore, evaluating the standard deviation of the signals represented a simple method to remove the windows without a true ECG acquisition.

Subsequently, a preliminary cleaning of the signal from the noise was done by filtering the data between 0.2Hz and 45Hz. High-frequency interference, greater than 45Hz, was eliminated. An example of high-frequency interference is that one due to the power supply of electrical devices. Even low-frequency artifacts below 0.2Hz were removed.

At that point the Pan-Tomkins algorithm was used to individuate the R peaks on the ECG signal coming from lead Y. The algorithm needs as input the signal coming from one of the available channels. Peaks from different leads and related to the same subject are in phase. Therefore, only a certain lead was used as input to the Pan-Tompkins algorithm. The choice of the lead was arbitrary.

After the detection and correction of R peaks, only windows with a number of R peaks between 60 and 230 were accepted for the consequent analysis. That choice reflected the necessity to identify only windows in which the number of R peaks is compliant with the normal heart rate. Indeed, being the subjects all healthy, their heart rate normally oscillates in the range of 30bpm (60 R peaks in 120s) and 115bpm (230 R peaks in 120s). Therefore, a number of R peaks lower than 60 or major than 230, was considered to be due to errors in correctly detecting the R peaks caused by a heavy noise presence. Thus, the noisy windows were not considered suitable for the study.

The R peaks detection, and the subsequent identification of the fiducial points, were necessary for the use of the EAMF method, therefore, for the actual study of the PWA, QRSA and TWA.

The EAMF method was chosen for its robustness to noise and its unique capability to detect all types of ECGA. Anyway, it was modified to be properly used with the data coming from the database taken into consideration. Indeed, in the original version of the EAMF, only the median sections' waveforms were computed, without any alignment of the sections and without correcting the median. So, in the original version, the median sections waveforms were calculated considering all the sections without previously aligning the sections and without removing those ones with a correlation lower than 0.3. That modification was introduced to identify median sections' waveforms as clean as possible of noise and interference and being truly representative of the sections' waveforms of each window. The correlation is a measure of the similarity of the signals it is computed between. The correlation between delayed signals results lower with respect to synchronous signals. Thus, the alignment represents an optimization of the method to have a reliable measure of the correlation between the sections' waveforms. Moreover, the calculation of the median sections' waveforms is performed to identify waveforms that are representative of each window. The median computed considering aligned signals and without those sections with a lower correlation than 0.3 (considered as affected by noise and interference) is more truly representative than the simple median calculated in the original version of EAMF. For the same reasons, each section and its representative median were first aligned, prior to the calculation of correlation between them.

At the end of the processing phase, results of ECGA-A, ECGA-D and ECGA-M for each subject were available. The amplitude, the number of altering beats and the magnitude are 3 ways to characterize the same phenome (ECGA) but with slightly variations. In fact, in literature thresholds in terms of amplitude are reported to be more suitable to identify TWA lasting few beats but with a high amplitude. On the contrary, thresholds in terms of altering beats are reported to be more suitable to identify TWA of long duration even if of low amplitude. Finally, thresholds in terms of magnitude (which is actually a combination of amplitude and number of altering heart beats) are reported to be more suitable to identify TWA with amplitude and duration in the middle [39]. Furthermore, in the original version of the EAMF method, the ECGA is described through a parameter called area. Anyway, because of how the area is defined, the modulations during the hours of the day in terms of amplitude or in terms of area have the same trend [25].

ECGA-A, ECGA-D and ECGA-M values were mediated each 10 minutes to have more easily manageable and visualizable data. Then, the data were mediated over all the subjects to have results representative of the entire population and fitted through a 2-sins-sum model. The R-squared values associated to that fittings were all major than 0.5. The R-squared is a measure of the goodness of the fitting that can range between 0 and 1. Even if there is no standard range of R-squared values for which a fitting can be defined good, it is generally acknowledged that between 0.5 and 0.9 the goodness oscillates from acceptable to very high. The results confirm that PWA, QRSA and TWA are modulated by a circadian pattern. Generally, the trends of all the 3 types of ECGA have an increase during daily hours reaching an absolute maximum in the afternoon (12:00-18:00) and then a decreasing reaching a minimum during the night as observable in Figure 21-47. That modulation is in line with the information reported by the papers reviewed in this thesis and with the modulation of the cardiac arrhythmias confirming the relationship between ECGA and higher cardiovascular risk. The trends of the 3 types of ECGA present a monophasic shape (unique maximum and unique minimum during the 24h) with the exception of TWA-A on lead Z and QRSA-A on leads X, Y and Z. TWA-A on lead Z and QRSA-A on leads X, Y and Z have a biphasic shape with an absolute maximum in the afternoon, a minimum between 24:00 and 2:00 and then an increasing with a second maximum in the morning. Anyway, the difference between the minimum and the second maximum is lower than 2μV. Being the difference so small and being the resolution of the EAMF method of 1μV, the biphasic shape can be due to artifacts and not representing a real biphasic physiological modulation. A difference among the 3 leads (X, Y and Z) is appreciable for ECGA-A, ECGA-D and ECGA-M. The difference is present for PWA, QRSA and TWA, confirming that ECGA is a lead dependent phenomenon [25].

The 2-sins-sum model was chosen because a single-harmonic (sine or cosine) model would not have been able to accurately capture the data trends. Indeed, the data were not conformed to a perfect sinusoidal pattern. That finding is explicable due to the lack of a perfect balance between waking and sleeping times over the 24-hour period. Moreover, it highlights that ECGA is influenced by the sleep-wake rhythm.

The values of ECGA-A, ECGA-D and ECGA-M mediated over the subjects were subsequently mediated over the 3 leads (X, Y and Z) to have an overview of the results

and to allow a clearer comparison between PWA, QRSA and TWA. Figure 48-50 indicate that T wave reaches higher value of alternans respect to the P wave and the QRS complex; the QRS complex reaches the lowest values. However, the circadian modulation is more clearly visible for the PWA and less for the QRSA in which the trend has fewer absolute variations in terms of amplitude, number of alternating beats and magnitude.

Finally, this thesis provided reference ranges of ECGA in healthy subjects. Having normal ranges may allow the establishment of thresholds for the risk assessment according to the hour of the day. The values of ECGA-A, ECGA-D and ECGA-M were compared to those in literature to determine the reliability of the ranges obtained in this thesis. A consistent comparison is possible just when the methods and conditions of examination are analogous. TWA has been already investigated through the X, Y and Z leads and the AMFM method in healthy subject, even if the ECG data were limited in time and not covering the entire day. Since the AMFM is a precursor of EAMF, a comparison is feasible. The values obtained in this thesis of TWA-A, TWA-D and TWA-M are in line with the ones reported in literature but slightly lower [51], [52]. The fact that they are lightly inferior is understandable because the EAMF was designed to make each wave (P, QRS, T) independent from the other by computing the P wave signal, QRS complex signal and T wave signal. When using the AMFM, instead, that improvement is absent so each of 3 types of ECGA (PWA, QRSA and TWA) can be influenced by the presence of the others, introducing a possible overestimation [53]. ECGA-A, ECGA-D and ECGA-M have been studied using the EAMF method in healthy subjects. Even in this case, the data were acquired through ECG limited to some minutes, not through the Holter instrument. Anyway, it is observable that the reported results are compliant with the ones in this thesis. Thus, the ECGA values obtained in this thesis seem plausible and respect to previous studies they add the possibility to have reference ranges during the different hours of the day [54].

The time needed to complete the pre-processing and processing of the real data required, as declared, between 24h and 48h for each subject. Thus, the analysis of the ECGA demanded an elevated computational effort. That is the reason beyond the fact that the subjects included in the population of this thesis were a subset of the entire database available. However, the population of this thesis can be considered

representative because it is heterogeneous in terms of variables such as age, BMI, gender and smoking habit. Furthermore, its dimension is bigger than the population size considered by 5 reviewed papers, underlining its appropriateness. It was tried to stratify the results according to the gender, the BMI and the smoking habit. Anyway, in that case the subpopulation sizes (divided in male/female, normal weight/underweight/overweight, not smoker/smoker) were too limited to allow a proper identification of the ECGA circadian pattern.

In conclusion, the information present in literature reveals the existence of the circadian periodicity of ECGA, in both healthy and diseased subjects. In the healthy population studied in this thesis, it is confirmed the physiological circadian modulation of ECGA. Future studies on larger population may highlight the influence of anthropometric data (e.g., BMI, age) and of lifestyle (e.g., smoking) on the modulation of ECGA during the hours of the day.

Appendix A

*Table 1A Population main features.*Beta_BLK=Beta blockers intake: 1=Yes, 0=No. **1=smoker, 0=not smoker. ***BMI=Body Mass Index. N.A.=not available*

Subject ID	Beta_BLK*	Smoking**	Age (years)	Gender	BMI***
1017	0	1	22	Female	22.22
1018	0	0	13	Male	20.4
1027	0	1	64	Male	24.45
1030	0	1	53	Female	21.78
1041	0	0	22	Female	24.38
1042	0	0	N.A.	Female	19.49
1043	0	N.A.	49	Female	33.77
1044	0	0	19	Male	21.46
1045	0	0	21	Male	19.84
1046	0	0	21	Male	22.68
1047	0	0	25	Female	20.94
1048	1	0	48	Male	26.85
1049	0	1	47	Female	23.94
1056	1	0	61	Female	25.76
2001	0	0	24	Male	27.69
2002	0	0	23	Male	25.25
2003	0	0	46	Male	26.59
2004	0	0	27	Female	25.95
2005	0	0	41	Male	27.73
2006	0	0	29	Female	23.34
2007	0	1	51	Female	N.A.
2009	0	0	23	Male	28.29
2010	0	0	34	Male	29.22
2011	0	0	54	Female	20.42
2012	0	0	47	Male	28.03
2013	0	0	27	Male	26.85
2014	0	0	34	Male	28.7
2015	0	1	55	Male	24.22
2016	0	1	65	Female	31.24
2017	0	1	48	Male	29.32
4034	0	0	40	Female	21.09
4035	0	1	40	Male	20.98
4038	0	0	44	Male	25.8
4043	0	0	44	Female	20.7
4050	0	0	24	Female	21.34
4057	0	0	36	Male	23.1
4058	0	0	31	Male	24.41
4073	0	0	19	Female	20.15
4076	0	0	22	Male	21.37
4085	0	1	40	Female	21.94
10022	0	0	48	Male	21.56

10023	0	0	28	Female	21.41
10050	0	1	32	Male	24.62
10048	0	1	49	Male	22.86
10069	0	0	17	Female	26.17
10082	0	0	48	Female	17.72
10083	0	1	45	Female	22.27
10084	0	1	56	Male	31.02
10085	0	1	76	Female	34.52
10086	0	0	16	Female	31.22
10087	0	0	75	Male	22.49
10090	0	0	32	Female	26.49
10091	0	0	33	Female	23.88
10094	0	1	43	Female	18.47
10095	0	0	27	Female	45.04
10096	0	0	68	Male	26.83
10101	0	1	58	Female	24.61
10102	0	0	42	Female	23.62
10103	0	1	47	Female	26.57
10106	0	0	N.A.	Male	21.14

Appendix B

*Table 1B Daily maximum and minimum P wave alternans values in terms of amplitude (PWA-A) for each subject. *Q1=first quartile; **Q3=third quartile*

	Lead X				Lead Y				Lead Z			
	Max		Min		Max		Min		Max		Min	
Subject ID	Value (μV)	Hour	Value (μV)	Hour	Value (μV)	Hour	Value (μV)	Hour	Value (μV)	Hour	Value (μV)	Hour
1017	12	21:00	8	17:00	14	6:00	5	14:00	13	12:00	7	17:00
1018	44	16:00	7	9:00	80	3:00	8	11:00	60	3:00	9	14:00
1027	13	09:00	8	20:00	18	8:00	8	23:00	16	10:00	7	20:00
1030	47	03:00	10	16:00	36	2:00	11	16:00	36	2:00	10	16:00
1041	25	18:00	10	6:00	20	12:00	10	16:00	41	18:00	11	1:00
1042	22	11:00	13	22:00	21	21:00	13	5:00	19	13:00	14	10:00
1043	20	10:00	8	4:00	22	1:00	9	0:00	21	2:00	7	0:00
1044	57	01:00	22	13:00	20	7:00	13	10:00	23	12:00	11	4:00
1045	29	19:00	13	7:00	26	12:00	11	5:00	35	11:00	13	7:00
1046	36	12:00	12	14:00	37	21:00	12	22:00	68	9:00	12	5:00
1047	56	14:00	17	5:00	40	9:00	12	18:00	19	22:00	9	17:00
1048	13	04:00	9	14:00	20	7:00	9	18:00	14	15:00	9	17:00
1049	25	14:00	9	5:00	28	9:00	8	3:00	32	9:00	8	3:00
1056	17	17:00	10	8:00	17	15:00	9	0:00	16	10:00	9	8:00
2001	13	00:00	8	8:00	13	2:00	8	18:00	13	9:00	8	18:00
2002	38	00:00	11	7:00	25	8:00	12	11:00	31	8:00	11	14:00
2003	18	10:00	7	0:00	21	15:00	8	2:00	13	9:00	8	2:00
2004	17	12:00	7	22:00	17	9:00	8	22:00	20	19:00	7	23:00
2005	17	13:00	9	22:00	17	12:00	9	22:00	13	7:00	9	0:00
2006	31	15:00	8	4:00	40	15:00	7	22:00	14	17:00	8	22:00
2007	16	19:00	7	22:00	32	14:00	7	22:00	17	20:00	7	22:00
2009	21	08:00	7	22:00	27	8:00	8	22:00	18	13:00	7	22:00
2010	21	12:00	11	9:00	31	2:00	10	18:00	24	3:00	11	18:00
2011	22	22:00	9	0:00	21	7:00	9	5:00	16	9:00	9	5:00
2012	27	12:00	8	22:00	19	12:00	10	20:00	32	12:00	10	22:00
2013	60	01:00	24	15:00	32	20:00	14	7:00	43	5:00	18	15:00
2014	14	21:00	6	10:00	12	21:00	8	9:00	12	15:00	7	20:00
2015	15	00:00	8	11:00	70	12:00	9	22:00	20	8:00	8	22:00
2016	15	05:00	6	11:00	14	13:00	6	1:00	12	9:00	6	20:00
2017	13	10:00	8	13:00	19	17:00	10	6:00	23	10:00	8	6:00
4034	25	10:00	8	1:00	17	19:00	8	1:00	26	23:00	8	1:00
4035	23	14:00	9	3:00	19	9:00	8	3:00	21	10:00	9	2:00
4038	24	13:00	9	9:00	26	12:00	10	9:00	28	12:00	11	1:00
4043	17	15:00	10	0:00	20	11:00	10	0:00	19	17:00	10	4:00
4050	15	17:00	8	11:00	24	9:00	7	0:00	10	5:00	7	0:00
4057	14	06:00	9	12:00	22	6:00	9	18:00	16	6:00	9	18:00
4058	14	14:00	8	8:00	16	3:00	7	8:00	14	14:00	7	8:00
4073	23	09:00	9	11:00	15	18:00	7	6:00	16	9:00	9	13:00
4076	35	18:00	11	5:00	35	4:00	10	23:00	50	4:00	9	22:00
4085	20	05:00	10	14:00	24	22:00	9	20:00	19	22:00	9	11:00
10022	34	04:00	17	2:00	18	16:00	9	22:00	36	10:00	10	22:00

10023	38	20:00	9	2:00	22	19:00	10	2:00	14	0:00	8	9:00
10048	24	11:00	13	23:00	25	18:00	10	3:00	35	10:00	12	3:00
10050	14	04:00	8	11:00	18	8:00	7	11:00	22	19:00	8	11:00
10069	20	09:00	7	5:00	20	8:00	8	4:00	20	9:00	7	3:00
10082	21	11:00	9	18:00	17	10:00	8	4:00	16	8:00	8	13:00
10083	18	13:00	10	0:00	28	17:00	9	0:00	14	22:00	7	7:00
10084	16	12:00	7	10:00	34	8:00	7	4:00	20	19:00	7	22:00
10085	24	03:00	8	4:00	21	12:00	9	1:00	20	3:00	7	22:00
10086	31	16:00	10	1:00	99	11:00	9	3:00	36	18:00	9	3:00
10087	16	02:00	7	4:00	19	17:00	8	2:00	42	15:00	9	8:00
10090	18	19:00	9	17:00	23	20:00	10	0:00	14	2:00	9	23:00
10091	18	12:00	7	2:00	16	20:00	9	10:00	13	3:00	7	9:00
10094	25	17:00	7	0:00	18	10:00	9	1:00	23	19:00	7	0:00
10095	18	08:00	8	18:00	15	10:00	8	15:00	22	8:00	8	0:00
10096	15	09:00	8	1:00	17	19:00	9	0:00	16	22:00	8	1:00
10101	18	15:00	10	8:00	27	1:00	12	8:00	17	1:00	11	8:00
10102	16	19:00	9	23:00	13	19:00	9	17:00	20	9:00	9	23:00
10103	100	20:00	7	1:00	21	23:00	8	21:00	16	10:00	7	2:00
10106	23	20:00	8	18:00	21	21:00	8	18:00	22	14:00	7	18:00
Median	20	15:00	9	12:30	21	15:00	9	22:00	20	15:00	9	22:00
Q1*	16	12:00	8	7:45	17	9:00	8	16:00	16	10:00	7	13:45
Q3**	26	20:00	10	22:00	27	20:15	10	1:00	27	22:15	9	0:00

*Table 2B Daily maximum and minimum QRS complex alternans values in terms of amplitude (QRSA-A) for each subject. *Q1=first quartile; **Q3=third quartile*

	Lead X				Lead Y				Lead Z			
	Max		Min		Max		Min		Max		Min	
Subject ID	Value (μV)	Hour	Value (μV)	Hour	Value (μV)	Hour	Value (μV)	Hour	Value (μV)	Hour	Value (μV)	Hour
1017	13	21:00	6	1:00	10	4:00	6	20:00	14	14:00	7	18:00
1018	106	12:00	7	22:00	33	3:00	9	12:00	13	21:00	6	1:00
1027	11	16:00	7	2:00	13	10:00	7	23:00	44	12:00	9	22:00
1030	20	2:00	9	16:00	18	2:00	10	16:00	12	15:00	7	22:00
1041	21	18:00	13	4:00	15	12:00	7	17:00	18	2:00	8	16:00
1042	15	15:00	12	22:00	14	16:00	10	11:00	20	18:00	9	2:00
1043	13	9:00	7	23:00	16	10:00	8	0:00	22	16:00	14	22:00
1044	36	1:00	16	13:00	38	7:00	14	17:00	15	9:00	7	23:00
1045	22	5:00	12	21:00	18	7:00	12	8:00	31	7:00	12	17:00
1046	24	9:00	12	11:00	23	21:00	12	13:00	37	9:00	12	16:00
1047	18	11:00	10	23:00	24	2:00	10	0:00	31	9:00	11	1:00
1048	13	5:00	8	17:00	13	7:00	8	17:00	21	11:00	12	1:00
1049	14	14:00	8	5:00	18	9:00	8	5:00	13	15:00	8	17:00
1056	18	17:00	10	8:00	18	17:00	10	8:00	21	9:00	7	3:00
2001	12	0:00	8	20:00	16	4:00	9	20:00	22	17:00	10	8:00
2002	24	0:00	10	14:00	21	1:00	12	14:00	14	4:00	8	20:00
2003	13	15:00	7	7:00	18	10:00	8	2:00	32	10:00	15	17:00
2004	12	2:00	6	22:00	16	8:00	7	22:00	13	11:00	7	2:00
2005	11	13:00	7	22:00	13	12:00	9	22:00	23	8:00	7	22:00
2006	18	15:00	8	22:00	21	15:00	7	22:00	14	10:00	8	18:00
2007	14	20:00	7	22:00	19	16:00	6	22:00	16	9:00	8	22:00
2009	24	8:00	8	22:00	18	8:00	7	22:00	16	20:00	8	22:00
2010	19	0:00	9	10:00	17	2:00	10	15:00	22	9:00	10	22:00
2011	15	13:00	9	5:00	21	13:00	12	3:00	20	3:00	10	20:00
2012	16	5:00	10	20:00	31	22:00	12	20:00	13	9:00	9	0:00
2013	40	5:00	21	15:00	28	21:00	12	19:00	32	12:00	11	20:00
2014	11	21:00	6	10:00	11	2:00	8	17:00	32	4:00	17	19:00
2015	16	3:00	7	9:00	32	12:00	9	22:00	13	2:00	8	8:00
2016	13	5:00	6	11:00	13	9:00	6	18:00	18	8:00	8	22:00
2017	13	0:00	8	13:00	13	17:00	9	13:00	14	5:00	6	1:00
4034	24	9:00	8	1:00	17	9:00	9	2:00	14	17:00	9	22:00
4035	14	11:00	8	2:00	18	5:00	7	13:00	22	19:00	8	1:00
4038	18	14:00	13	0:00	22	12:00	11	9:00	22	16:00	10	0:00
4043	14	11:00	9	18:00	14	11:00	8	10:00	21	12:00	11	1:00
4050	13	10:00	8	19:00	15	17:00	9	3:00	18	12:00	9	14:00
4057	24	5:00	10	17:00	23	5:00	9	9:00	16	18:00	9	2:00
4058	16	0:00	7	8:00	14	3:00	6	8:00	18	6:00	10	18:00
4073	15	0:00	9	11:00	13	9:00	7	13:00	18	1:00	8	16:00
4076	22	1:00	13	22:00	23	15:00	8	5:00	22	20:00	12	1:00
4085	17	5:00	9	13:00	15	23:00	9	20:00	31	11:00	11	19:00
10022	22	4:00	11	12:00	35	11:00	17	22:00	28	3:00	12	9:00

10023	24	20:00	10	9:00	28	22:00	12	2:00	35	11:00	17	22:00
10048	22	11:00	12	23:00	25	10:00	10	3:00	28	22:00	12	2:00
10050	12	15:00	9	11:00	17	2:00	8	11:00	25	10:00	10	3:00
10069	11	8:00	7	4:00	23	9:00	7	4:00	17	2:00	8	11:00
10082	14	11:00	10	4:00	25	18:00	11	4:00	23	9:00	7	4:00
10083	16	15:00	10	5:00	13	16:00	9	3:00	25	18:00	11	4:00
10084	32	12:00	13	10:00	18	19:00	7	22:00	13	16:00	9	3:00
10085	14	12:00	8	4:00	12	3:00	7	1:00	18	19:00	7	22:00
10086	26	15:00	9	3:00	24	18:00	8	3:00	12	3:00	7	1:00
10087	19	11:00	10	16:00	37	21:00	12	8:00	24	18:00	8	3:00
10090	14	16:00	8	21:00	11	15:00	8	0:00	37	21:00	12	8:00
10091	12	20:00	8	2:00	16	10:00	7	18:00	11	15:00	8	0:00
10094	20	17:00	7	0:00	18	19:00	7	0:00	16	10:00	7	18:00
10095	11	8:00	7	15:00	15	8:00	7	22:00	18	19:00	7	0:00
10096	13	9:00	9	6:00	13	9:00	8	1:00	15	8:00	7	22:00
10101	18	15:00	11	4:00	19	20:00	12	17:00	13	9:00	8	1:00
10102	11	6:00	9	23:00	17	6:00	10	0:00	19	20:00	12	17:00
10103	19	20:00	7	2:00	16	10:00	7	1:00	17	6:00	10	0:00
10106	13	20:00	7	18:00	14	14:00	7	18:00	16	10:00	7	1:00
Median	16	16:30	9	20:30	18	15:30	9	20:00	18	15:00	9	22:00
Q1*	13	12:00	7	12:45	14	10:00	7	13:00	15	10:00	8	19:00
Q3**	21	0:00	10	0:00	23	22:00	10	0:00	23	20:00	11	1:00

*Table 3B Daily maximum and minimum T wave alternans values in terms of amplitude (TWA-A) for each subject. *Q1=first quartile; **Q3=third quartile*

	Lead X				Lead Y				Lead Z			
	Max		Min		Max		Min		Max		Min	
Subject ID	Value (μV)	Hour	Value (μV)	Hour	Value (μV)	Hour	Value (μV)	Hour	Value (μV)	Hour	Value (μV)	Hour
1017	16	6:00	5	19:00	18	6:00	4	14:00	20	15:00	5	2:00
1018	62	3:00	8	22:00	103	16:00	7	20:00	103	1:00	9	22:00
1027	12	14:00	7	22:00	19	8:00	6	23:00	14	23:00	5	5:00
1030	96	3:00	10	16:00	88	2:00	11	16:00	70	11:00	8	1:00
1041	46	0:00	11	6:00	35	0:00	7	17:00	44	3:00	14	15:00
1042	35	15:00	21	22:00	24	10:00	11	22:00	31	19:00	17	20:00
1043	29	3:00	7	4:00	34	1:00	6	4:00	33	11:00	6	8:00
1044	68	1:00	20	13:00	44	7:00	17	20:00	67	16:00	22	8:00
1045	48	19:00	20	8:00	42	12:00	10	16:00	66	20:00	22	13:00
1046	65	6:00	14	1:00	44	21:00	12	5:00	76	18:00	18	10:00
1047	102	14:00	18	5:00	75	9:00	15	18:00	35	13:00	13	10:00
1048	19	1:00	8	11:00	20	7:00	7	18:00	17	4:00	8	19:00
1049	29	14:00	8	5:00	29	14:00	5	3:00	40	9:00	6	3:00
1056	31	15:00	8	8:00	28	15:00	9	7:00	26	11:00	9	23:00
2001	15	0:00	6	17:00	11	0:00	5	20:00	15	9:00	6	5:00
2002	87	0:00	13	7:00	50	1:00	11	7:00	35	10:00	16	3:00
2003	18	10:00	6	0:00	19	10:00	5	2:00	14	19:00	6	11:00
2004	24	3:00	5	22:00	24	2:00	6	22:00	20	11:00	5	7:00
2005	18	13:00	8	5:00	17	13:00	7	0:00	15	16:00	7	3:00
2006	41	8:00	8	4:00	53	8:00	6	22:00	17	16:00	4	7:00
2007	22	19:00	5	22:00	29	17:00	5	22:00	18	5:00	5	7:00
2009	28	15:00	6	22:00	30	5:00	6	22:00	27	5:00	6	7:00
2010	37	3:00	12	18:00	70	2:00	10	18:00	56	11:00	14	3:00
2011	36	19:00	10	0:00	20	13:00	7	4:00	12	7:00	6	14:00
2012	35	12:00	8	20:00	23	12:00	9	17:00	34	21:00	11	5:00
2013	47	1:00	15	19:00	42	15:00	12	7:00	40	14:00	10	4:00
2014	25	21:00	6	12:00	20	23:00	5	9:00	16	12:00	6	2:00
2015	26	0:00	7	11:00	81	12:00	10	22:00	24	9:00	11	20:00
2016	11	13:00	4	4:00	12	5:00	4	0:00	8	22:00	3	10:00
2017	18	10:00	7	6:00	20	9:00	7	6:00	28	19:00	7	13:00
4034	23	13:00	6	1:00	18	9:00	5	1:00	30	8:00	10	10:00
4035	26	14:00	8	2:00	16	10:00	5	13:00	26	1:00	9	19:00
4038	28	13:00	9	9:00	29	7:00	10	9:00	22	21:00	11	18:00
4043	25	21:00	10	6:00	23	15:00	10	7:00	30	2:00	11	13:00
4050	21	2:00	6	6:00	12	9:00	6	19:00	13	2:00	6	10:00
4057	20	2:00	10	7:00	40	3:00	8	18:00	28	22:00	12	18:00
4058	21	3:00	8	8:00	30	3:00	6	8:00	23	3:00	5	8:00
4073	46	4:00	8	11:00	14	17:00	4	6:00	19	15:00	8	2:00
4076	89	4:00	15	23:00	75	4:00	12	14:00	126	4:00	10	19:00
4085	39	5:00	7	13:00	41	3:00	8	20:00	29	5:00	9	10:00
10022	33	4:00	19	12:00	23	3:00	7	6:00	37	15:00	16	0:00

10023	34	13:00	9	10:00	24	13:00	8	9:00	21	12:00	5	21:00
10048	34	11:00	17	11:00	30	6:00	13	3:00	62	18:00	13	1:00
10050	14	22:00	7	11:00	18	21:00	8	11:00	27	6:00	5	20:00
10069	17	8:00	5	5:00	17	8:00	6	5:00	17	19:00	5	10:00
10082	34	11:00	10	5:00	25	17:00	8	4:00	21	20:00	8	4:00
10083	36	2:00	13	0:00	23	17:00	8	6:00	15	14:00	6	10:00
10084	30	10:00	15	0:00	40	8:00	5	4:00	24	4:00	7	7:00
10085	32	16:00	6	22:00	26	18:00	6	22:00	27	15:00	5	7:00
10086	35	23:00	11	17:00	132	11:00	7	2:00	42	7:00	7	12:00
10087	27	18:00	8	3:00	17	18:00	6	23:00	47	22:00	6	16:00
10090	31	2:00	8	13:00	28	2:00	10	6:00	18	11:00	6	8:00
10091	21	12:00	7	16:00	16	20:00	8	10:00	17	12:00	5	5:00
10094	18	20:00	4	0:00	21	10:00	7	2:00	18	20:00	4	9:00
10095	18	8:00	6	0:00	16	9:00	7	22:00	21	19:00	7	9:00
10096	20	22:00	7	0:00	15	19:00	8	0:00	20	6:00	7	9:00
10101	27	15:00	12	8:00	56	1:00	14	16:00	27	5:00	12	7:00
10102	18	19:00	8	23:00	15	16:00	5	17:00	18	15:00	8	8:00
10103	46	20:00	7	4:00	18	10:00	6	4:00	17	19:00	5	13:00
10106	36	3:00	5	18:00	23	21:00	4	18:00	27	23:00	5	15:00
Median	29	0:00	8	0:00	24	2:00	7	0:00	26	9:00	7	7:30
Q1*	21	15:00	7	21:30	18	17:00	6	19:45	18	3:00	6	3:00
Q3**	36	3:00	11	6:00	40	8:00	10	6:00	35	15:00	11	10:15

*Table 4B Daily maximum and minimum P wave alternans values in terms of number of heart beats (PWA-D) per window for each subject. *Q1=first quartile; **Q3=third quartile*

	Lead X				Lead Y				Lead Z			
	Max		Min		Max		Min		Max		Min	
Subject ID	Value	Hour	Value	Hour	Value	Hour	Value	Hour	Value	Hour	Value	Hour
1017	112	4:00	97	6:00	115	17:00	54,5	18:00	122	3:00	67	18:00
1018	124	18:00	43	16:00	126	23:00	44	11:00	117	6:00	45	23:00
1027	121	10:00	43	8:00	121	5:00	38	2:00	118	5:00	42	17:00
1030	115	21:00	18	20:00	118	12:00	33	6:00	120	12:00	38	15:00
1041	126	2:00	51	4:00	121	19:00	52	9:00	119	8:00	48	11:00
1042	109	16:00	35	11:00	110	15:00	39	18:00	113	2:00	26	10:00
1043	114	0:00	20	18:00	121	15:00	34	18:00	105	4:00	23	18:00
1044	122	3:00	37	3:00	125	13:00	46	14:00	121	7:00	37	2:00
1045	122	18:00	59	0:00	122	6:00	68	16:00	120	21:00	68	22:00
1046	125	3:00	57	5:00	127	21:00	51	1:00	129	3:00	53	13:00
1047	114	2:00	39	1:00	116	7:00	31	14:00	127	6:00	33	21:00
1048	116	6:00	47	18:00	123	6:00	57	21:00	110	7:00	43	4:00
1049	119	6:00	14	22:00	121	14:00	39	23:00	110	9:00	31	23:00
1056	124	21:00	41	1:00	116	4:00	63	0:00	124	19:00	48	1:00
2001	118	1:00	32	7:00	118	11:00	46	4:00	127	4:00	39	5:00
2002	118	9:00	41	1:00	116	7:00	54	22:00	118	23:00	49	18:00
2003	106	8:00	22	7:00	107	7:00	45	7:00	102	6:00	33	5:00
2004	120	13:00	28	21:00	121	10:00	43	10:00	116	13:00	46	16:00
2005	121	1:00	44	18:00	124	17:00	59	12:00	130	12:00	43	19:00
2006	123	8:00	62	7:00	126	23:00	52	14:00	123	1:00	44	7:00
2007	117	1:00	30	7:00	109	16:00	27	5:00	116	0:00	48	3:00
2009	123	20:00	60	10:00	122	19:00	59	16:00	122	21:00	66	15:00
2010	127	0:00	38	9:00	127	23:00	49	22:00	126	4:00	45	3:00
2011	123	17:00	41	17:00	121	12:00	38	17:00	124	20:00	42	19:00
2012	122	14:00	34	21:00	119	12:00	36	7:00	126	14:00	46	23:00
2013	105	11:00	58	10:00	124	16:00	56	10:00	114	12:00	67	20:00
2014	124	11:00	37	5:00	124	23:00	47	11:00	116	12:00	40	0:00
2015	117	19:00	81	7:00	111	18:00	39	16:00	122	6:00	39	13:00
2016	115	22:00	34	23:00	112	15:00	19	11:00	120	23:00	29	1:00
2017	119	8:00	35	13:00	119	5:00	33	11:00	128	8:00	34	5:00
4034	117	15:00	38	9:00	114	5:00	40	3:00	112	8:00	34	4:00
4035	109	23:00	37	13:00	116	23:00	36	9:00	113	23:00	38	16:00
4038	121	9:00	67	19:00	120	9:00	59	19:00	121	1:00	53	9:00
4043	111	23:00	40	1:00	114	15:00	28	9:00	111	13:00	30	16:00
4050	114	8:00	36	21:00	113	14:00	43	18:00	124	11:00	46	22:00
4057	119	8:00	38	3:00	117	2:00	41	19:00	122	10:00	45	3:00
4058	126	18:00	40	18:00	122	4:00	52	7:00	120	22:00	48	8:00
4073	122	10:00	44	4:00	129	2:00	46	10:00	118	11:00	34	11:00
4076	114	1:00	26	21:00	111	1:00	43	0:00	99	12:00	25	0:00
4085	119	19:00	24	17:00	119	22:00	30	19:00	117	4:00	30	7:00
10022	118	13:00	18	1:00	122	11:00	41	13:00	121	11:00	31	13:00

10023	113	21:00	25	18:00	117	15:00	41	2:00	119	7:00	34	19:00
10048	116	3:00	31	15:00	117	11:00	33	12:00	111	7:00	42	17:00
10050	115	7:00	16	3:00	116	10:00	21	9:00	114	1:00	19	11:00
10069	128	13:00	26	13:00	114	19:00	40	17:00	122	18:00	44	9:00
10082	126	5:00	90	15:00	119	9:00	58	7:00	122	23:00	76	15:00
10083	121	14:00	29	9:00	118	6:00	39	9:00	128	6:00	27	12:00
10084	115	10:00	30	11:00	122	9:00	44	6:00	119	9:00	35	11:00
10085	122	13:00	51	23:00	124	12:00	62	15:00	122	18:00	50	15:00
10086	116	1:00	41	8:00	119	1:00	50	2:00	115	11:00	25	1:00
10087	121	14:00	42	13:00	117	11:00	49	18:00	120	23:00	49	17:00
10090	136	5:00	44	18:00	129	17:00	33	18:00	126	9:00	48	18:00
10091	119	23:00	21	12:00	116	6:00	32	10:00	119	12:00	34	12:00
10094	117	20:00	36	21:00	122	2:00	43	12:00	124	19:00	40	11:00
10095	119	8:00	21	14:00	122	9:00	28	21:00	126	7:00	35	0:00
10096	110	10:00	13	5:00	112	11:00	30	9:00	115	16:00	18	10:00
10101	114	13:00	21	21:00	117	14:00	39	9:00	121	22:00	20	7:00
10102	111	6:00	51	20:00	112	13:00	30	10:00	116	4:00	44	16:00
10103	124	15:00	34	21:00	122	18:00	24	18:00	125	15:00	17	20:00
10106	122	17:00	34	11:00	117	3:00	46	3:00	120	0:00	35	13:00
Median	119	6:00	37	5:30	119	11:00	42	18:30	120	11:00	40	2:00
Q1*	115	16:00	29	16:45	116	15:00	34	22:45	116	11:45	33	6:30
Q3**	122	5:45	44	18:00	122	7:30	50	9:15	123	23:30	46	16:15

*Table 5B Daily maximum and minimum QRS complex alternans values in terms of number of heart beats per window (QRSA-D) for each subject. *Q1=first quartile; **Q3=third quartile*

	Lead X				Lead Y				Lead Z			
	Max		Min		Max		Min		Max		Min	
Subject ID	Value	Hour	Value	Hour	Value	Hour	Value	Hour	Value	Hour	Value	Hour
1017	103	4:00	88	6:00	125	18:00	71	22:00	128	22:00	70	14:00
1018	115	2:00	26	9:00	117	0:00	18	8:00	115	22:00	34	5:00
1027	110	10:00	23	16:00	109	5:00	21	14:00	112	8:00	17	9:00
1030	98	12:00	17	2:00	108	7:00	18	10:00	116	12:00	16	20:00
1041	116	9:00	18	5:00	116	4:00	26	10:00	111	4:00	20	3:00
1042	107	9:00	19	16:00	118	9:00	13	12:00	115	10:00	34	23:00
1043	101	0:00	15	1:00	119	22:00	30	6:00	79	4:00	20	18:00
1044	113	4:00	70	3:00	114	21:00	27	5:00	115	7:00	11	10:00
1045	108	16:00	25	0:00	117	5:00	42	22:00	105	5:00	7	8:00
1046	136	0:00	20	6:00	124	22:00	34	7:00	123	5:00	13	1:00
1047	112	17:00	31	11:00	110	2:00	37	23:00	120	20:00	43	13:00
1048	106	7:00	6	16:00	111	7:00	36	15:00	87	7:00	12	14:00
1049	104	6:00	0	0:00	117	14:00	11	10:00	108	16:00	15	3:00
1056	120	22:00	23	21:00	97	18:00	32	17:00	119	22:00	18	18:00
2001	103	21:00	8	5:00	97	19:00	19	17:00	104	4:00	13	19:00
2002	109	9:00	17	8:00	106	7:00	24	21:00	107	9:00	18	7:00
2003	94	22:00	1	15:00	99	23:00	11	13:00	99	9:00	17	4:00
2004	112	13:00	6	9:00	101	9:00	17	3:00	106	11:00	19	7:00
2005	120	1:00	17	3:00	114	17:00	27	13:00	121	2:00	6	17:00
2006	119	23:00	0	7:00	119	23:00	19	1:00	112	6:00	17	3:00
2007	113	0:00	26	10:00	94	23:00	12	5:00	101	0:00	29	11:00
2009	100	13:00	0	22:00	97	19:00	18	14:00	114	21:00	9	14:00
2010	110	3:00	11	9:00	110	23:00	14	13:00	118	4:00	19	6:00
2011	110	15:00	14	6:00	109	14:00	18	22:00	108	4:00	10	18:00
2012	122	15:00	24	4:00	112	1:00	11	4:00	122	14:00	10	10:00
2013	83	20:00	0	11:00	63	5:00	9	22:00	112	12:00	32	22:00
2014	119	18:00	14	9:00	110	10:00	26	5:00	100	9:00	13	10:00
2015	111	19:00	35	13:00	100	21:00	24	10:00	108	19:00	5	5:00
2016	106	22:00	13	4:00	100	19:00	0	2:00	112	9:00	19	20:00
2017	120	6:00	16	8:00	111	5:00	14	8:00	125	8:00	23	5:00
4034	91	19:00	5	10:00	112	15:00	19	22:00	93	23:00	11	0:00
4035	85	23:00	17	12:00	106	21:00	16	9:00	97	21:00	10	12:00
4038	105	6:00	28	19:00	113	7:00	19	14:00	123	6:00	14	9:00
4043	91	23:00	17	7:00	107	23:00	22	7:00	105	15:00	11	23:00
4050	99	8:00	7	4:00	107	7:00	38	20:00	108	18:00	23	22:00
4057	114	10:00	18	23:00	111	2:00	21	0:00	117	17:00	20	14:00
4058	118	18:00	24	6:00	115	23:00	42	8:00	115	12:00	18	0:00
4073	111	2:00	19	19:00	114	0:00	24	21:00	114	10:00	19	17:00
4076	92	11:00	0	5:00	107	2:00	5	18:00	98	12:00	12	13:00
4085	109	0:00	10	9:00	117	0:00	20	20:00	116	2:00	18	12:00
10022	105	6:00	3	12:00	114	15:00	1	21:00	127	12:00	17	13:00

10023	96	10:00	19	18:00	119	15:00	21	4:00	115	7:00	21	23:00
10048	108	10:00	30	15:00	111	11:00	18	17:00	110	7:00	30	8:00
10050	97	9:00	12	10:00	109	14:00	33	21:00	90	15:00	0	0:00
10069	111	3:00	18	18:00	112	15:00	27	7:00	118	19:00	31	23:00
10082	114	7:00	61	7:00	102	10:00	23	17:00	117	21:00	66	4:00
10083	107	14:00	6	11:00	113	20:00	12	5:00	124	6:00	5	19:00
10084	102	0:00	18	20:00	117	5:00	30	6:00	118	23:00	29	14:00
10085	107	11:00	13	9:00	122	2:00	30	9:00	121	21:00	17	16:00
10086	106	16:00	10	11:00	112	1:00	25	4:00	110	1:00	10	4:00
10087	116	14:00	17	11:00	113	15:00	27	1:00	114	14:00	25	0:00
10090	117	22:00	24	19:00	120	3:00	18	17:00	123	0:00	63	11:00
10091	109	12:00	4	11:00	109	6:00	12	10:00	121	0:00	7	10:00
10094	88	20:00	5	23:00	102	17:00	15	18:00	103	6:00	18	16:00
10095	113	21:00	1	6:00	120	4:00	10	6:00	113	7:00	14	15:00
10096	101	10:00	5	8:00	108	18:00	0	19:00	112	16:00	8	9:00
10101	114	20:00	11	14:00	109	20:00	17	13:00	106	14:00	26	8:00
10102	105	19:00	22	21:00	92	7:00	2	16:00	122	21:00	29	9:00
10103	119	15:00	31	18:00	118	15:00	6	18:00	123	13:00	31	13:00
10106	105	15:00	26	3:00	107	9:00	7	8:00	118	17:00	55	10:00
Median	109	2:00	17	3:30	111	14:30	19	22:00	114	11:00	18	18:00
Q1*	102	19:45	7	8:30	107	21:45	13	5:45	107	11:45	12	4:00
Q3**	114	6:00	23	11:00	116	2:45	27	10:45	118	22:45	25	9:00

*Table 6B Daily maximum and minimum T wave alternans values in terms of number of heart beats per window (TWA-D) for each subject. *Q1=first quartile; **Q3=third quartile*

	Lead X				Lead Y				Lead Z			
	Max		Min		Max		Min		Max		Min	
Subject ID	Value	Hour	Value	Hour	Value	Hour	Value	Hour	Value	Hour	Value	Hour
1017	123	6:00	103	16:00	121	23:00	88	20:00	126	18:00	100	1:00
1018	122	8:00	90	4:00	124	4:00	77	19:00	123	1:00	80	2:00
1027	122	22:00	89	9:00	123	5:00	87	17:00	125	13:00	83	7:00
1030	123	10:00	85	2:00	124	12:00	80	9:00	121	15:00	77	3:00
1041	127	17:00	88	10:00	128	1:00	90	11:00	122	8:00	83	8:00
1042	122	9:00	79	15:00	129	4:00	73	9:00	121	4:00	73	9:00
1043	123	21:00	87	10:00	123	19:00	73	14:00	114	14:00	50	13:00
1044	128	20:00	103	5:00	126	11:00	73	0:00	124	22:00	79	12:00
1045	124	18:00	89	8:00	129	6:00	88	10:00	126	18:00	78	1:00
1046	130	3:00	100	6:00	128	22:00	82	12:00	125	20:00	91	20:00
1047	126	0:00	79	5:00	121	16:00	82	11:00	124	8:00	93	18:00
1048	126	6:00	84	22:00	125	15:00	89	15:00	120	6:00	73	10:00
1049	128	6:00	78	3:00	125	5:00	90	2:00	123	14:00	70	10:00
1056	129	21:00	80	1:00	122	23:00	90	13:00	129	22:00	76	13:00
2001	124	15:00	71	2:00	126	11:00	84	8:00	124	1:00	80	19:00
2002	123	12:00	84	16:00	121	11:00	83	5:00	122	10:00	88	1:00
2003	117	21:00	79	13:00	119	0:00	82	21:00	118	9:00	80	17:00
2004	124	11:00	75	7:00	123	15:00	82	8:00	123	16:00	86	15:00
2005	122	19:00	83	18:00	122	18:00	85	18:00	127	14:00	76	19:00
2006	128	23:00	94	13:00	128	23:00	77	15:00	124	13:00	84	15:00
2007	122	0:00	89	23:00	123	2:00	66	20:00	120	5:00	75	8:00
2009	121	11:00	74	12:00	124	21:00	83	12:00	123	21:00	83	0:00
2010	128	21:00	92	0:00	128	23:00	83	9:00	126	20:00	72	16:00
2011	126	19:00	91	6:00	124	15:00	83	19:00	128	8:00	84	7:00
2012	129	17:00	89	21:00	130	18:00	85	22:00	125	17:00	85	5:00
2013	114	6:00	81	11:00	124	16:00	77	22:00	114	6:00	91	20:00
2014	128	18:00	79	5:00	126	19:00	79	6:00	128	10:00	81	4:00
2015	120	19:00	79	8:00	119	19:00	68	5:00	118	23:00	71	5:00
2016	124	23:00	78	2:00	120	19:00	58	8:00	125	1:00	72	16:00
2017	125	21:00	76	10:00	121	5:00	71	8:00	132	6:00	71	22:00
4034	126	3:00	85	21:00	125	9:00	67	22:00	123	7:00	80	20:00
4035	122	20:00	75	11:00	122	23:00	81	0:00	121	23:00	75	12:00
4038	122	4:00	96	7:00	123	5:00	86	19:00	127	12:00	87	14:00
4043	120	13:00	70	21:00	120	23:00	74	17:00	117	7:00	77	8:00
4050	119	18:00	82	21:00	123	4:00	83	16:00	122	11:00	86	11:00
4057	123	8:00	79	4:00	119	7:00	78	13:00	121	10:00	83	22:00
4058	126	17:00	87	3:00	125	17:00	85	9:00	126	5:00	86	8:00
4073	132	20:00	82	12:00	122	5:00	90	18:00	121	22:00	87	16:00
4076	124	13:00	70	8:00	120	11:00	67	16:00	124	13:00	73	5:00
4085	123	19:00	79	21:00	124	0:00	78	19:00	132	2:00	70	16:00
10022	123	6:00	74	3:00	124	18:00	73	3:00	121	11:00	62	13:00

10023	118	21:00	82	12:00	121	0:00	80	3:00	120	10:00	80	16:00
10048	123	22:00	90	10:00	123	12:00	84	17:00	120	12:00	87	18:00
10050	128	10:00	77	4:00	118	15:00	80	23:00	119	15:00	51	11:00
10069	126	13:00	71	8:00	120	17:00	67	12:00	121	10:00	71	18:00
10082	125	5:00	80	7:00	118	6:00	71	15:00	122	3:00	83	18:00
10083	127	14:00	85	14:00	122	20:00	78	9:00	122	6:00	76	22:00
10084	120	20:00	87	15:00	124	9:00	83	9:00	124	12:00	78	11:00
10085	125	13:00	80	1:00	127	2:00	87	3:00	128	8:00	66	8:00
10086	123	1:00	81	14:00	118	1:00	83	12:00	119	5:00	76	15:00
10087	122	14:00	79	9:00	120	21:00	75	17:00	121	0:00	89	10:00
10090	130	13:00	91	11:00	124	14:00	84	19:00	128	9:00	85	19:00
10091	123	3:00	75	12:00	122	3:00	73	12:00	122	1:00	78	6:00
10094	123	16:00	81	15:00	126	2:00	83	15:00	124	10:00	85	13:00
10095	122	6:00	60	15:00	122	8:00	57	17:00	113	7:00	55	1:00
10096	116	8:00	68	13:00	117	12:00	70	6:00	116	4:00	60	5:00
10101	122	19:00	74	7:00	122	13:00	82	9:00	126	23:00	80	11:00
10102	125	2:00	83	15:00	123	4:00	61	9:00	120	7:00	79	16:00
10103	126	13:00	67	22:00	124	13:00	67	7:00	124	13:00	67	7:00
10106	128	17:00	84	11:00	124	9:00	84	1:00	124	3:00	83	4:00
Median	124	14:30	81	22:30	123	18:30	82	1:30	123	4:00	79	19:30
Q1*	122	3:45	78	2:30	121	23:45	73	18:30	121	0:15	73	10:45
Q3**	126	3:00	87	11:00	125	23:15	84	12:00	125	22:15	84	8:30

*Table 7B Daily maximum and minimum P wave alternans values in terms of magnitude (μV*number of alternating beats) per window (PWA-M) for each subject. *Q1=first quartile; **Q3=third quartile*

	Lead X				Lead Y				Lead Z			
	Max		Min		Max		Min		Max		Min	
Subject ID	Value (μV*n)	Hour	Value (μV*n)	Hour	Value (μV*n)	Hour	Value (μV*n)	Hour	Value (μV*n)	Hour	Value (μV*n)	Hour
1017	3232	6:00	1634	16:00	3283	6:00	1163	16:00	4202	22:00	680	18:00
1018	5844	3:00	332	16:00	5050	21:00	371	11:00	1571	4:00	492	10:00
1027	2945	21:00	474	8:00	2871	10:00	409	2:00	6620	0:00	485	17:00
1030	1848	21:00	174	20:00	1900	21:00	327	21:00	4554	22:00	311	3:00
1041	4380	2:00	358	7:00	4233	2:00	441	9:00	2369	8:00	422	7:00
1042	4465	16:00	230	11:00	2687	21:00	283	22:00	3657	2:00	260	22:00
1043	2845	18:00	180	18:00	2138	18:00	258	18:00	1495	17:00	174	18:00
1044	6064	3:00	250	3:00	3085	3:00	175	14:00	5501	21:00	312	2:00
1045	5125	0:00	487	18:00	4397	0:00	496	14:00	4977	18:00	453	15:00
1046	5729	0:00	551	5:00	4202	19:00	516	7:00	5657	22:00	512	3:00
1047	2323	2:00	265	1:00	2238	9:00	341	10:00	8069	8:00	384	21:00
1048	2552	6:00	439	18:00	2519	6:00	556	18:00	1918	16:00	391	4:00
1049	3355	18:00	108	22:00	3275	18:00	308	23:00	1318	20:00	268	21:00
1056	4449	11:00	297	1:00	3414	8:00	520	0:00	3503	19:00	388	1:00
2001	2663	1:00	272	7:00	2031	1:00	357	4:00	4508	4:00	391	5:00
2002	3471	9:00	364	5:00	2336	18:00	404	22:00	2362	13:00	352	18:00
2003	2176	18:00	241	19:00	2288	19:00	482	10:00	2221	0:00	358	13:00
2004	5187	11:00	273	21:00	3174	13:00	304	8:00	3007	14:00	350	16:00
2005	21061	20:00	354	18:00	20943	20:00	457	5:00	5195	2:00	318	19:00
2006	3944	23:00	400	16:00	3818	23:00	440	7:00	3527	5:00	346	3:00
2007	2005	9:00	247	7:00	1518	16:00	245	5:00	2028	6:00	419	5:00
2009	7706	0:00	388	10:00	9206	0:00	587	16:00	9669	19:00	611	8:00
2010	1699	19:00	265	9:00	2249	19:00	378	20:00	3848	14:00	364	3:00
2011	9286	22:00	459	18:00	7608	22:00	468	22:00	5507	15:00	433	19:00
2012	4099	14:00	339	21:00	2994	4:00	442	20:00	7176	14:00	497	6:00
2013	2406	22:00	925	13:00	2362	22:00	711	15:00	2638	22:00	766	20:00
2014	3215	20:00	296	5:00	3022	20:00	374	13:00	3679	11:00	305	0:00
2015	6029	6:00	1650	13:00	5461	8:00	1122	13:00	3390	21:00	461	4:00
2016	4354	18:00	479	23:00	4743	18:00	281	11:00	5741	23:00	335	1:00
2017	5681	0:00	318	13:00	5392	0:00	584	11:00	16978	4:00	345	9:00
4034	14313	19:00	510	9:00	13932	19:00	705	9:00	3453	1:00	397	16:00
4035	1620	5:00	350	13:00	1809	5:00	383	9:00	1962	22:00	431	16:00
4038	4638	18:00	552	9:00	4397	18:00	468	21:00	4235	9:00	355	9:00
4043	1855	19:00	332	1:00	1987	1:00	364	0:00	2408	21:00	306	18:00
4050	1910	19:00	249	21:00	1959	19:00	358	4:00	2886	5:00	337	4:00
4057	4320	3:00	404	3:00	4618	23:00	445	3:00	4563	2:00	503	3:00
4058	3003	21:00	271	18:00	2879	18:00	337	23:00	2011	20:00	307	8:00
4073	2734	13:00	333	4:00	2460	13:00	383	1:00	3469	3:00	239	11:00
4076	2649	8:00	236	21:00	2517	8:00	369	21:00	1592	12:00	201	6:00
4085	6122	6:00	160	6:00	8272	6:00	218	19:00	1998	14:00	259	7:00
10022	3121	19:00	144	16:00	3015	19:00	305	23:00	2549	21:00	239	13:00

10023	3114	15:00	229	18:00	2954	15:00	420	17:00	5962	7:00	363	0:00
10048	3658	9:00	276	15:00	3040	12:00	387	14:00	4547	6:00	454	17:00
10050	2839	14:00	112	3:00	2455	7:00	243	9:00	2012	21:00	135	11:00
10069	5923	15:00	238	11:00	4589	15:00	229	18:00	6805	19:00	460	15:00
10082	8733	9:00	2055	4:00	8064	9:00	2041	17:00	6337	6:00	1247	22:00
10083	1525	14:00	238	9:00	1661	23:00	312	9:00	2712	6:00	240	12:00
10084	1851	10:00	293	19:00	1847	10:00	331	19:00	3447	20:00	355	19:00
10085	2533	7:00	274	23:00	2337	6:00	376	23:00	2143	15:00	264	15:00
10086	2169	1:00	367	6:00	2169	1:00	495	5:00	4381	16:00	190	1:00
10087	4455	0:00	342	11:00	4196	0:00	469	11:00	3906	5:00	454	10:00
10090	3584	9:00	357	18:00	3555	9:00	271	18:00	3027	17:00	404	18:00
10091	3129	23:00	232	12:00	3107	6:00	279	10:00	4208	6:00	407	15:00
10094	2118	20:00	337	1:00	2307	20:00	431	15:00	2921	6:00	366	11:00
10095	3416	7:00	172	14:00	3337	7:00	184	1:00	2716	7:00	264	0:00
10096	3093	10:00	154	5:00	3072	10:00	289	9:00	2904	16:00	197	10:00
10101	2015	23:00	194	21:00	2330	20:00	378	9:00	2104	20:00	187	7:00
10102	3212	1:00	444	15:00	2244	1:00	380	9:00	3295	17:00	443	13:00
10103	7269	15:00	337	21:00	6995	15:00	239	18:00	6029	15:00	196	20:00
10106	3038	13:00	360	11:00	3113	13:00	442	3:00	3417	0:00	365	3:00
Median	3224	12:00	325	1:00	3031	2:30	379	11:00	3461	9:30	361	19:00
Q1*	2547	11:45	240	4:45	2324	0:45	307	18:45	2399	21:00	296	7:30
Q3**	4760	7:30	391	18:00	4274	3:45	468	9:15	4666	18:00	436	9:30

*Table 8B Daily maximum and minimum QRS complex alternans values in terms of magnitude (μV*number of alternating beats) per window (QRSA-M) for each subject. *Q1=first quartile; **Q3=third quartile*

	Lead X				Lead Y				Lead Z			
	Max		Min		Max		Min		Max		Min	
Subject ID	Value (μV*n)	Hour	Value (μV*n)	Hour	Value (μV*n)	Hour	Value (μV*n)	Hour	Value (μV*n)	Hour	Value (μV*n)	Hour
1017	1931	6:00	1002	4:00	2066	6:00	938	3:00	6944	22:00	1388	18:00
1018	3445	15:00	256	4:00	2511	1:00	284	17:00	2996	12:00	379	9:00
1027	1950	3:00	370	16:00	1846	22:00	290	12:00	3315	10:00	178	9:00
1030	1104	12:00	146	19:00	1225	9:00	192	15:00	2839	12:00	160	12:00
1041	1941	8:00	149	3:00	1648	2:00	223	2:00	2506	8:00	144	3:00
1042	2086	16:00	164	16:00	1770	10:00	110	12:00	3156	19:00	370	23:00
1043	1835	22:00	127	2:00	1964	22:00	260	1:00	1107	17:00	176	18:00
1044	3463	1:00	757	8:00	3065	1:00	473	11:00	2550	7:00	93	10:00
1045	2206	18:00	219	10:00	1741	5:00	283	10:00	1907	5:00	46	8:00
1046	7368	0:00	176	5:00	4825	21:00	219	17:00	3963	13:00	81	1:00
1047	2658	10:00	393	4:00	1677	20:00	434	23:00	4463	20:00	429	13:00
1048	1427	7:00	86	16:00	1594	0:00	345	16:00	812,4	6:00	103	14:00
1049	1666	6:00	45	21:00	1512	14:00	91	10:00	1771	16:00	145	7:00
1056	3663	11:00	172	1:00	3500	11:00	286	0:00	2734	21:00	118	18:00
2001	1228	21:00	60	5:00	907,8	0:00	155	17:00	2630	19:00	111	19:00
2002	1807	9:00	183	8:00	1247	20:00	209	7:00	1756	23:00	133	12:00
2003	1832	22:00	38	8:00	1768	22:00	214	14:00	1947	5:00	195	4:00
2004	1958	11:00	65	9:00	1254	8:00	167	2:00	2142	19:00	174	14:00
2005	3960	1:00	133	19:00	3878	1:00	217	17:00	3713	12:00	65	17:00
2006	2202	23:00	85	16:00	2227	23:00	159	16:00	2241	10:00	97	3:00
2007	1846	21:00	130	10:00	818,7	2:00	107	5:00	1648	4:00	166	9:00
2009	4207	3:00	54	13:00	4627	3:00	251	11:00	3864	19:00	110	14:00
2010	1909	3:00	109	9:00	1643	3:00	93	13:00	3181	4:00	164	6:00
2011	2619	22:00	129	3:00	2068	22:00	187	22:00	2126	8:00	88	7:00
2012	2781	15:00	292	4:00	2847	21:00	114	4:00	3761	14:00	80	10:00
2013	1465	20:00	25	11:00	922,6	20:00	109	22:00	3085	6:00	361	22:00
2014	1535	5:00	145	2:00	1586	11:00	223	5:00	1571	9:00	137	10:00
2015	3915	8:00	486	14:00	2671	0:00	543	13:00	3593	20:00	48	5:00
2016	2333	18:00	191	4:00	2100	18:00	0	2:00	4657	9:00	238	20:00
2017	3716	6:00	217	17:00	2357	23:00	192	8:00	5777	4:00	275	11:00
4034	2911	19:00	77	12:00	2302	19:00	257	22:00	2211	17:00	130	0:00
4035	942	17:00	195	2:00	1032	21:00	204	22:00	1277	21:00	123	0:00
4038	2277	23:00	230	19:00	2391	23:00	162	14:00	3422	5:00	100	9:00
4043	1908	6:00	197	7:00	1969	6:00	229	7:00	2084	6:00	123	23:00
4050	1209	19:00	84	4:00	1326	18:00	330	1:00	2178	5:00	199	1:00
4057	3631	23:00	229	23:00	3244	23:00	213	21:00	3755	12:00	341	13:00
4058	3467	0:00	200	18:00	1828	15:00	329	8:00	1960	7:00	131	0:00
4073	1767	2:00	134	19:00	1711	2:00	199	21:00	3700	3:00	143	7:00
4076	1142	11:00	41	10:00	1147	11:00	51	18:00	1062	10:00	128	13:00
4085	3454	6:00	90	9:00	3860	6:00	161	20:00	2318	21:00	174	12:00

10022	1621	6:00	44	12:00	1583	16:00	9	21:00	2280	14:00	131	13:00
10023	4047	4:00	254	18:00	3161	4:00	204	18:00	4631	7:00	234	23:00
10048	2875	10:00	312	15:00	2452	10:00	253	17:00	3102	6:00	250	8:00
10050	1523	13:00	122	10:00	1923	14:00	301	6:00	1272	12:00	30	1:00
10069	2126	14:00	207	18:00	2091	15:00	386	1:00	3764	12:00	418	23:00
10082	5107	9:00	1319	17:00	5691	9:00	709	17:00	3601	21:00	1092	5:00
10083	1722	14:00	71	12:00	1555	14:00	93	2:00	1592	6:00	85	19:00
10084	1320	19:00	146	20:00	1474	19:00	247	14:00	2433	2:00	244	14:00
10085	1669	13:00	81	9:00	1737	13:00	158	9:00	2153	8:00	136	7:00
10086	1324	16:00	88	11:00	1423	1:00	240	4:00	2507	1:00	87	11:00
10087	2790	14:00	114	11:00	2306	11:00	226	12:00	2750	14:00	231	2:00
10090	1951	20:00	215	19:00	2019	20:00	157	17:00	4785	0:00	515	13:00
10091	2340	12:00	73	11:00	2231	12:00	171	10:00	2774	0:00	83	10:00
10094	1353	20:00	67	23:00	1304	18:00	136	18:00	1874	3:00	176	16:00
10095	1901	8:00	51	6:00	1952	4:00	101	1:00	1694	19:00	119	15:00
10096	2314	10:00	91	19:00	1999	12:00	0	19:00	2259	18:00	119	13:00
10101	1750	20:00	106	14:00	1512	20:00	125	13:00	2459	2:00	230	4:00
10102	1360	8:00	208	16:00	1069	19:00	17	16:00	3457	5:00	327	9:00
10103	3638	13:00	454	11:00	3407	15:00	102	18:00	4706	13:00	417	21:00
10106	2293	5:00	284	21:00	1863	21:00	86	8:00	3647	21:00	796	8:00
Median	1954	9:30	145	0:30	1893	0:00	204	17:00	2590	9:00	145	12:30
Q1*	1668	6:00	85	2:00	1545	20:45	123	8:30	2053	20:45	110	13:45
Q3**	2884	2:45	217	12:30	2366	22:15	258	8:00	3613	3:15	240	9:00

*Table 9B Daily maximum and minimum T wave alternans values in terms of magnitude (μV*number of alternating beats) per window (TWA-M) for each subject. *Q1=first quartile; **Q3=third quartile*

	Lead X				Lead Y				Lead Z			
	Max		Min		Max		Min		Max		Min	
Subject ID	Value (μV*n)	Hour	Value (μV*n)	Hour	Value (μV*n)	Hour	Value (μV*n)	Hour	Value (μV*n)	Hour	Value (μV*n)	Hour
1017	4057	6:00	2056	4:00	3851	16:00	2044	4:00	4674	18:00	1578	20:00
1018	4725	21:00	658	11:00	4939	21:00	617	11:00	3816	22:00	504	0:00
1027	7593	4:00	1194	8:00	7513	3:00	1239	20:00	8762	18:00	664	4:00
1030	2357	0:00	465	19:00	2153	12:00	507	19:00	4123	22:00	479	23:00
1041	3803	16:00	425	7:00	3771	16:00	426	9:00	1847	15:00	354	8:00
1042	4510	22:00	692	12:00	4244	4:00	753	8:00	4785	2:00	443	12:00
1043	7951	18:00	830	7:00	7190	18:00	676	17:00	2392	11:00	259	13:00
1044	5545	20:00	1476	17:00	4036	20:00	1161	17:00	6924	21:00	487	10:00
1045	8374	0:00	441	13:00	8223	0:00	438	13:00	5700	18:00	385	15:00
1046	6327	0:00	654	7:00	6180	19:00	578	7:00	7938	11:00	545	4:00
1047	4228	9:00	623	19:00	4489	9:00	619	19:00	10853	8:00	598	20:00
1048	4904	14:00	655	12:00	4862	14:00	715	9:00	2917	16:00	400	2:00
1049	4669	6:00	445	3:00	4279	6:00	541	3:00	2564	12:00	334	10:00
1056	3697	22:00	292	1:00	2733	13:00	391	1:00	3700	22:00	322	6:00
2001	2690	2:00	362	2:00	2744	2:00	427	8:00	4118	9:00	413	7:00
2002	3472	9:00	397	7:00	2563	6:00	384	5:00	3259	23:00	454	5:00
2003	4049	18:00	746	17:00	3925	17:00	710	17:00	6306	0:00	837	17:00
2004	5475	11:00	489	0:00	3514	18:00	339	8:00	2908	12:00	544	15:00
2005	7090	20:00	538	5:00	7152	20:00	551	5:00	4116	1:00	338	19:00
2006	7356	8:00	375	16:00	6783	8:00	375	21:00	6822	18:00	336	21:00
2007	2801	16:00	420	18:00	2902	16:00	342	19:00	3394	14:00	391	7:00
2009	9764	0:00	417	12:00	9708	0:00	510	12:00	12017	1:00	704	10:00
2010	1997	18:00	515	14:00	2007	23:00	559	9:00	2853	20:00	345	12:00
2011	18496	22:00	941	6:00	17904	22:00	861	6:00	10370	17:00	661	2:00
2012	7696	1:00	793	22:00	8133	1:00	568	6:00	10155	18:00	1037	3:00
2013	5426	20:00	1533	15:00	6008	20:00	1464	22:00	4944	22:00	1303	20:00
2014	7034	20:00	542	5:00	6641	20:00	608	6:00	6492	11:00	456	0:00
2015	9184	19:00	2041	5:00	9229	19:00	1984	5:00	5897	23:00	1268	7:00
2016	9678	18:00	1481	11:00	9414	18:00	1324	11:00	12561	20:00	1499	6:00
2017	8333	6:00	1029	9:00	7726	6:00	986	9:00	13804	1:00	941	9:00
4034	39076	19:00	1391	11:00	40699	19:00	1316	11:00	6298	1:00	858	20:00
4035	2415	18:00	585	5:00	2234	8:00	626	0:00	2599	6:00	544	14:00
4038	6545	18:00	723	20:00	7495	18:00	620	20:00	6502	1:00	403	14:00
4043	4323	19:00	501	21:00	3991	19:00	600	3:00	3001	17:00	658	3:00
4050	3947	1:00	473	21:00	3675	1:00	489	5:00	2633	5:00	428	16:00
4057	11121	23:00	938	21:00	10967	23:00	828	21:00	5073	10:00	1101	16:00
4058	3517	15:00	500	13:00	3547	15:00	464	13:00	2995	12:00	417	1:00
4073	5264	14:00	457	12:00	4945	14:00	479	15:00	4422	18:00	356	16:00
4076	2821	10:00	429	5:00	2721	10:00	411	18:00	2424	0:00	500	12:00
4085	8181	6:00	576	6:00	8797	6:00	511	3:00	2368	9:00	361	16:00
10022	4723	19:00	321	3:00	4518	19:00	357	3:00	2737	13:00	265	13:00

10023	4934	23:00	458	17:00	5377	23:00	492	18:00	7610	5:00	425	17:00
10048	10177	9:00	737	20:00	9112	9:00	727	20:00	9521	12:00	937	15:00
10050	5248	7:00	613	4:00	4658	7:00	717	4:00	1814	13:00	270	11:00
10069	8906	15:00	523	18:00	8848	15:00	595	18:00	4176	10:00	668	14:00
10082	9198	10:00	1085	4:00	9470	10:00	954	4:00	7330	9:00	1004	22:00
10083	2929	6:00	355	14:00	3196	6:00	324	10:00	2050	22:00	388	7:00
10084	3648	8:00	542	13:00	3731	7:00	599	21:00	4102	4:00	687	11:00
10085	1645	10:00	301	1:00	1696	13:00	342	4:00	1550	13:00	171	8:00
10086	2551	1:00	550	16:00	2706	16:00	543	16:00	5902	16:00	472	12:00
10087	3362	22:00	304	9:00	3750	22:00	345	9:00	6487	0:00	461	9:00
10090	3454	22:00	536	17:00	3296	22:00	576	13:00	5554	0:00	681	17:00
10091	3958	12:00	681	8:00	3931	12:00	654	16:00	3506	20:00	651	16:00
10094	5473	22:00	517	15:00	4809	22:00	569	15:00	7482	21:00	714	13:00
10095	3155	7:00	376	15:00	3089	7:00	356	1:00	1848	7:00	308	1:00
10096	4272	12:00	633	13:00	4239	12:00	692	13:00	3374	10:00	770	5:00
10101	3623	18:00	493	2:00	3903	18:00	449	2:00	3733	18:00	323	1:00
10102	6731	1:00	482	16:00	6990	1:00	482	19:00	3625	7:00	414	13:00
10103	11051	1:00	807	18:00	11148	1:00	884	18:00	13612	0:00	833	13:00
10106	7103	10:00	544	20:00	6784	10:00	542	20:00	5062	0:00	615	10:00
Median	4919	8:30	542	11:00	4588	1:00	573	11:00	4299	11:30	483	7:00
Q1*	3642	16:00	454	20:45	3643	9:00	461	21:00	2976	8:30	388	12:00
Q3**	7619	11:15	740	16:15	7499	1:30	716	17:00	6582	11:15	691	1:30

References

[1] R. L. Drake, et al., *Anatomia del Gray. I fondamenti*. Edra, 2015.
[2] C. P. Anthony, et al., *Fondamenti di anatomia e fisiologia dell'uomo*. Casa editrice ambrosiana, 1977.
[3] S. Kumar, et al., «Sarcomeric Gene Variants and Their Role with Left Ventricular Dysfunction in Background of Coronary Artery Disease», 2020.
[4] A. Guyton, et al., *Guyton and Hall textbook of medical physiology*, 12th ed. Philadelphia, Pa: Saunders/Elsevier, 2011.
[5] A. Smiley, «Evolutionary optimisation of atrial fibrillation diagnostic algorithms», 2014.
[6] R. Di Pietro, *Elementi di Istologia*. EdiSES, 2017.
[7] University Hospital of Leicester, *Cardiology Guidelines*. 2021.
[8] Y. Guo, et al., «Circadian Rhythm in the Cardiovascular System: Considerations in Non-Invasive Electrophysiology», *Card Electrophysiol Rev*, 2002.
[9] V. V. Shusterman, et al., «Nocturnal Peak in Atrial Tachyarrhythmia Occurrence as a Function of Arrhythmia Burden», *J. Cardiovasc. Electrophysiol.*, 2012.
[10] B. Maron, et al., «Circadian patterns in the occurrence of malignant ventricular tachyarrhythmias triggering defibrillator interventions in patients with hypertrophic cardiomyopathy», *Heart Rhythm*, 2009.
[11] F. Portaluppi, et al., «Circadian rhythms in cardiac arrhythmias and opportunities for their chronotherapy», *Adv. Drug Deliv. Rev.*, 2007.
[12] D. Jeyaraj, et al., «Circadian rhythms govern cardiac repolarization and arrhythmogenesis», *Nature*, 2012.
[13] E. A. E. Schroder, et al., «The cardiomyocyte molecular clock regulates the circadian expression of Kcnh2 and contributes to ventricular repolarization», *Heart Rhythm*, 2015.
[14] J. Cinca, et al., «Circadian variations in the electrical properties of the human heart assessed by sequential bedside electrophysiologic testing», *Am. Heart J.*, 1986.
[15] A. Mubarik, et al., «Holter Monitor», 2022.
[16] E. Jovanov, et al., «Real Time Holter Monitoring of Biomedical Signals», 1999.
[17] S. Salinari, *Strumentazione biomedica, trasduzione e manipolazione*. La Goliardica Editrice, 1982.
[18] M. J. Cutler, et al., «Explaining the clinical manifestations of T wave alternans in patients at risk for sudden cardiac death», *Heart Rhythm*, 2009.
[19] D. Sprenkeler, et al., «Circadian pattern of short-term variability of the QT-interval in primary prevention ICD patients - EU-CERT-ICD methodological pilot study», *PLOS ONE*, 2017.
[20] R. S. Khandpur, *Biomedical Instrumentation*, 2ª ed. New Delhi: McGraw-Hill Offices, 2003.
[21] G. E. Burch, «The history of vectorcardiography», *Med. Hist.*, 1985.
[22] R. Jaros, et al, «Comparison of Different Electrocardiography with Vectorcardiography Transformations», *Sensors*, 2019.
[23] H. Bonnemeier, et al., «Circadian Profile of QT Interval and QT Interval Variability in 172 Healthy Volunteers», *Pacing Clin. Electrophysiol.*, 2003.
[24] K. Mayuga, et al., «Circadian and Gender Effects on Repolarization in Healthy Adults: A Study Using Harmonic Regression Analysis», *Ann. Noninvasive Electrocardiol.*, 2010.
[25] I. Marcantoni, et al., «Enhanced adaptive matched filter for automated identification and measurement of electrocardiographic alternans», *Biomed. Signal Process. Control*, 2021.
[26] E. V. Garcia, et al., «T-Wave Alternans: Clinical Performance, Limitations and Analysis Methodologies», *Clin. Update*., 2011.
[27] M. Haghjoo, et al., «Microvolt T-wave alternans: A review of techniques, interpretation, utility, clinical studies, and future perspectives», *Int. J. Cardiol.*, 2006.
[28] A. Suszko, et al., «Microvolt QRS Alternans Without Microvolt T-Wave Alternans in Human Cardiomyopathy: A Novel Risk Marker of Late Ventricular Arrhythmias», *J. Am. Heart Assoc.*, 2020.
[29] P. Chakraborty, et al., «Microvolt QRS Alternans in Hypertrophic Cardiomyopathy: A Novel Risk Marker of Late Ventricular Arrhythmias», *J. Am. Heart Assoc.*, 2021.
[30] I. Marcantoni, et al., «Electrocardiographic Alternans: A New Approach», in *XV Mediterranean Conference on Medical and Biological Engineering and Computing – MEDICON 2019*, Cham: Springer International Publishing, 2020.
[31] K. Kulkarni, et al., «Low-Level Tragus Stimulation Modulates Atrial Alternans and Fibrillation Burden in Patients With Paroxysmal Atrial Fibrillation», *J. Am. Heart Assoc.*, 2021.
[32] E. Siniorakis, et al., «P-wave alternans predicting imminent atrial flutter», *Cardiol. J.*, 2017.
[33] L. Burattini, et al., «Comparative analysis of methods for automatic detection and quantification of microvolt T-wave alternans», *Med. Eng. Phys.*, 2009.

[34] I. Marcantoni, et al., «Automatic T-Wave Alternans Identification in Indirect and Direct Fetal Electrocardiography», presented at 40th Annual International Conference of the IEEE Engineering in Medicine and Biology Society (EMBC), 2018.
[35] B. Nearing, et al., «Modified moving average analysis of T-wave alternans to predict ventricular fibrillation with high accuracy», *J. Appl. Physiol.*, 2002.
[36] J. M. Smith, et al., «Electrical alternans and cardiac electrical instability.», *Circulation*, 1988.
[37] B. D. Nearing, et al., «Dynamic Tracking of Cardiac Vulnerability by Complex Demodulation of the T Wave», *Science*, 1991.
[38] J. P. Martinez, et al., «Methodological principles of T wave alternans analysis: a unified framework», *IEEE Trans. Biomed. Eng.*, 2005.
[39] L. Burattini, et al., «Assessment of Physiological Amplitude, Duration, and Magnitude of ECG T-Wave Alternans», *Ann. Noninvasive Electrocardiol.*, 2009.
[40] «http://thew-project.org/».
[41] I. Marcantoni, et al., «Circadian Modulation of Electrocardiographic Alternans in Kidney Failure Patients on Dialysis», presented at CinC2022, 2022.
[42] Page MJ, et al. The PRISMA 2020 statement: an updated guideline for reporting systematic reviews. BMJ, 2021.
[43] F. Cruz Filho, et al., «Electrical behavior of T-Wave polarity alternans in patients with congenital long QT syndrome», *J. Am. Coll. Cardiol.*, 2000.
[44] N. Takasugi, et al., «Sleep apnoea induces cardiac electrical instability assessed by T-wave alternans in patients with congestive heart failure», *Eur. J. Heart Fail*, 2009.
[45] L. Makarov, et al., «Microvolt T-Wave Alternans during Holter Monitoring in Children and Adolescents», *Ann. Noninvasive Electrocardiol.*, 2010.
[46] S. Yamada, *et al.*, «Sleep-disordered breathing increases risk for fatal ventricular arrhythmias in patients with chronic heart failure», *Circ. J.*, 2013.
[47] A. Martin-Yebra, et al., «Circadian modulation on T-wave alternans activity in chronic heart failure patients», presented at CinC2015, 2015.
[48] S. Sakamoto, *et al.*, «Utility of T-wave alternans during night time as a predictor for ventricular fibrillation in patients with Brugada syndrome», *Heart Vessels*, 2016.
[49] K. Hashimoto, et al., «Diurnal variation of frequency domain T-wave alternans on 24-hour ambulatory electrocardiogram in subjects without heart disease: Significant effect of autonomic nervous activity of the heart», *Ann. Noninvasive Electrocardiol.*, 2019.
[50] M. Uson, et al., «Cosinor-Based Circadianity of T-Wave Alternans Activity as a Predictor of Sudden Cardiac Death in Heart Failure: a Post-Hoc Analysis of the GISSI-HF Holter Substudy», presented at CinC2022, 2022.
[51] L. Burattini, et al., «Identification of Gender-Related Normality Regions for T-Wave Alternans: Gender-Related T-Wave Alternans», *Ann. Noninvasive Electrocardiol.*, 2010.
[52] L. Burattini, et al., «Is T-wave alternans T-wave amplitude dependent?», *Biomed. Signal Process. Control*, 2012.
[53] I. Marcantoni, et al., «Electrocardiographic Alternans: A New Approach», presented at 15th Mediterranean Conference on Medical and Biological Engineering and Computing (MEDICON), 2012.
[54] I. Marcantoni, et al., «Initial Reference Values of Electrocardiographic Alternans by Enhanced Adaptive Matched Filter», presented at CinC2022, 2022.